SIXTH FRAMEWORK PROGRAMME

Project no. 018412

IRASMOS

Integral Risk Management of Extremely Rapid Mass Movements

Specific Targeted Research Project

Priority VI: Sustainable Development, Global Change and Ecosystems

D1.1 – Catalogue of causes, triggers, and triggering thresholds for extremely rapid mass movements for a range of environmental boundary conditions

Due date of deliverable: 31/05/2008

Actual submission date: 15/07/2008

Start date of project: 01/09/2005 Duration: 33 months

WSL Swiss Federal Institute for Snow and Avalanche Research

Revision [2]

Project co-funded by the European Commission within the Sixth Framework Programme (2002-2006)		
Dissemination Level		
PU	Public	
PP	Restricted to other programme participants (including the Commission Services)	
RE	Restricted to a group specified by the consortium (including the Commission Services)	
CO	Confidential, only for members of the consortium (including the Commission Services)	

SIXTH FRAMEWORK PROGRAMME
PRIORITY VI
Sustainable Development, Global Change and Ecosystems

SPECIFIC TARGETED RESEARCH PROJECT

irasmos

INTEGRAL RISK MANAGEMENT OF EXTREMELY RAPID MASS MOVEMENTS

WORK PACKAGE 1:
FROM CAUSES TO FORECASTING

DELIVERABLE D1.1

Catalogue of causes and triggering thresholds

Edited by:
DIETER RICKENMANN (BOKU)
RICCARDO RIGON (UNIV. TRENTO)

Contributions by:
D. RICKENMANN (BOKU)
D. LAIGLE, G. CHAMBON (CEMAGREF)
M. DALL'AMICO (UNIV.TRENTO)
C. RULLI (UNIV.MILANO)
V. KVELDSVIK, F. SANDERSEN (NGI)
O. KORUP, T. PREUTH (WSL)

DATE: AUGUST 31, 2007 – **0.6-VERSION**

	TABLE OF CONTENTS	
Chapter 1		
		8
		12
		24
Chapter 2		
Chapter 3		

	3.2.1 Snow crystal types 3.2.1.1 Crystal before metamorphism 32.2.2 Crystal after metamorphism 3.2.2 Snow physical parameters 3.2.2.1 Liquid water content 3.2.2.2 Density 3.2.2.3 Main mechanical properties 3.2.2.4 Thermal properties 3.2.2.5 Energetic budget at the surface 3.2.3 Metamorphism 3.2.3.1 Mechanical transformation 3.2.3.2 Thermodynamical metamorphism	
	3.3 Instability factors and prodedures	
	3.3.1 Meteorological causes 3.3.1.1 Snowfall 3.3.1.2 Rain 3.3.1.3 Wind 3.3.1.4 Temperature and temperature gradient 3.3.1.5 Snowpack conditions: the slab structure 3.3.2 Environmental causes (Terrain in the avalanche starting zone) 3.3.3 Instability procedures and break process	
	3.4 Avalanches description and definition	
	3.4.1 Triggering classification 3.4.2 Avalanche classification 3.4.3 Avalanche zones and flows	
	3.5 Triggering causes and mechanisms	
	3.5.1 Recent-snow avalanches 3.5.1.1 Powder avalanches 3.5.1.2 Soft-lab avalanches 3.5.2 Slab avalanches 3.5.3 Wet-snow avalanches	
	3.6 Main triggering thresholds	
	3.6.1 Recent-snow avalanches 3.6.1.1 Quantity of new snow 3.6.2 Slab avalanches 3.6.3 Wet-snow avalanches 3.6.3.1 Rain 3.6.3.2 Significant and rapid temperature rises	

	3.7 Typical meteorological situations causing major spontaneaous avalanches	
	3.7.1 French Alps 3.7.2 Corsica 3.7.3 French Pyrenees 3.7.4 Spanish Pyrenees 3.7.5 Italy (provided by AINEVA)	

	LIST OF FIGURES
Chapter 1	
Figure 1	(upper): Scheme of shallow landslides in a basin; below: shallow landslide example (courtesy of Enzo *Farabegoli)*
Figure 2	Landslide and subsequent debris flow
Figure 3	Alpine like debris flow
Figure 4	Geomorphic
Figure 5	Ranges of lower limit of slope gradient from many sites worldwide for various types of landslides. The shaded area above the solid bar for debris avalanches, slides, and flows represents only one area in India [Sidle and *Ochiai 2006]*
Figure 6	Schematic of three-dimensional connectivity of different types of preferential flow pathways in forested soils [Sidle and Ochiai *2006]*
Figure 7	Anthropogenic hazard increase. On the left, due to roadcut, on the right due to infiltration change originated by cultivation purposes
Figure 8	Morphological map of the Super-Sauze earthflow
Figure 9	type of shallow landslide in steep terrain [Sidle Ochiai *2006]*
Figure 10	initiation of a debris flow [Sassa 1985]
Figure 11	overview of the Armancette catchment
Figure 12	Zone of debris flow triggering
Chapter 2	
Figure 18	Rock type affected by rock avalanches in the European Alps
Figure 32	Triggers of rock avalanches in the European alps
Figure 33	Relation of maximum distance between trigger and event (Keefer *1984)*
Figure 35	Cumulative rainfall diagram of the Val Pola area June-July 1987 (Crosta 2004)
Figure 36	Diagram of rainfall-equivalent snowmelt and rainfall in comparison to long-term mean values (Gertseema et.al.2006)
Figure 37	Climatic conditions before and during the Zymoetz rock avalanche (ZRRA) (Boultbee et.al.2005)
Chapter 3	
Figure 38	Short wave, long wave radiation and turbulent exchange at the snow surface
Figure 39	Scheme exhibiting the different snow metamorphisms according to the grain type
Figure 40	Rounding and size increasing mechanisms in wet snow metamorphism (from CEN/CS)
Figure 41	Different topographies that can produce wind slabs
Figure 42	The slab structure
Figure 43	Skier on a snowpack with a slab structure. In this case, the weak layer undergoes an additional stress due to the skier weight
Figure 44	Point start
Figure 45	Linear start
Figure 46	Powder avalanche
Figure 47	The fracture line is clear and an aerosol (powder cloud) rapidly forms in front of the flow
Figure 48	The fracture line spans the entire slope. Note the overhanging cornice, a sign of wind accumulation
Figure 49	The fracture is linear, the snow compact (likely deposited under windy conditions) and

	blocks are found along the track

	LIST OF TABLES

Chapter 1

TRIGGERING OF DEBRIS FLOWS AND SHALLOW LANDSLIDES

1.1 Introduction

Defining debris flow

A **debris flow** is a mixture of water, poorly sorted sediment and other debris, typically flowing rapidly, with one or more surges and a coarse-grained front, down steep mountain channels to a fan. Both solid and fluid forces strongly influence the motion, distinguishing debris flows from related phenomena such as rock avalanches and sediment-laden floods.

A debris flow has a higher solid concentration than normal or hyperconcentrated streamflow on the one end, and a higher water content than a landslide or rock avalanche on the other end of a spectrum defined by sediment-water ratio. The material involved in debris flows usually includes particles from clay size up to boulders, and organic components such as woody debris may also be present. Debris flows in the more restrictive sense transport a significant amount of coarse particles particularly near the front region.

A **mud flow** is a mixture of water and predominantly clay-, silt- and sand-sized particles, making up a viscous slurry and typically flowing rapidly, with one or more surges and occasionally including organic debris, down steep and also gentler mountain channels. The term mud flow usually refers to fine-grained debris flows. The presence of fine cohesive particles such as clay and a high solid concentration imply that the mixture is viscous and the flow behaviour is often laminar. The viscous slurry prevents rapid drainage of water. Mud flows generally attain longer runout distances

	than coarse-grained debris flows. However, debris and mud flows show similar general characteristics. The bulk behaviour of both debris and mud flows is characterised as a non-Newtonian fluid. At low shear stresses or shear rates the mixture may stop flowing at non-zero slope gradients (e.g. due to a yield stress). Debris flows including a substantial amount of coarse particles are probably more frequent in torrential catchments of the European Alps than mud flows. However, depending also upon the local geology and lithology large areas are recognized to produce essentially mud flows or so-called muddy or viscous debris flows. Debris flows derived from hillslopes have a similar material composition as debris or mud flows. In contrast to debris or mud flows, these hillslope debris flows do not occur in any preexisting channel or drainage line. A hillsope debris flow usually does not occur repeatedly within a historic time scale at a given location. In its initial stage, it may be similar to a landslide (i.e. a debris slide), but after internal dislocation and development of higher velocities it has a flow character similar to that of debris flows. Multiple surges are uncommon. There is **no uniform terminology** to distinguish between different flow types. This instance reflects to some degree the complexity of these phenomena. For some terms, even contradictory definitions have been proposed. Here, we adopt the most common use in the scientific English literature. Debris flow is often used as a general expression referring to all the three flow types discussed above. In the following, we also use the term in this general sense and only refer to mud flows and hillsope debris flows where an explicite distinction is necessary. Table 1 gives an overview on the most commonly used terms for the different flow types in several European languages.

Table 1 Expressions for debris flows and related processes in some European languages

	Debris flow	Mud flow	Hillslope debris flow	Hyper-concen-trated flow	Normal streamflow, flood including fluvial sediment transport
English terminology adopted here					
Englisch alternate expressions	[Debris torrent]	Mudflow	Debris avalanche, mudslide	Debris flood, mud flood, (immature debris flow)	
German	(Granularer) Murgang	Schlamm-strom, feinkörniger Murgang	Hangmure	Intensiver Geschiebe-transport *	Hochwasser mit Geschiebe-transport
French	Lave torrentielle (granulaire)	Coulée de boue, lave torrentielle boueuse	Coulée boueuse	Charriage hyper-concentré *	Crue avec charriage
Italian	Colata di detrito, lave torrentizie	Colata di fango	Scivolamento di detrito		Piena con trasporto solido
Spanish	Corriente de derrubios lava torrencial		Deslizamiento de derrubios		

*These expressions refer to the sediment transport conditions (immature debris flow) occurring in hyperconcentrated flow or in normal streamflow at steep slopes.

For a more detailed discussion of the characteristics and proposed classifications of solid-water flows, see for example Hungr et al. [2001]. Flowing sediment-water mixtures with solid concentrations higher than encountered in debris or mud flows are generally called landslides or earth flows, but there is a number of other expressions among which also debris avalanche is used, which thus contradict the use of this term for hillslope debris flows.

Hyperconcentrated flows have sediment concentrations higher than thosce occurring during fluvial sediment transport, but lower ones than those in debris and mud flows. Hyperconcentrated flows are not associated with a surging flow behaviour (as debris and mud flows), and the fluid mixture is characterised as a non-Newtonian fluid with a yield stress (contrary to normal streamflow), implying low settling velocities of sand-sized paricles. Hyperconcentrated flows occur through dilution of debris or mud flows, or by further entrainment of solid material through sediment transporting flows.

The volumetric solid concentration in the frontal and main part of a debris-flow surge is of the order of 50% to 85%. In the case of channelised debris and mud flows there is a close relationship to hyperconcentrated and normal streamflow, which are characterised by decreasing sediment concentrations. In hyperconcentrated flows, the volumetric solid concentration is of the order of 25% to 50%. The exact limits between different flow types are generally unknown, partly because they also depend on grain-size distribution and on grain composition.

The transition between different process types may occur towards the rear part of a

debris-flow surge or through dilution by normal streamflow as the flow enters higher order channels. A transition between debris flows, hyperconcentrated and normal streamflow is also possible in a given torrent channel during the same rainstorm event. With normal streamflow conditions prevailing over a longer time period, fluvial sediment transport may also result in a considerable throughput of solid material to the fan area.

Introduction

In this contribution we focus on the triggering conditions and mechanisms of debris flows in the broader sense. Table 2 points out that debris flows also share many commonalities with other types of mass movements.

Table 2 Classification and characteristics of the major trypes of mass movements

TYPE OF MASS MOVEMENT	TRANSPORTED MATERIALS	MOISTURE CONTENT	TYPE OF STRAIN AND NATURE OF MOVEMENT	RATE OF MOVEMENT
Dry granular flow	Sand or silt	Very low	Funnelled flow down steep slopes of non-cohesive sediments	Rapid to extremely rapid
Debris flow	Mixture of fine and coarse debris (20-80% of particles coarser than sand-sized)	High	Flow usually focused into pre-existing drainage lines	Very rapid
Debris or rock avalanche (sturzstrom)	Rock debris, in some cases with ice and snow	Low	Catastrophic low-friction movement of up to several kilometres, usually preceded by a major rock fall and capable of overriding significant topographic features	Extremely rapid
Rock slide	Unfracured rock mass	Low	Translational to rotational movement of coherent rock mass along single fracture	Very slow to extremely rapid
Debris/earth slide	Rock debris or soil	Low to moderate	Shallow slide of deformed masses of soil	Very slow to rapid
Rock fall	Rock blocks	low	Fall of individual blocks from vertical faces	Rapid to extremely rapid

Debris flows are complex mass movement processes determined by hydraulic flow behaviour, which is strongly dependent on the composition of the solids [Hungr et al. 2001]. One of the first monographs specifically devoted to debris flows was published by Stiny [1910]. The most recent textbook on debris flows and debris avalanches is edited by Jakob and Hungr. The methods used to assess debris flows on a site-specific scale range from general empirical geometric relations to advanced numerical process modelling. Current research on debris flows is summarised in Chen [1997], Wieczorek and Naeser [2000], Rickenmann and Chen [2003].

	In a pure flow, shear occurs throughout the moving mass of material and there is no well-defined shear plane. Flow is distinguished from creep by having discrete boundaries or narrow peripheral zones experiencing shear. Shear is at maximum at the base of the flow, but here the rate of flow is relatively slow and nearly all the movement occurs as turbulent motion within the body of the flowing mass. Dry flows can occur, but abundant water is usually present. They are often initiated by fall or slides, becoming flows when the moving soil or rock mass breaks up. Flows are categorized as avalanches, debris flows, eathflows or mudflows depending on wether they consist of predominantly snow and ice, rock fragments, sand-sized material or clay. IRASMOS Deliverable 1.3 deals in a more detailed way about the movements of debris flow and hence this is not treated here. As was noted above, debris flows are often initiated from shallow landslides. The term "landslide" is a widespread form of mass movement, and part of our everyday vocabulary. This presents some problems when using it in a specific technical sense, because landslide in general usage simply means the rapid downslope movements of slope material. Applied in this sense many landslides also involve fall and flow. However, a pure sliding failure occurs along a well-defined shear plane. Any resisting forces decrease sharply immediately following the initial failure, and downslope movement continues until there is a sufficient increase in resistance, often related to decrease in slope angle, to halt it. Most landslides typically involve a length-width ratio of 10:1. Excellent reviews of the problem related to landslide or debris-flow triggering have been compiled by Sidle [2006] and Glade and Crozier [2006].
	1.2 Physical causes
Introduction	The occurrence of debris flows depends on several factors such as the geological, groundwater, and topographic conditions. The following criteria must be satisfied: (i) availability of sediment, (ii) steep slopes, and (iii) sufficient water input. The parameters (i) and (ii) define the disposition or susceptibility of a catchment to produce debris flows. The conditions (iii) points to triggering conditions: if the stress in the soil induced by water infiltration and runoff exceeds a threshold value, slope instabilities and debris flows may occur. Long-lasting rainfalls may increase the susceptibility to slope instabilities. In a catchment with limited sediment availability, weathering may be important to replenish a certain sediment potential necessary for debris-flow occurrence. The sediment sources may be concentrated in the headwater area linked to distinct source locations such as moraines, talus slope or other glacio-fluvial deposits. Alternatively or additionally, the sediment is being entrained along the flow path. In this case there may be regular sediment input from small tributaries, or the bulk of the material may result from incision of the main torrent bed in readily erodable rock formations.

	The most common trigger of debris flows is sufficient water input during precipitation events. Other important sources of water infiltration into steep debris- or soil-mantled slopes are snowmelt during spring and early summer, melting ice during a volcanic eruption, glacial lake outburst floods, and sudden release of subsurface water stored near the outlet of a glacier drainage system.
Initiation mechanisms	Among the three main initiation mechanisms are (1) landslide-type failures (which may also result in hillslope debris flows); (2) channel-bed failure; and (3) temporary blockage of sediment and water flows in the channel, enhancing the surge-like flow behavior [e.g. Rickenmann and Zimmermann, 1993]. Berti and Simoni [2003] mention two broad approaches which may be used to quantitatively assess the first two initiation mechanisms. The appraisal of landslide derived debris flows typically relies on a Coulomb failure criterion coupled with critical-state soil mechanics to explain failure-induced liquefaction of material. For the channel-bed initiation a hydraulic approach may be used to define critical conditions for debris flow formation [Tognacca et al., 2000; Berti & Simoni, 2005; Armanini et al. 2000]. The controls on landslide susceptibility in a given area may be subdivided into two categories: quasi-static and dynamic. The quasi-static variables comprise geology, geotechnical properties, long-term climatic conditions, slope gradient, aspect and long-term drainage patterns. The dynamic variables include hydrological processes, vegetation and surface cover, and also human activities.
	1.2.1 Landslide type initiation
	Mass wasting is the major landform-shaping process in mountainous and steep terrain. Many shallow landslides involving mostly soil or debris result from infrequent meteorological or seismic events that induce unstable conditions on otherwise stable slopes or accelerate movements on unstable slopes. Thus, the delicate equilibrium between the resistance of the soil to failure and the gravitational forces tending to move the soil downslope can be easily upset by external factors, such as rainstorms, snowmelt, but also vegetation cover or land-use management. One of the most important hydrological triggering mechanisms for slope failures is the build-up of soil pore water pressure. This can occur not only at the contact between the soil mantle and the bedrock, but also at the discontinuity surface determined by the wetting front during heavy rainfall events. In addition to precipitation and infiltration, other factors deeply affect instability. We can summarize these aspects in the following categories: presence of debris, geological factors, geotechnics and mineralogical properties, geomorphic-topographic factors, hydrological and meteorological conditions, vegetation, and anthropogenic influence.
Shallow landslide definition	Shallow soil and debris slides represent one important precusory process of debris-flow triggering. It is therefore important to introduce some features regarding shallow-landslide classification and predisposing factors. This includes a detailed focus on slope-stability analysis, in order to quantify the parameters and the governing equations

	affecting the triggering of hillslope debris flows. We can distinguish shallow landslides from deep rock landslides according to the following characteristics: • The topographic surface is nearly parallel to the sliding surface; • The ratio length/depth is commonly >20; • The dominant control is the variation of depth of the water table. ***Figure 1*** (upper) shows that shallow landslide usually occur in hydrographic concave cells (b), where the hydrology is subject to a convergent regime, as opposed to divergent hillslope elements such as triangular factes (e).
Figure 1 (upper): Scheme of shallow landslides in a basin; below: shallow landslide example (courtesy of Enzo Farabegoli)	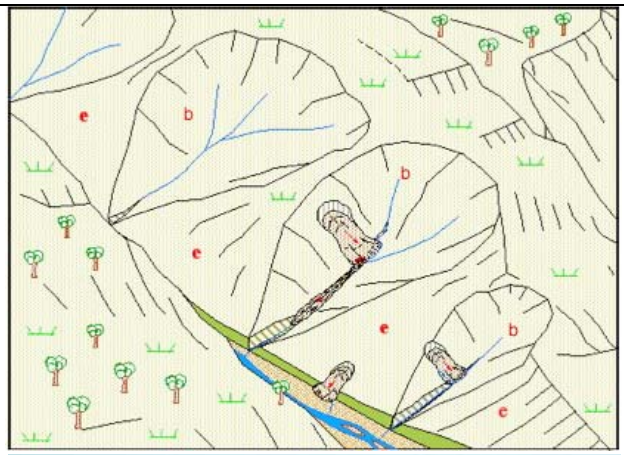 
Shallow landslides and debris flow	Importantly, an initially sliding motion of can turn into a much more mobile flow along the river bed. In the event depicted in ***Figure 2***, the material initially slid and most of the debris accumulated in the river bed (on the left). Then, after ten days of rainfall, it was mobilized and eventually obstructed the course of the torrent, invading the road below. On hillslopes with an abundance of coarse material, such as in alpine environments, the dynamics of such instability may be different, as the material commonly changes from soil to debris of various granulometry (***Figure 3***).

Figure 2 Landslide and subsequent debris flow	 
Figure 3 Alpine like debris flow	 

Presence of debris	The presence of debris is a condition *sine qua non* for the occurrence of a shallow landslide. Apart from its size characteristics, it is crucial to determine also the type of debris (clay, ravel, glacial deposits…) in order to assess its friction angle, coherence, permeability and propensity to result in a future debris flow. Numerous techniques are exploited to describe and quantify the material, for example direct *in situ* surveys and geophysical analysis, or indirect Earth Observation methods.
Topographic features	Profile and plan form of the slopes, slope angle, lengths of slope above the torrent channels, longitudinal and planar characteristics of the slopes (e.g. convergence, curvature, aspect) are the driving factors of water flow, both above and below the surface. This is important for stability, because high hydraulic gradients of hypodermic flows can weaken the stability of superficial deposits. As a consequence, critical gradients and quick and boiling conditions can occur, with the corresponding liquefaction processes in static conditions [Tharmit, 1999]
Geological factors	Geological causes of shallow landslides primarily involve rock characteristics and weathering. Mechanical or physical weathering consists of frost action, salt weathering, hydration, thermal stress caused by temperature fluctuation and mechanical unloading. While many lithologies are strongly associated with active landsliding, the extent and nature of the weathering processes and its influence on water infiltration and interaction with the rock mass more accurately describe the susceptibility of these substrates to mass movement [Sidle 2006]. Structural features of bedrock can promote landslide initiation in several ways, by forming weak surfaces that are prone to sliding, facilitating the exfiltration of groundwater onto the overlying soil mantle and creating the opportunity of weathering. The bedrock-soil interface is often of crucial importance in setting the susceptibility to shallow landslides. For instance, debris slides, avalanches and flows are common occurrences in coastal Alaska and British Columbia in terrain sculpted by recent glacial retreat, where hillslopes have been oversteepened and relatively impermeable glacial till has been deposited over bedrock, forming a barrier to water penetration and an effective sliding surface [Sidle 2006, Brandinoni and Hassan 2006].
Geotechnics and mineralogy	Geotechnical slope stability analyses, by methods of limiting equilibrium, require a quantitative determination of soil shear strength. Some parameters like cohesion, grain-size distribution, and internal friction angle can be determined *in situ* or through laboratory analysis. Additional parameters, such as presence of vegetation and relative apparent cohesion, presence of erosions, type of geology, can be determined by indirect measures or derived, where available, from maps. Remote-sensing data can help to identify areas where the cohesion has been drastically reduced, for example through the recognition of areas affected by recent forest fires or deforestation. All these parameters, in order to account for uncertainty, ought to be assigned a probability distribution rather than a fixed value. Furthermore, their characterization should take into account the particular instability model and its parameters requirements. Moreover, the mineralogy and chemistry of clays affect certain physical and

	engineering properties of soils and regoliths, thereby influencing the stability of cohesive materials [Yatsu 1966, Torrance 1999, Duzgoren-Aydin 2002]. Clay mineralogy influences the stability of cohesive soils, especially in slump-earth flow movements, deep-seated soil creep, shallow quick clay slides and flows and shallow slides in non-sensitive clay soils. The importance of clay mineralogy is minimal in shallow, rapid failures of cohesionless soils unless there is an underlying failure plane rich in clay.
Geomorphic-topographic features	Hillslopes that are convergent or concave in plan form tend to concentrate subsurface water into small areas of the slope, thereby generating rapid pore-water pressure increase during storms or periods of snowmelt [Sidle 1984a, Fernandes 1994, Montgomery 1997, Tsuboyama 2000]. Thus, shallow, rapid landslides frequently occur in slope depressions and gullies and these topographic hollows have been the topic of renewed interest. Planar slope segments are intermediate in susceptibility to landsliding between divergent and convergent slopes.
Figure 4 Geomorphic landform elements	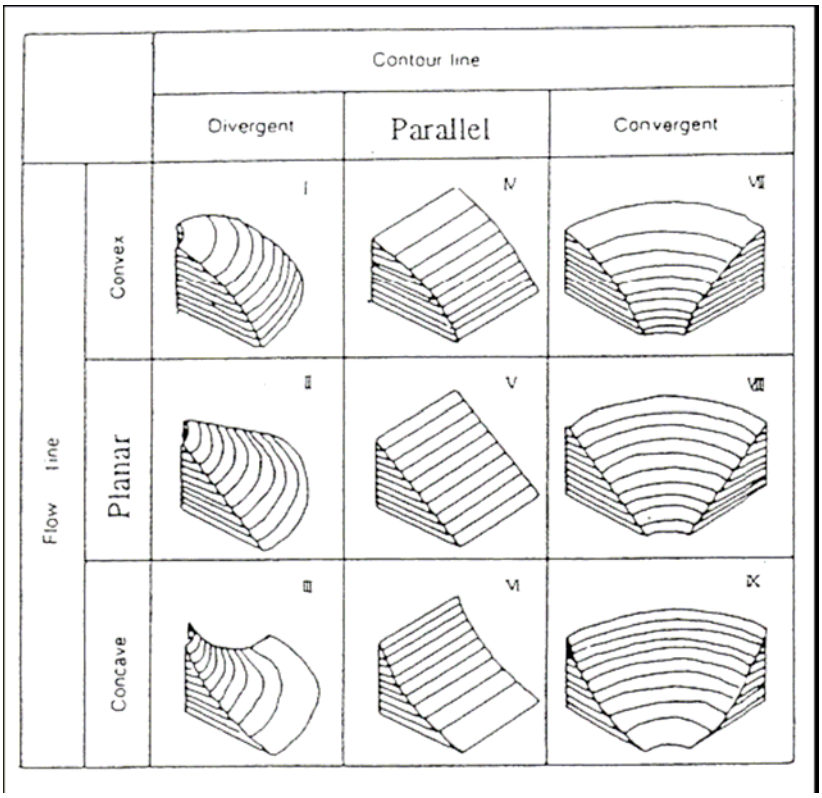
	When a landslide occurs, a channel can be eroded into the hillslope linking the hollow to an existing channel. This linkage is more likely to occur if the landslide is large and transforms directly into a debris flow. In the case of smaller landslides in hollows, the depositional material may remain on the hillslope, at least temporarily as the infilling or accretion of soil in hollows may last for long time. A lower limit of slope gradient for various soil slides is difficult to ascertain, and high variations in typical gradients for various processes have been reported (***Figure 5***) Furthermore, interpretations ot these gradients are confounded by complex combination mass movements as well as inconsistent measurement and classification criteria. However, it appears that debris slides, debris avalanches and debris flows

	initiate on the steepest slopes, while earthflows, slumps and soil creep (generally deep-seated mass movements) typically initiate on more gentler slope. Also altitude, by virtue of other factors such as slope gradient, lithology, weathering, precipitation, ground motion, soil thickness and land use, is usually associated with landslides. While many studies have drawn strong statistical relationships between elevation and landslide occurrence, it does not provide any plausible physical explanation.
Figure 5 Ranges of lower limit of slope gradient from many sites worldwide for various types of landslides. The shaded area above the solid bar for debris avalanches, slides, and flows represents only one area in India [Sidle and Ochiai 2006]	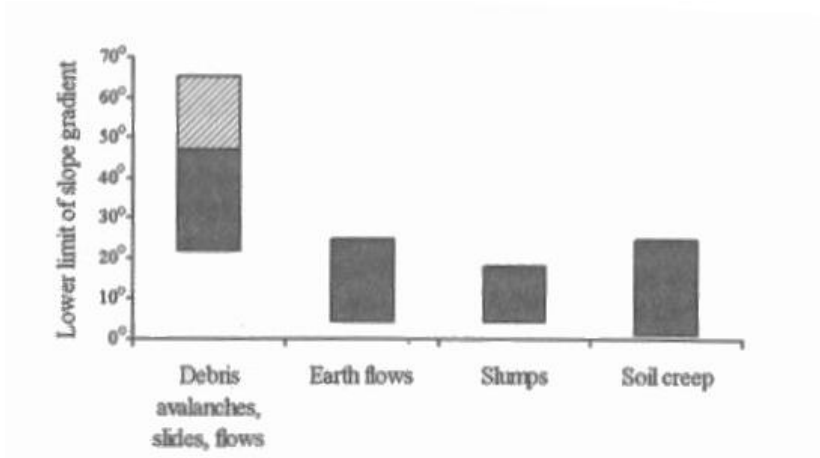
Hydrology and meteorology	Meteorologic factors such as temperature also play a major role during the snow melting period, particularly in areas where permafrost exists. Raindrop and hailstone impacts, with firehose effects and runoff, may result in loss of structure and direct mobilization of elementary particles and soil aggregates. At the moment, the grid of meteorological models is not sufficiently small to cope with the required hydrological scale, and should therefore properly downscaled. Spatial patterns of rainfall and snow accumulation (and melt) are closely associated with landslide initiation. Typically, higher mountain elevations experience larger volumes of precipitation, both rain and snowfall. In such areas, altitude may be used as an approximate surrogate for precipitation to help stratify landslide hazard because few remote regions have detailed distributed precipitation data. According to Sidle [2006], four attributes strongly affect landslide initiation: total rainfall, short-term intensity, antecedent storm precipitation and storm duration. These attributes all influence the generation of pore-water pressure in unstable hillslopes, including hollows. At the most general level of prediction, 73 shallow landslide/debris flow occurrences from around the world were assessed on the basis of mean rainfall intensity and storm duration [Caine 1980]. The lower bound of this log-linear relationship is given by a monomial expression which involves the intensity of the rainstorm and the storm duration. In principle, this equation could be used to assess the likelihood of shallow landslide and debris flows on hillslopes for different magnitudes and frequencies of rainfall. If at any time during a storm the average rainfall intensity exceeds the threshold value, shallow, rapid landslide may occur. After some studies the relation was modified, and, to assess the effects of antecedent rainfall on the mean intensity-duration relationship with respect to shallow landslides, all data complied by Caine [1980] that included two-day antecedent rainfall were

plotted

To account for the effects of antecedent soil moisture on landslide initiaition during rainfall events, an Antecedent Water Status Model (AWSM) was developed that uses daily rainfall and estimates soil water status based on a climatic water balance [Crozier and Eyles 1980, Crozier 1999]

The most important physical properties of soils that affect slope stability are those that govern the rate of water movement onto and through the hillslope, as well as the water holding capacity. Additionally, the structure, density and orientation of fractures and interstices in bedrock or other substrate that underlie the soil profile are important in determining whether subsurface water will drain from the soil or enter the soil from below (***Figure 6***).

The water-holding capacity of the soil influences antecendent soil moisture and thus the amount of rainfall or snowmelt required to recharge the soil mantle. While the physical properties of the soil matrix are important as related to water movement and pore-pressure accretion in unstable hillslope soils, it is often the larger-scale physical attributes of the soil catena and regolith that ultimately dictate where and when landslides will occur. Estimating the role of preferential flow systems over appropriate scales in indeed problematic [Sidle et al, 2000a, 2001].

Figure 6 Schematic of three-dimensional connectivity of different types of preferential flow pathways in forested soils [Sidle and Ochiai 2006]

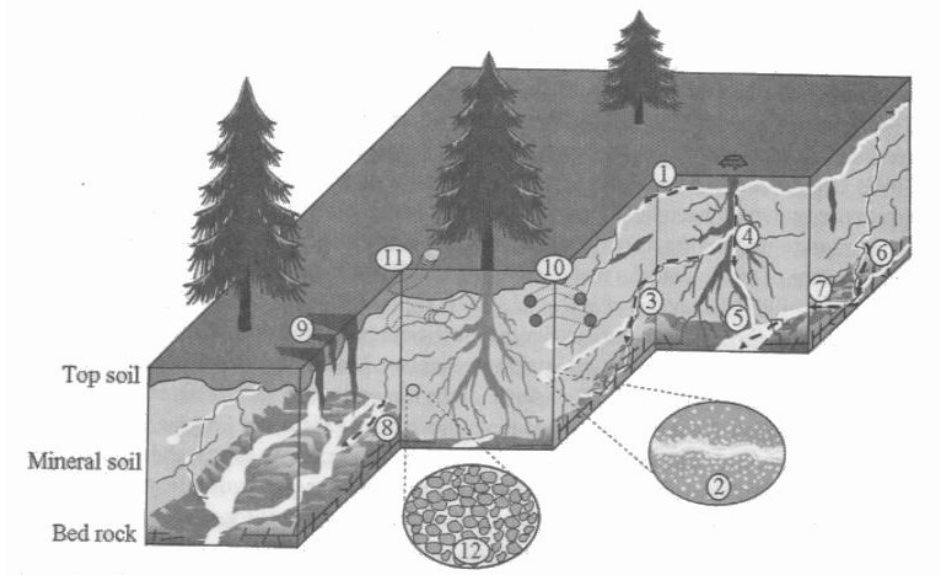

1. preferential flow occurring in the organig horizon above the mineral soil
2. macropores interacting with surrounding mesopores to enlarge these preferential flow paths during wet conditions
3. connection of individual macropores via physical interaction
4. preferential flow through buried organic matter and decayed roots
5. flow along a lithic contact
6. preferential flow into and through bedrock fractures or joints
7. exfiltration of water from shallow bedrock fractures or joints
8. flow over microchannels on the bedrock or other substrate (i.e. substrate topographic control
9. flow through soil cracks
10. flow in worm holes
11. flow in animal (including insect) burrows or cavities
12. preferential flow through inter aggregate spaces

Infiltration refers to the actual flux of water into the soil and is dependent upon

	physical, biological, topographic and coltural factors as well as the water delivery rate (i.e. rainfall intensity or snowmelt rate). While important, it is difficult to directly relate infilration characteristics to slope stability. Theoretically, reducing recharge into the soil mantle should stabilize hillslopes by reducing pore pressures that develop during storms. While at the micro-scale this may be true, much unstable terrain is replete with tension cracks, especially around potential landslide initiation zones, thus providing preferential pathways for any overland flow into that does not infiltrate into the soil matrix. Such water may be rapidly redirected to the failure planes of deep-seated or even shallow landslides, thereby actually increasing the probability of slope failure. Thus, maintaining a viable vegetation cover that promotes infiltration, will generally benefit slope stability as peak inputs of water into the soil mantle will likely be dispersed. Processes of subsurface flow influence both the temporal and spatial characteristics of pore-water pressure distribution. Subsurface flows at the hillslope or small catchment scale are usually modeled on the basis of Richard's equation and Darcy's law for unsaturated and saturated flow, respectively. Similar to vertical infiltration, slope-parallel movement of water is strongly affected by networks of preferential flow. Spatial and temporal variability in subsurface flow may be strongly liked to three-dimensional preferential flow networds at the hillslope scale [Carey and Woo, 2000]. These networks in turn influence the spatial and temporal accretion of pore-water pressure that is typically responsible for landslide initiation.
Vegetation influences	Woody vegetation, particularly trees, augments the stability of hillslopes in primarily two ways: removing soil moisture through evapotranspiration and providing root cohesion to the soil mantle [Philips and Watson, 1994, Ekanayake and Phillips, 2002]. Effects of evapotranspiration on the soil water budget can be partitioned as follows: - canopy interception of rainfall or snow and subsequent evaporation loss to the atmosphere - transpiration of infiltrated water to meet the physiological demands of vegetation - evaporation from the soil or litter surface According to [Sidle 2006] the potential for vegetation to affect slope stability through evapotranspiration depends primarily on vegetation cover and the climatic setting. In general, evapotranspiration rates in temperate regions are lowest from bare soil, several times higher form grassland and 5 to 10 times higher compared to bare soil from forests [Jones, 1997]. The seasonal influence of evapotranspiration on soil water budgets, especially in temperate and dry regions, determines whether these losses influence landslide probability. The contribution of vegetation roots to soil shear strength is generally recognized as more important in stabilizing hillslopes compared to evapotranspiration losses [Wu et al 1979, Gray and Megaham 1981, Greenway 1987, Phillips and Watson 1994]. Many field investigations in steep forested terrain worldwide have noted a two- to more than tenfold increase in rates of mass erosion three to 15 years after timber harvesting [Bishop and Stevens 1964, Endo and Tsuruta 1969, Fujiwara 1970, Swanson and Dyrness 1975]. This increase in landslide frequency and volume is related to the period of minimum rooting strength after clearcut harvesting and prior to substantial regeneration. Thus, the root strength minimum does not imply that a landslide will occur at any specific time; rather, it indicates that the probability of a landslide is higher given the likelihood of a triggering rainfall or snowmelt event. Described a bit

	differently, the threshold for a landslide triggering storm at a particular site would be lowest during the root strength minimum [Sidle 1992]. When hillslope soils are in a tenuous state of equilibrium, reinforcement by tree roots may provide the critical difference between stability and instability during storm or snowmelt [Sidle 1992]. Although conclusive evidence has linked root systems of forests with enhanced soil strength, there remains a high level of variability in mass erosion from mountainous forested areas [Guthrie 2002]. Evaporation from vegetation canopies and transpiration lead to drier soil conditions, thus potentially reducing pore water pressure accretion during storms or snow melt. Conversely, vegetated land surfaces have higher infiltration capacities due to greater surface roughness, organic matter and depletion of soil moisture by deep-rooted vegetation may enhance the formation of desiccation cracks. Thus, typically, the benefits of evapotranspiration and enhanced subsurface draining would outweigh disadvantages of greater infiltration, not to mention surface erosion benefits. The presence of trees increases both the normal and slope-parallel force components on potential sliding surfaces. For cohesionless soils, if the slope angle is less than the internal angle of friction, tree surcharge should have a net stabilizing effect of hillslopes; when the slope angle exceeds the friction angle, then surcharge would have a small destabilizing effect. Beneficial effects of greater surcharge on low cohsion soils are slightly greater when groundwater tables are higher [Gray and Megahan 1981,Sidle 1984b]. For most steep sites with some soil and root cohesion, decreasing surcharge by removing trees has only a minor stabilizing effect on hillslopes [Sidle 1992].

Table 3 Anthropogenic influence and release factors (Tharmit 1999)

Main land modification	Vegetation Evapotrans--piration	Run-off	Infiltration	Water concentration velocity	Flow rate	Erosion	Torrent pavement
Deforestation	↘	↗	↘	↗	↗	↗	↘
Road construction	↘	↗	↘	↗	↗	↗	↘
Earthwork	↘	↗	↘	↗	↗	↗	↘
Buildings	↘	↗	↘	↗	↗	↗	↘
Ski piste drainage		↘		↘	↘	↘	
Ski piste compaction	↘	↗	↘	↗	↗	↗	↗
Artificial snow	↘	↗	↘	↗	↗	↗	↗

Figure 7 Anthropogenic hazard increase. On the left, due to roadcut, on the right due to infiltration change originated by cultivation purposes

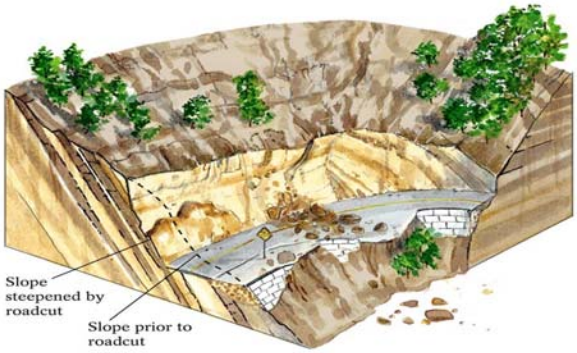

Anthropogenic influence

Hydraulic balance (runoff, infiltration, evapotranspiration) and slope stability are highly affected by the action of man. For example, slope cultivation, roadcut for construction, drainage, modification of landscape due to resort constructions, loss of water from pipelines are part of the man-induced modifications that can influence the hydrology and stability of a slope. ***Table 3*** gives an overview on the relationship between anthropogenic modification and release factors. ***Figure 7*** shows the instability provoked on a slope by a roadcut and on a field by drainage modification consequent to cultivation.

1.2.2 Snowmelt and freezing-thawing induced instabilities

Dave and Savage [2005] outline that snowpack conditions commonly cause or contribute to triggering debris flows in alpine areas throughout the world. The most current and comprehensive research on the subject is centered in the Swiss Alps. Among the other causes, we can classify the contribution of snowpack to the triggering of debris flow as follows:

1. Melting of perennial snow patch [Rickenmann and Zimmerman, 1993]. The melting of old snow patches during the spring and summer months enhances local water saturation of the underlying unconsolidated sediments. In the Swiss Alps the combination of this melting and a pulse of rain precipitation led to over 600 recorded debris flows during the summer of 1987.
2. Breaching of proglacial lakes. Four potentially hazardous periglacial lakes were studied near Valais in the Swiss Alps [Haeberli, et. al 2001]. From the late 1980s to the present, during a general warming trend, the lakes have been enlarged by successive snow and ice melt toward the glaciers. The authors warn that the formation of slush avalanches in snow covering the outflow of these lakes can cause a sudden increased discharge towards two of the lakes during spring and early summer. Single-flow and multiple-flow GIS-models were created for the assessment of hazards from glacier lake outbursts [Huggel, et. al. 2003]. The models are topography based and use primarily ASTER satellite-derived digital elevation models. The model was applied to the Tasch Lake area of Switzerland, which experienced a devastating debris flow on June 25, 2001, during a period without any significant precipitation. Considerable parts of the village of Tasch were destroyed or damaged by the event. Elevated air temperatures during the period prior to the event led to high snowmelt input to the lake. Tasch Lake had previously been dammed by pieces of lake ice and snow deposits. The elevated water level caused larger hydraulic gradients and piping in the core of the moraine dam. The snow and ice blockage ruptured and the resulting water initiated the debris flow that devastated the village. The single-flow GIS model was able to more accurately recreate the event than the multiple-flow version and was suggested as a possible predictive tool for the regional assessment of debris-flow hazards.
3. Snow avalanche deposits in gullies [Bardou and Delaloye, 2004] in the Valais Alps of southwest Switzerland were shown to be both potential amplifying and reducing factors of debris flows. On the one hand, these serve as enhancing factors by increasing the base flow under the snowpack and creating a sliding plane for sediments covering it, on the other they are reducing factors, as they decrease the impact energy or raindrops, mainly during the time of winter storms. Consequent debris flows can result simply from the alternation of snowmelt events with sediment slips.

During the summers of 1999 and 2000, small debris flows occurred in many of the upper watersheds throughout the European Alps. Some of these debris flows occurred during clear weather and were not triggered by rain precipitation and were observed to contain large amounts of snow. [Bardou and Niggli, 2003] performed a statistical analyses over selected watersheds to correlate winter snowfall with the number of

	floods occurring during the following summers, concluding that snow precipitation is often the underlying cause of debris flows in mountainous torrents during the first thunderstorms of the summer, and that temperature and antecedent climatic history of the watershed must be examined in addition to rainfall to give a complete picture of debris-flow triggers. Global warming is creating numerous concerns about its relation to triggering landslides. According to [Sidle 2006], the occurrence and rates of deep-seated mass movements may increase in some regions characterized by winter rainfall and rain-on-snow events in response to predicted increases in winter precipitation in latitudes above 45° N [Sidle and Dhakal, 2002]. However, with predicted shorter winters, the period of deep-seated mass movement may decrease. Increased temperatures may accelerate weathering processes and increase the susceptibility and rate of slow, deep-seated mass movement. In northern latitudes, where snowpacks increase, mass movements will probably occur earlier (due to climate warming), have increased seasonal rates of movement, and experience a longer period of activity. Glacial thinning and retreat in western Canada associated with climate warming during the last 100-150 yr triggered landslides due to debuttressing effects, and additionally, outburst floods and debris flows initiated form moraine- and ice-dammed lakes [Evans and Clauge 1994, Hewitt, 1998]. Bovis and Jones [1992] used recent records of climate change, dendrochronological data, and stratigraphic records to show that movement of large earthflows in British Columbia responded to Holocene climatic changes. Since high temperatures related to climatic change are likely to affect high-elevation permafrost distribution, thawing of permafrost may also induce ravel and dry creep at higher elevations [Sidle and Dhaka, 2002]. Climate changes that promote more frequent freezing-thawing ro wetting-drying cycles would induce greater dry ravel and dry creep on steep, disturbed or partially vegetated hillslopes. Coversely, fewer of these cycles would tend to reduce dry ravel and creep. Various authors have studied the dependence of snowmelt and infiltration. Horton [1938] found that snowmelt provides a more continuous supply of water over longer time periods than infiltration from rain, Matthewson [1990] found that snowmelt may also recharge shallow fractured bedrock and raise pore-water pressures beneath shallow soils, thus triggering debris flow. Spatial variability from infiltration of snowmelt is not as high as that from intense rainstorm cells. The rate of snowmelt depends on air temperature, which in turn relates to the timing of debris flows [Choleborad, 1997, 1998]. [Choleborad, 1997] found a threshold on a six-day moving average of daily maximum temperature for anticipating the onset of snowmelt-generated landslides in the central Rocky Mountains. Debris flows have also been found in south-western British Columbia to be associated with moderate rainfall with snowmelt, low intensity rainfall and heavy snowmelt, and heavy rainfall onto deeply froze, thawing ground [Church and Miles, 1987].
	1.3 Phases of instability
Triggering conditions and safety factor	In a general simplified scheme, the triggering occurs when, in the debris of the slope under consideration, the sliding active forces are superior to the resisting forces. The

active forces, neglecting the presence of earthquakes or volcanic explosions, are the gravity of the weight of material and water, and the deformation - sliding forces deriving from infiltration. As resisting forces, we consider the cohesion and intergranular forces deducted by the buoyancy due to interstitial water.

Usually, the action of these forces is accounted for in a safety factor, which expresses the tendency of the slope to instability.

Meteorological triggering conditions must be searched in the variation of pore pressures in the soil. A comprehensive analysis of the triggering conditions must account for the effects of this variation, both in saturated and unsaturated soils from a dynamic perspective. The analysis of the temporal variation in slope stability examines the role of pore water pressures on the soil shear strength. In general, the pore-pressure field, u(x,y,z,t), is three-dimensional and time-dependent. However, in most slope stability analyses, four assumptions are commonly used to simplify the quantification of the pore-pressure field in the vicinity of a hillslope:

1. The temporal response of the pore-pressure field to infiltration is ignored, and a "worst-case" is assumed, replacing the actual transient field, u(x,y,z,t) with a steady-state surrogate u(x,y,z);

2. The analysis of the three-dimensional steady pore-pressure field u(x,y,z), is represented by a two-dimensional approximation, u(x,z). This approximation is appropriate only for cases where the geometry of the slope and geology do not vary normal to a cross section;

3. The hillslope hydrology is almost always considered isotropic and homogeneous, ignoring any structural complexities that exist in form of layering, lensing or fracturing;

4. The unsaturated zone between the water table and the ground surface is commonly ignored.

While these assumptions may be adequate for the engineering design of man-made slopes, they may be inappropriate for regional, time dependent analysis of natural slopes stability. On natural slopes the assumption of homogeneous, isotropic conditions may lead to assessments and forecasts with unacceptable large errors. Recently, several models that incorporate the transient pore-water pressure distribution in regional slope-stability analysis have been proposed and developed [Iverson, 2000; Baum et al., 2002; Savage et al., 2004; Rigon et al., 2004].

Historically landslide-triggering problems have been tackled from a macroscopic point of view. The effective stress approach which quantifies the part of the total stress that produces measurable effects, such as compaction or an increase of the shearing resistance, while, for instance, [Terzaghi, 1936] only accounts for forces propagating through the soil skeleton. It accurately describes the soil behavior under saturated conditions because the soil-water system can be treated as an equivalent continuum medium with macroscopic stresses defined at the boundary. In this framework the pore

water, which acts over the entire grain surface, constitutes a neutral, isotropic stress; therefore the system can be described by macroscopic stress state variables such as the total stress, the pore-water pressure and the intergranular bonding stress that provides cohesion at zero normal stress.

When the water content decreases, the soil starts desaturating and the pore-water pressure is no longer a neutral stress in a soil-water-air system. The macro-scale variables do not adequately describe the forces acting on the system, since local interparticle forces arise through the different phases and their interfaces. According to Lu and Likos [2004], these forces are physicochemical forces, surface tension and forces arising from negative pore water pressure.

The triggering mechanisms in natural slopes can then be summarized as follows:

a. Reduction in soil shear strength due to an increase in positive values of pore water pressure, i.e. saturated conditions.

b. Reduction in soil shear strength due to an increase in negative values of pore water pressures, which occurs under partially saturated conditions.

The Safety Factor (SF) for these scenarios can be described with only one equation:

$$SF = \frac{\tan\varphi'}{\tan\alpha} + \frac{(-u_w)S\tan\varphi'}{\gamma z sen\alpha\cos\alpha}$$

where the drained cohesion is considered to be zero, φ' is the internal friction angle, α is the slope angle, γ is the specific soil weight, z is the soil thickness, u_w is the pore water pressure, ϑ is the volumetric soil water content, ϑ_{sat} is the volumetric soil water content at saturation and ϑ_r is the residual volumetric soil water content. According to the sign of pore water pressures, the contribution of the pore water presure to the safety factor can be positive or negative. If the water table is above the sliding surface, pore water generally has adverse effect on the safety of the slope since it is positive or compressive. In this case the effective stress , σ', defined by Terzaghi, and consequentely the shear strength decreases:

$$\sigma' = \sigma_{tot} - u_w$$
$$\tau = \sigma' \cdot \tan\varphi' = (\sigma_{tot} - u_w)\tan\varphi'$$

where σ_{tot} is the total stress.

When the moisture variation in the vertical direction is important, the consequent effective stress in partially saturated soil above the water table may need to be considered. In this case the effective stress is no longer the difference between the total stress and pore water pressure. The generalized effective stress unifying both saturated and unsaturated conditions was recentely given by Lu and Likos [2006]:

$$\sigma' = \sigma_{tot} - \sigma_s$$

$$\left.\begin{array}{l} \sigma_s = u_w \\ \sigma_s = f(u_a - u_w) \end{array}\right\} \left\{\begin{array}{l} u_w > u_b \\ u_w < u_b \end{array}\right.$$

where σ_s is the soil suction stress due to capillary forces, u_b is the air-entry pressure and u_a is the air pressure (which is usually considered to be zero). Lu and Likos [2005] also demonstrate that an expression for the suction stress can be described by the following relation:

$$\sigma_s = -\frac{\vartheta(z) - \vartheta_r}{\vartheta_{sat} - \vartheta_r}(u_a - u_w) \quad .$$

At saturation $\vartheta(z) = \vartheta_{sat} \Rightarrow S(z) = 1$ and $u_w > 0$, therefore the expression for the Safety Factor reduces to:

$$SF = \frac{\tan\varphi'}{\tan\beta} - \frac{u_w \tan\varphi'}{\gamma z sen\alpha \cos\alpha},$$

clearly indicating a reduction in the Safety Factor.

For partially saturated soil $\vartheta(z) < \vartheta_{sat} \Rightarrow 0 < S(z) < 1$ and $u_w < 0$; therefore the expression for the Safety Factor becomes:

$$SF = \frac{\tan\varphi'}{\tan\alpha} + \frac{u_w \dfrac{\vartheta(z) - \vartheta_r}{\vartheta_{sat} - \vartheta_r} \tan\varphi'}{\gamma z sen\alpha \cos\alpha}$$

Since suction stress is tensile in nature, the overall effect is to hold soil together, thus increasing the Factor of Safety. Suction stress generally reduces as soils become wetter, and this phenomenon is regarded as the physical mechanism triggering many shallow landslides when soil is subjected to intensive precipitations.

For a given slope angle, possible triggering conditions due to an increase in pore water are summarized in following table.

Table 4 Safety conditions for slope and friction angles)

#	Slope Angle & Friction Angle	Stable if	Unstable if
1	$\alpha < \varphi'$	$u_w > 0$	$u_w + \Delta u = 0$
2	$\alpha << \varphi'$	$u_w > 0$	$u_w + \Delta u < 0$
3	$\alpha > \varphi'$	$u_w < 0$	$u_w + \Delta u < 0$
4	$\alpha = \varphi'$	$u_w < 0$	$u_w + \Delta u = 0$

Figure 8 Morphological map of the Super-Sauze earthflow

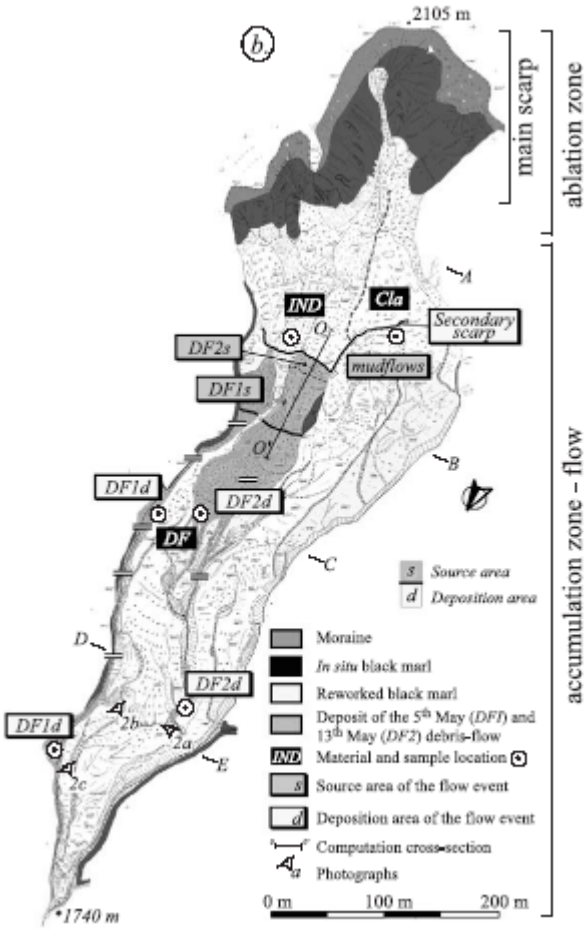

Condition for movement

Exampe: Super-Sauze earthflow

Rheometrical analyses have been carried out on undisturbed samples collected (***Figure 8***) on the secondary main scarp (IND), on the western slope area (C1a) and in the deposits of DF1 and DF2 events. All the materials exhibit a viscoplastic behaviour over the range of shear rates in consideration, well represented by a Herschel–Bulkley constitutive equation. Herschel–Bulkley parameters (yield-stress τc, consistency K) increase with the total solid fraction. For total solid fractions between ϕ=0.30 and ϕ=0.60, the yield stress may vary by as much as three times, while the consistency varies only by twice as much. Laboratory results are consistent with those estimated at the field scale by the shape of the slurries at stoppage (***Table 5***). The differences are comprised between the margin of error specified by Coussot and Ancey [1999] who indicate that the difference in the yield stress estimation using several methods is

between 10% to 25%.

Rheological parameters clearly distinguish two types of material in the debris source area: the cohesive silty clayey matrix (C1a) presents high yield stress and viscosity and the sandy silty matrix (IND) that presents lower rheological characteristics. This means that a higher volume of water is necessary to initiate a fluid behaviour in C1a material than in IND material. Combined with the hydrological and geotechnical characteristics, it appears that the main potential source of debris is therefore the eastern part of the secondary scarp cut in the IND material (***Figure 8***). The geometrical and morphological characteristics of this zone being also favourable to the release of debris, it was important to define the stability conditions of this zone.

Table 5 Rheological properties of the debris source area material and of the muddy debris flow deposits for ϕ=0.45

Rheological properties of the debris source area material and of the muddy debris flow deposits for ϕ=0.45

	Rheometry			Inclined plane	Deposit shape
	τ_e	κ	n	τ_e	τ_e
	Pa	Pa s	/	Pa	Pa
C1a	182	120	0.31	211	/
IND	103	84	0.30	126	/
DF1	84	52	0.32	89	132
DF2	75	41	0.35	93	146
AM	142	86	0.29	168	/

τ_e is the yield stress; κ is the Herschel–Bulkley shape parameter or consistency; n is the power law exponent; ϕ is the total solid fraction.

Landslide-debris flow linkages

According to [Sidle 2006], small landslides occur on steep hillslopes or within geomorphic hollows may behave in the following ways (***Figure 9***):

1. Initially transform into a debris flow and proceed downslope to a channel [Wang et al 2002a, 2003b]
2. Enter headwater channels and immediately trigger a debris flow [Sidle and Chigira 2004, Chen 2006]
3. Transport sediment and organic debris into the channel heads and channels, but not immediately initiate a debris flow [Gomi et al, 2002]
4. Deposit debris on the hillslope that can potentially be transported to the headwater channel during future hydrogeomorphic events [Peart et al, 2005]

Figure 9 type of shallow landslide in steep terrain [Sidle Ochiai 2006]	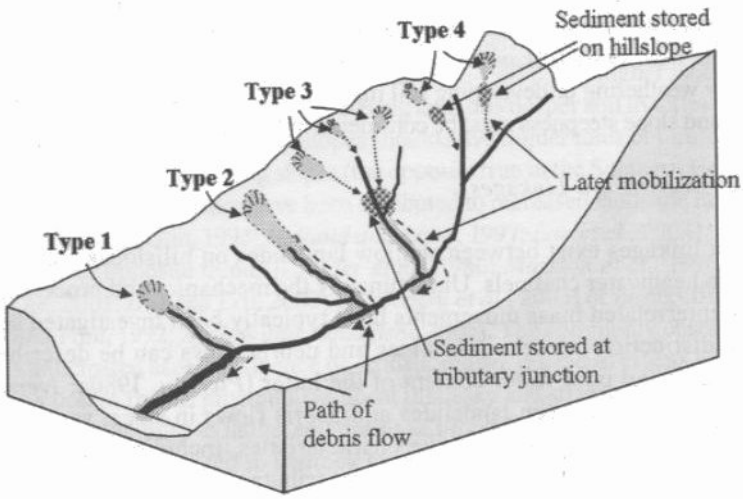
	Type 1 and 2 occur directly in response to the landslide. The stress-strain and strength properties of soil combined wit the effects of pore water have significant implications for the formation, speed and travel distance of landslides. Soils that deform contractively do so by reducing their pore space that, in saturated or nearly saturated soil results in an immediate increase in pore pressure, with consequent loss of soil strength. Therefore failure of a loose, contractive soil may result in a rapid evolution from soil slide to debris flow. In contrast, failure of a relatively dense, dilatant soil tends to proceed incrementally; expansion of pore space in a soil reduces pore pressure and may result in matric suction If sufficient water is available the suction will draw water onto the zone of failure in the dilatant soil. The additional water thus drawn reduces the suction (or increases the pore pressure) and may allow an additional increment of dilatant failure Moore and Iverson [2002]. Fleming et al [1989] showed from field studies that contractive soils tend to fully mobilize into fluid debris flows that travel relatively long distances and that soil slides in dilatant soils will either mobilize only partially into flows of relatively short runout or will remain perched on the hillside and coherent slide masses. Iverson et al [2000] confirmed these observations experimentally and showed that an initial critical porosity of at least 20.5% is required for rapid failure and debris flow fluidization in a sandy-loam soil. For type 2 and 3 it is apparent that critical levels of sediment and debris inputs are needed together with the occurrence of a large runoff event to trigger an in-channel debris flow [Placios et al, 2003, Iaizumi et al, 2005]. For cases where landslides do not immediately mobilize into debris flows, the timing of landslide initiation is separated, but not independent from, the timing of the debris flow initiation processes. Factos that contribute to landslide initiation on slopes (e.g. rain intensity) may be more stochastic, compared to the partly deterministic factors that control in-channel debris flows (e.g. sediment and woody debris accretion, channel storage sites) [Lancaster et al, 2003]. Sediment deposited near channel heads by stochastically triggered hillslope landslides reaches a critical level of accomulation after which time the material falis as a debris flow. Similar phenomenon would lidely apply to landslides and the resulting debris flow triggered by snowmelt or rain-on-snow events [Wieczorek et al, 1989, Buchanan et al, 1990, Toews 1991].

Figure 10 initiation of a debris flow [Sassa 1985]	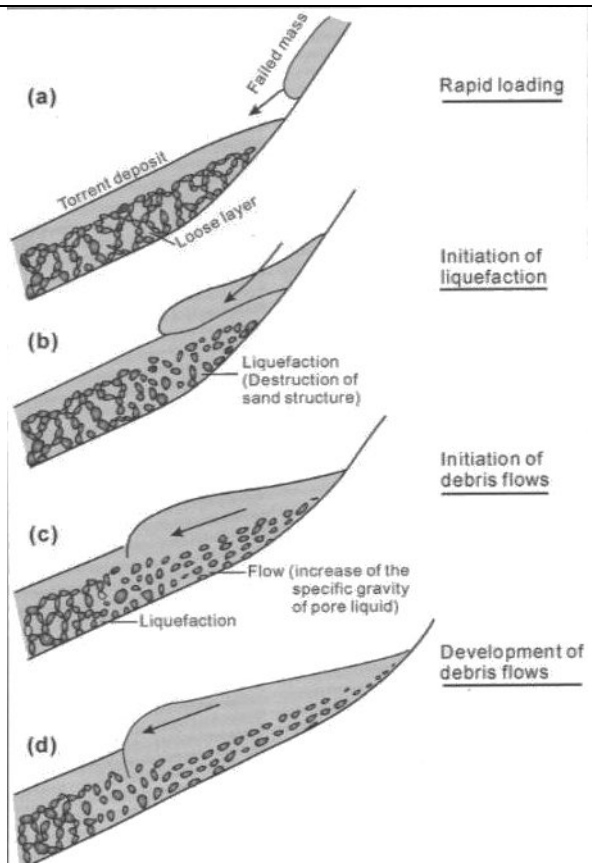
	Liquefaction failure phenomenon of torrent deposits may result in a debris flow. As described by [Sassa 1985] (***Figure 10***), torrent deposits with loose and unstable structure can collapse structurally under rapid loading, and the displaced debris mass becomes seated on a liquefied layer. The torrent deposit starts to flow, causing liquefaction at its front and increasing its volume. Similar mechanisms were proposed by Htchinson and Bhandari [1971], Tabata and Ichinose [1973] Costa and Williams [1984]. Liquefaction can take place in meta-stable granular soils. The collapse of the soil structure causes volume reduction and results in excess pore-water pressure generation. Liquefaction takes place only in soils with very loose meta-stable structure. On the other hand, sliding-surface liquefaction can take place in loose, medium, or even dense soils so long as grain crushing and the resulting volume reduction takes place under the given overburden pressure. When a landslide mass moves onto slope or torrent deposits, drained or undrained loading can be involved, and either liquefaction or sliding-surface liquefaction can occur.
	1.3.1 Channel type initiation (entrainment of bed material)
	The channel-type starting zone can broadly be divided into two subgroups [Rickenmann & Zimmermann, 1993]: (a) Rock gullies (couloirs) filled with debris. Both on the bed and on the sides it is rock that limits the erosion. In the high-alpine zones, these debris masses were often ice-covered some decades ago. In the Swiss Alps, typical gradients from 24° to 35° were observed. (b) Larger, temporary debris accumulations in a channel or gully are suddenly mobilized under increased runoff conditions. In the Swiss Alps, gradients from 3° to 33° were observed. Often the erosion is progressive and the starting volume is small compared to the overall event

	magnitude. For the channel-type debris-flow initiation, the shear stress by the flowing water (possibly mixed already with transported sediment) is an important factor for further material entrainment. At steep slopes close to the angle of repose of the bed material, the mechanisms mentioned for the slope-type initiation may additionally play a role, resulting in a more extensive (deeper reaching) bed destabilisation. If the mobilised bed material leads to volume solid concentrations of the flowing mixture higher than about 50 %, a rapid transformation into a debris will occur at steep slopes. A simple slope stability analysis predicts a theoretical limiting slope of about 12° to 17° for typical bed material properties (i.e. angle of repose from 33° to 37°) [Takahashi, 1987, Hungr et al. 2005] extend this approach to undrained conditions, and they also discuss field observations related to channel bed erosion by debris flows. According to laboratory experments by Tognacca et al. [2000], the critical slope for channel bed debris-flow initiation appears to depend on the water discharge and grain size; a thershold criterion similar to the threshold for bedload transport has been proposed. The influence of hydraulic conditions for bed destabilization and debris flow formation in channels are discussed by Papa et al. [2004], Armanini and Gregoretti [2005], Berti and Simoni [2005].
Other or combined mechanism	A temporary blocking of the solid and or water discharge in a stream channel may support the formation of debris flows. The blocking may be associated with pulsing bed load movement including coarse particles, and with channel constrictions, possibly favoured by woody debris. Alternatively, it may be caused by a sudden input of a large mass of solid material, either through a slope failure or by a debris flow from a tributary channel. Mountain torrents are often characterised by a very irregular channel morphology. Channel constrictions may be due to large boulders or bedrock outcrops. At such locations a temporary blockage of water and sediment flow may occur, possibly favoured by the presence of woody debris. The combination of woody debris and coarse particles is very effective in blocking a flow path, as is known from slit type outlet structures of sediment retention basins. Upstream of the temporary blockage, more sediment is accumulated until the pressure is sufficient to cause a collapse, suddenly releasing large quantities of sediment and water. Such a “dam-break” flow can transform into a debris flow. Glacial lake outburst floods (GLOF’s) are characterised by the release of large quantitites of water and much greater peak flows as compared to a rainfall-induced flood in the same catchment. Below moraine-dammed lakes there are often ideal conditions for the intitation of debris flows: steep gradients and and easily erodable material with a wide grain size distribution. Therefore, many of the largest debris flows observed in alpine environments are the result of glacial lake outburst floods [Haeberli, 1983].

Observation of an Alpine event	A debris flow event occurred in the Armancette torrent (Contamines-Montjoie, Haute-Savoie, France) on August 22, 2005. The event began at 5:00 pm with a first surge reaching the Bonnant river (valley bottom). The event, constituted of at least four surges, finished at 7:00 pm. The total volume of material deposited on the alluvial fan of the Armancette torrent ranges between 170 000 m^3 et 200 000 m^3. This event presented large similarities with a previous one which occurred in 1964. The deposited material contained a large fraction of boulders up to several meters in diameter. The slope of the deposited material was about 14%. The analysis of the grain size distribution of the deposit material led us to conclude that this debris flow is of granular type (after Bardou's [2002] classification). In fact, the material seemed to come essentially from moraines eroded by the flow along the torrent channel. Even though the rainfall in the valley has been moderate, one can suspect that at high elevation, the rainfall has been intense and maintained over a long time period of more than 24 hours. It is noticeable that during the same period, a large number of debris flows have been observed in Switzerland, mainly in Bernese Oberland. The Armancette catchment (***Figure 11***) elevation ranges from about 1200 m to 3400 m a.s.l., It covers about 7.5 km2 and its main channel develops over about 4 km.
Figure 11 overview of the Armancette catchment	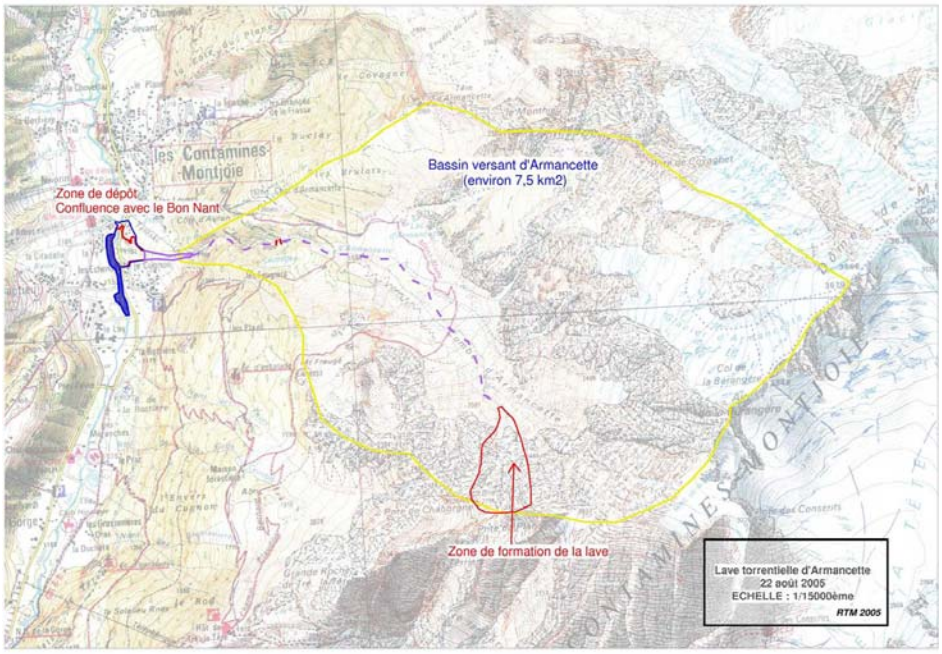
	Field observations of the August 22, 2005 event. The debris flow triggering area The debris flow triggering zone is located above 2000 m a.s.l. in a steep rocky face, below the pointe de Chaborgne. Several gullies present incisions about 5 m (***Figure 12***): - the central gully with a firn covered by blocks; - the western gully, with a S shape which has a junction with the previous one at elevetation 2050 m a.s.l.; probably also the eastern gully which has a junction with the central gully at elevation

	2150 m a.s.l. - The main channel at the bottom of the rocky face presents also traces of intense erosion.
Figure 12 Zone of debris flow triggering	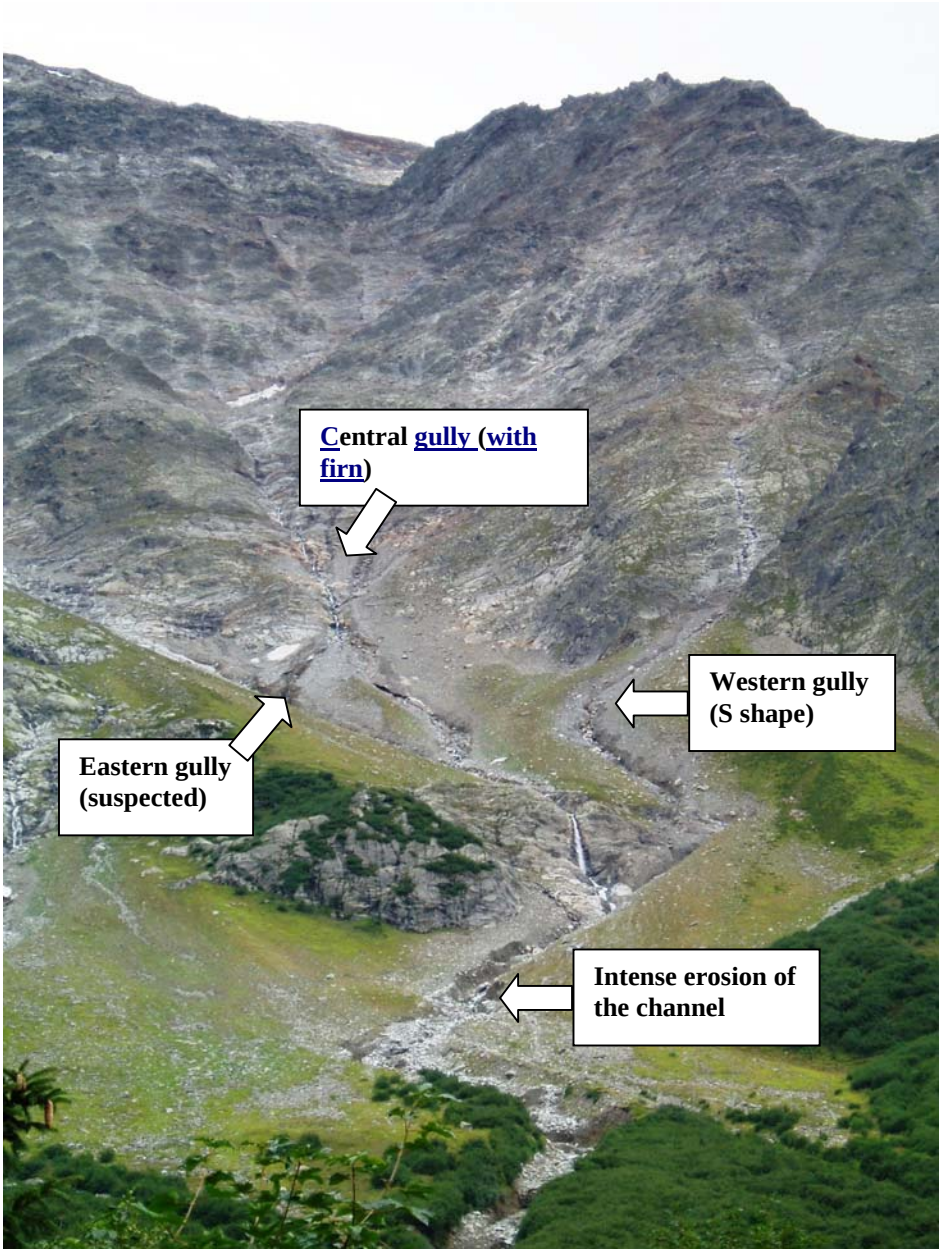
Comments:	General features of this triggering area are classically encountered. A steep rocky face, incised by gullies inside which weathered material is likely to accumulate by gravity and inside which intense rainfall concentrates, leading to some "fire-hose" effect is clearly favourable to debris flow triggering. However in the present case, material entrainment in these gullies has been able to provide a limited volume of material of a few thousands cubic meters (most probably less than 10000 to 20000 m^3), that is one or two orders of magnitude below the event magnitude. Furthermore, it is difficult to explain the intense channel erosion observed at the very bottom of the rocky face, which probably results from some intense flow over some previously saturated material.

The channelized area	Below the triggering area, down to the alluvial fan, develops the main channel of the Armancette torrent over a distance of about 4 km. In the upper part of this area form about 2000 m to 1500 m a.s.l, the channel takes place over a wide inclined plane of moraine deposits whose slope is about 35% in its upper part. The channel observed after the event is very deeply incised (about 10 m). This contrasts with its tributaries which seem to have very similar features (similar rocky faces dominating the moraine inclined plane) but are not incised (channel about 10 m wide and 1 m deep). Downstream this upper part, between about 1500 m and 1250 m a.s.l., the channel enter a forest area where lateral banks are steeper. Once again, over the all reach, the channel has very deeply incised its bed of 5 to 10 m and sometimes much more. In some place, although extremely high, the erosion has been limited by the bedrock which can then be seen completely cleaned up. Just before reaching the deposition zone on the alluvial fan, the channel has a slope about 20% and the flow cross-section according to traces has been estimated to 100 m^2. Along the whole channel, the soil is constituted of moraines or easily weathered formations like gypsum for example. In some places, the erosion could reach values as high as 150 to 200 m^3/m. Some more comments help to put this event into perspective: The most astonishing feature of the August 22, 2005 event in Armancette torrent is the intense erosion that occurred all along the channel. By a simple computation, the total volume of the event (about 200 000 m^3) corresponds to a mean erosion rate of 50 m^3/m over the 4 km of channel. Locally, this erosion rate can be as high as 150 à 200 m^3/m. In reference to the literature, [after Hungr et al. 1984] erosion rates higher than 30 m^3/m are generally observed only in zones of destructured moraines with steep, unstable channel banks generally more than 20 m high and presenting sliding areas. This is not the kind of "vision" we had a priori of the Armancette torrent which did not present evidence of high and generalized instability before the 2005 event. The only evidence of the capacity of the torrent to generate huge debris flows was in fact the historical reference to the 1964 event which had a similar volume of material and similar extension on the alluvial fan.
Conclusions	Even though not perfectly indentified, the triggering mechanisms of August 22, 2005 debris flow in the Armancette torrent seems to be quite classical (accumulation of weathered material in very steep gullies and "fire-hose" effect of the water flow in this gullies resulting from some high intensity of rainfall maintained over a long time period). The triggered volume explained by this phenomenon is however at least one order of magnitude below the volume of the whole event. The additional volume clearly originates from the huge erosion which took place all along the channel down to the alluvial fan. The mean erosion rate along this channel is extremely high compared to the geomorphological pieces of evidence observed in the field. It is noticeable that most probably an expert of torrential phenomena analysing the hydraulic and geomorphological features of the Armancette catchment before the August 22, 2005 would have concluded that such a scenario was very unlikely to occur. Only historical data proved the validity of such scenario.

Chapter 2

TRIGGERING OF ROCK AVALANCHES

2.1 Introduction

Introduction

Rock avalanches are extremely rapid (>10m/s) and large (>10^6 m^3) gravitational mass movements originating mainly from solid rock. During flow, they may entrain substantial amounts of soil, debris, water, and ice [Pierson and Janda 1994, Hungr and Evans 2004]. Rock avalanches that originate from volcanic edifices are generally termed debris avalanches, although much of the underlying dynamics and physics relating to the failure and flow process appear to be essentially the same.

We note that various velocity and size thresholds have been proposed [e.g. Hsü 1975], but retain the above definition for the sake of brevity. What all rock avalanches have in common is that the mass moves as a granular flow over an excess runout with respect to predictions of conventional friction physics. Therefore, the runout of rock avalanches is considerably larger than that of other extremely rapid mass movements such as snow avalanches and debris flows. The types of movement involved during rock avalanching may combine sliding, flowing, and occasionally, free fall [e.g. Keefer 1999].

The occurrence of rock avalanches depends on several causes, triggers, and critical thresholds that are closely linked to geotechnical rock-slope stability, and which will be summarised below. It is important to realise that most of these dispositional and triggering factors may also condition other large rock-slope failures such as rockfall or slow deep-seated rock-mass deformation (sackung, creep, etc.); yet in most cases they are also applicable to catastrophic rock avalanches. The actual transition from an initial rock slide or fall to a long-runout rock avalanche takes place a short time after the

initial onset of motion, i.e. after a given rock slope has succumbed to catastrophic failure [e.g. Davies et al. 2006]. Likewise, rock avalanches may subsequently transform into debris flows [e.g. Vallance and Scott 1997, Evans et al. 2001, Capra et al. 2002], thus representing only one phase during a complex and extremely rapid mass-movement event.

2.2 Causes

The underlying factors that serve as preconditions for rock-slope instability are variably (and synonymously) termed causes, causative factors, disposition, or dispositional factors. It is useful to further distinguish between a basic and variable disposition.

Basic dispositional factors include those that are invariant over longer, usually geological, time periods, such as e.g. large-scale topography, tectonics, lithology, faulting and jointing pattern.

Variable dispositional factors generally describe short-term fluctuations around these basic conditions, and include, for example, pore-water pressure fluctuations, dynamic loads, fluvial undercutting, etc. the superposition of variable disposition and basic disposition allows the attainment of critical conditions that may contribute the ratio between shear strength and shear stresses in a rock slope. Variable dispositional factors may also be of volcanic origin, and include hydrothermal alteration, or flank steepening through magma chamber growth or degassing.

These critical conditions are commonly marked by the force or limit equlibrium between shear strength and shear stresses, at which a rock slope is considered to be metastable. Attaining this critical threshold typically requires a triggering mechanism that provides the necessary additional force input (also termed “loading”), which serves to either reduce the slope shear strength or increase the shear stresses.

2.2.1 Topographic conditions

Topography is generally considered a first-order control on rock-slope stability, at least under static conditions. Hillslope height is a proxy of the potential energy of a rock slope per unit width, whereas hillslope angle modulates gravitational forces, and thus, shear stresses acting on the slope. Valley cross-sectional shape further controls the development of topographically-induced stress fields [Augustinus 1995]. For example, it has been argued that glacially carved trough valleys may concentrate tensile stresses near toes of hillslopes, thus preconditioning rock slopes to large failures.

Hence, some of the key parameters for quantitatively describing topographic

susceptibility to catastrophic rock-slope failure include hillslope height and mean hillslope angle [Selby 1992, Schmidt and Montgomery 1995, Korup et al., in press]. These parameters are contained in the Culmann wedge-failure criterion for dry soil cliffs, which is one of the simplest approximations to geotechnical slope stability. Schmidt and Montgomery [1995] argued that, at the landscape scale, hillslope relief is limited by either rock-mass strength or fluvial incision, and used the Culmann criterion to derive the maximum stable hillslope height H_c,

$$H_c = \frac{4c \sin\beta \cos\phi}{\gamma_r \left[1 - \cos(\beta - \phi)\right]}, \qquad (1)$$

where c is cohesion, β is mean hillslope angle, ϕ is the angle of internal friction, and γ_r is the mean unit weight of the slope material.

Long-runout rock and debris avalanches make up about two-third of the largest terrarestrial landslides on Earth, and may mobilise volumes of up to 10^{10} m^3 in, geologically speaking, instanteous time [Korup et al., in press]. The influence of topography on the occurrence of rock avalanches, however, is seldomly constrained quantitatively, and supported by only scattered empirical observations throughout the world. This is complicated by the fact that large rock-slope failures, including rock avalanches, leave locally much more profound geomorphic imprints on the landscape than do smaller landslides. In many cases, rock avalanches have considerably reduced local hillslope height and hillslope angles, often to a degree that does not allow a reliable reconstruction of the pre-failure topography [Korup, 2006].

Figure 13 Topography of the source area of the 1984 rock avalanche at head of Avalanche Creek, Canada [Evans et al. 2001]. In this example, pre-failure topography could be reasonably well reconstructed.

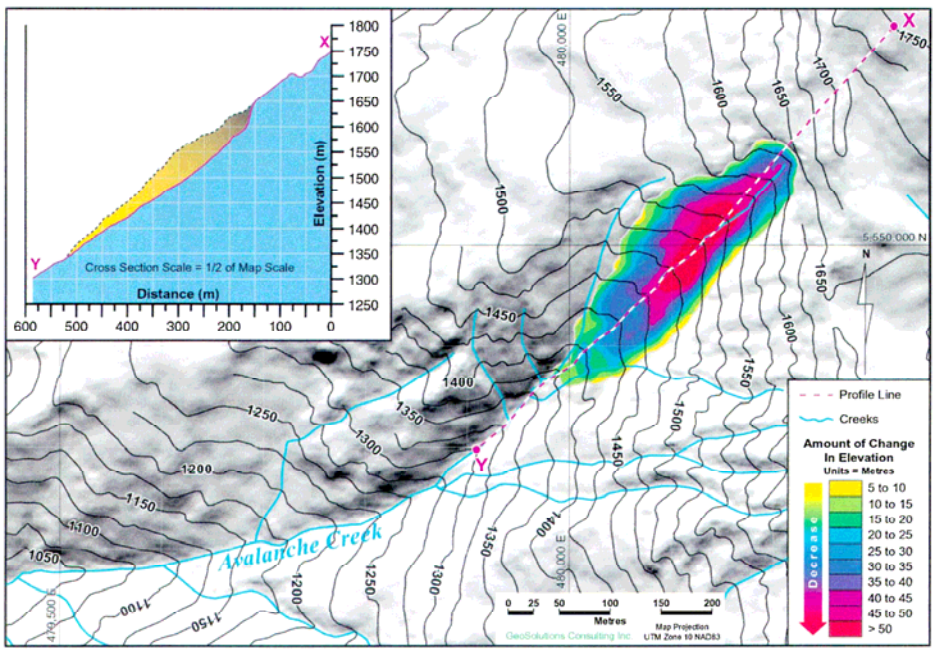

This observation also holds for large debris avalanches, which often remove large parts of the volcanic edifice, leaving a conspicuous amphitheatre-shaped detachment area

[Wadge et al. 1995]. Hence, the topographic constraints on the occurrence of large rock and debris avalanches often have to be estimated from adjacent hillslopes that remained stable, thus containing an unquantifiable degree of error. Moreover, in the case of volcanic edifices, topography may be regenerated by intrusion of magatic bodies, thus raising the potential for episodic recurrence of large debris avalanches [Beget and Kienle 1992] that may successively obliterate the detachment geometries of preceding events.

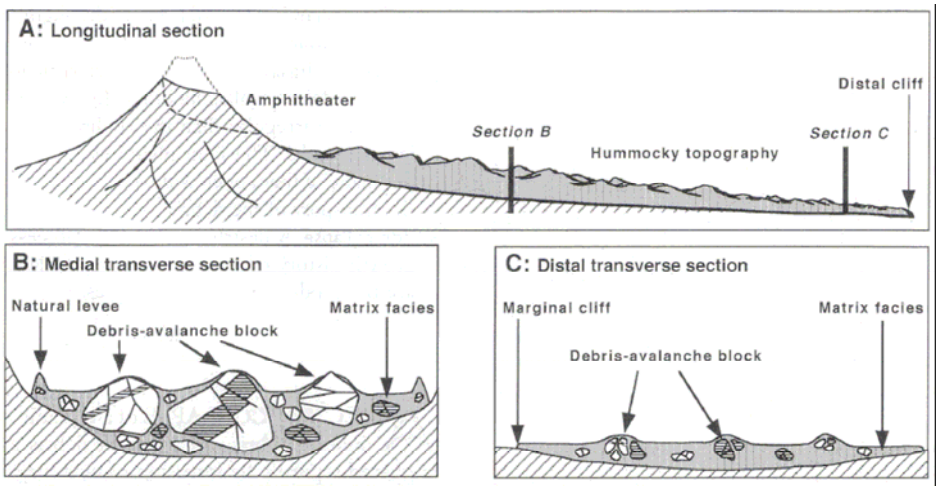

Figure 14 Schematic section for a debris avalanche deposit: (A) longitudinal section stretching from the source amphitheater to the distal end; (B) transverse section of the medial region; (C) transverse section for the distal region. Size of hummocks gradually decreases toward the distal area. Debris-avalanch blocks are smaller and scarce at the distal area [Ui et al. 2000].

Some of these observations come from landslide-triggering earthquake episodes. Under these conditions of additional dynamic loading, the slopes where rock avalanches have occurred have had vertical heights of at least 150 m [Keefer 1984]. The hillslope angles may vary between 25° and 40°, whereas higher inclinations did not seem to be conducive to rock avalanching [Keefer 1984]. These values were empirically derived for a sample of about only 100 rock avalanches triggered during 40 earthquakes [Keefer 1984], and half of the rock avalanches were triggered in one single event, i.e. the M = 9.2 Alaska earthquale in 1964. Therefore, these topographical constraints are preliminary at best, and should under no circumstances be assumed as representative for a given site.

Sufficiently hillslope heights and hillslope angles are generally present only in alpine regions, in deeply cut and former glaciated valleys, as well as on volcanic edifices. Indeed, essentially all of the earthquake-triggered rock avalanches documented by Keefer [1999] appear to have been uncercut by channel erosion or recent glacial activity. Investigating several extremely large (> 10^9 m^3) rock avalanches in the Tien Shan mountains of Central Asia, Strom and Korup [2006] found little evidence of a topographic control on their distribution, which they argued was more closely tied to the pattern of active tectonic faults in the region.

However, Korup et al. [in press] showed that large rock avalanches are not exclusively restricted to formerly glaciated terrain. This partly undermines the notion that the occurrence of large and catastrophic rock avalanches would mainly be manifest as a response to deglaciation [e.g. Seijmonsbergen et al. 2005, Wilson and Smith 2006]. Korup et al. [in press] also demonstrated that, at the mountain-belt scale, a high local relief (defined on a ~0.9-km resolution grid as the maximum difference in elevation

	within a 5-km radius) was a sufficient, but not necessary, condition for large rock avalanches. They found that most of the rock avalanches with volumes >10^9 m^3 have occurred in areas with mean local relief >1 km, which makes up less than 5% of the Earth's surface. In volcanic arcs, such as southeast Kamchatka, this not surprising, as debris avalanches are limited to individual volcanic edifices that contain most of the regional relief within a very small fraction of the landscape. However, rock avalanches are known to have occurred in areas of comparatively low relief, such as the British Isles or the Scandinavian mountain belts, during postglacial times [e.g. Jarman 2002, Ballantyne and Stone 2004, Wilson and Smith 2006]. Volcanic edifices also provide some of the highest local terrestrial relief together with steep hillslope inclinations. Notably, some of the largest terrestrial rock (debris) avalanches, measured by volume, drop height, or runout, have originated from large volcanoes [e.g. Stoopes and Sheridan 1992, Reid et al. 2001, Ponomareva et al. 2006].

Figure 15 Slope angle vs. slope height for rock avalanche sites (TOPO LS) and adjacent hillslopes (TOPO NON LS), derived from GTOPO30 DEM.

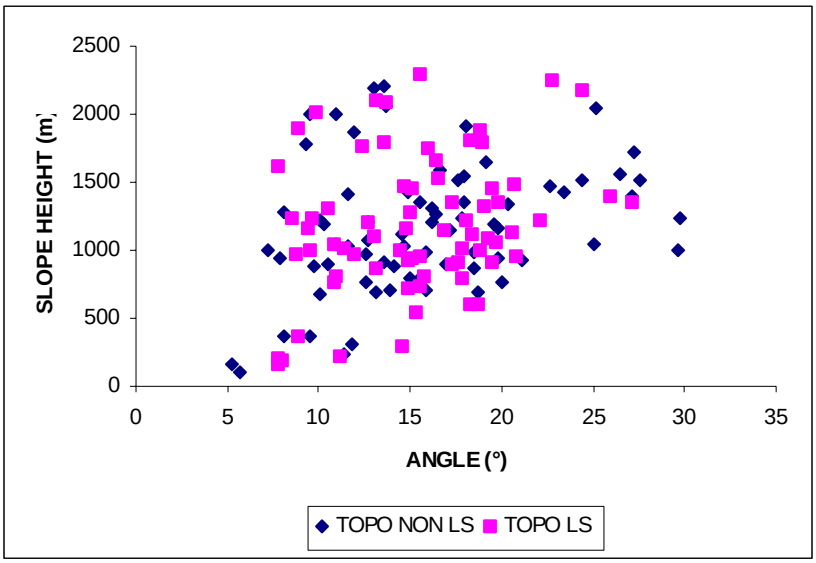

The topographic conditions at rock-avalanche sites in the European Alps vary greatly. The values of local relief (measured as maximum elevation difference within a 10-km raster window) where rock avalanches may occur ranges between 1000 and 2600 m whereas the hillslopes on which rock avalanches occur have a relief of about 100 to 2300 m and lengths between 1 and 12 km. The slope angles of rock avalanche sites vary between 5 and 30°, but without a significant difference between rock avalanche sites and adjacent "undisturbed" slopes. The mean direction into which rock avalanches in the Alps do fail is more or less south oriented with a mean of about 137°.

Figure 16 Aspect of rock avalanche scar areas in the European Alps

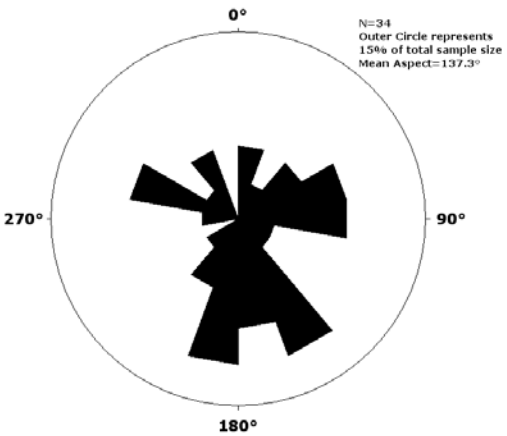

In the Norwegian Caledonides, for example, massive rock-slope failures that transformed into rock avalanches are preferentially located along steep and often sub-

	vertical fjord walls [Bjerrum and Jørstad 1968, Braathen et al. 2004].
	2.2.2 Geological conditions
	From a worldwide perspective, rock avalanches may occur in all major rock types [Korup et al. in press]. At a regional scale, however, the tectonic, seismic, geologic history puts many more constraints on their distribution. Rock-mass conditions are a major local control on the occurrence of rock avalanches. It is generally recognised that laboratory-derived measurements on small intact rock samples overestimated the strength of rock masses at the hillslope scale. This is because of scale effects and the neglectance of three-dimensional fracturing and faulting patterns throughout the hillslope, let alone ambient and dynamic cleft-water pressures. Also, laboratory samples do not reflect properties of fracture fillings such as clay-rich fault gouges or weak cementing materials. Consequently, research on rock-slope stability has partly focused on determining the total rock-mass strength that combines material strength with properties of discontinuities [e.g. Selby 1992, Watters et al. 2000]. Moreover, there are few quantitative data as to ascertain as to whether rock avalanches would preferentially occur in weak or strong rocks. This is because weak rocks are assumed to fail more readily and more frequently, thus not favouring the sudden detachment of very large rock masses. Keefer [1999] notes that most earthquake-triggered rock avalanches occurred in well-indurated, but intensely fractured, rocks. Rocks on both active and extinct volcanic slopes may show distinctive variations in degree of consolidation, fracturing, hydrothermal alteration, as well as water and clay content [e.g. Friele and Clague 2004, Carrasco-Nunez et al. 2006, Opfergelt et al. 2006]. In the European Alps, for example, sedimentary rock appears to show higher susceptibility to rock avalanching than metamorphic or volcanic rocks(***Figure 18***). This is visible in the density distribution of rock avalanches, where the highest densities are apparent in areas with a) sediment rock, which is b) not or only little experienced with metamorphosis (***Figure 18***).

Figure 17 Density distribution of rock avalanches in the European Alps (from Veit 2002)

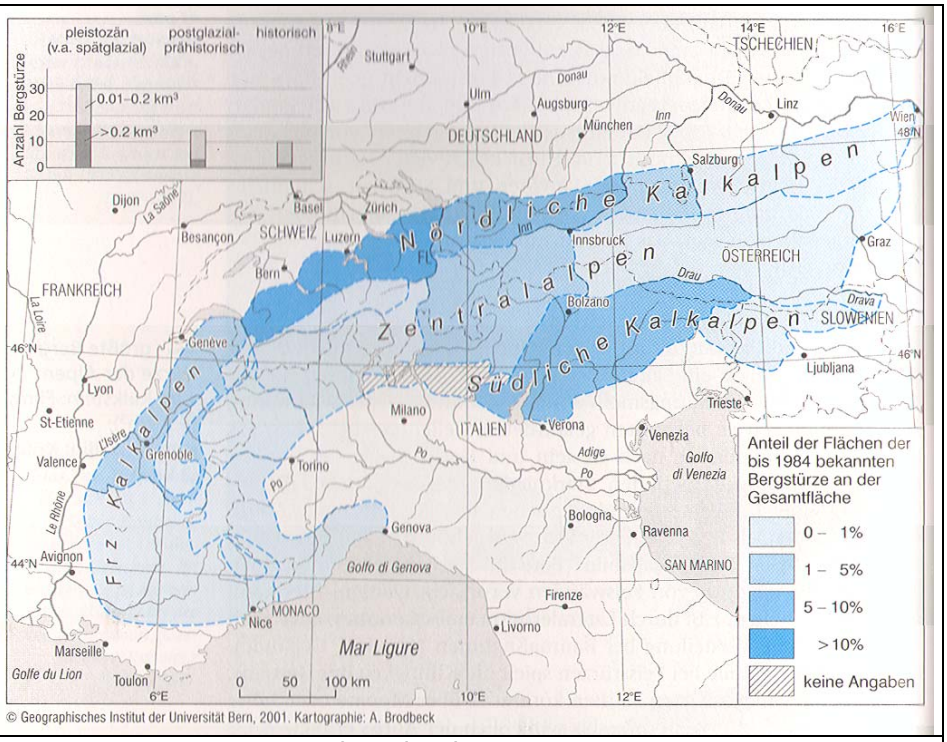

Table 6 Main geologic formations in the European Alps, their area, their rock avalanche occurrence and the distribution of rock avalanches per km² in every formation

Geologic Formation	Rock avalanches per geologic formation	Area of geologic formation km²	Rock avalanches per km²
Austroalpine Cover	9	18223	0.00049
South Alpine Basement	19	46009	0.00041
Tauern Window	3	5672	0.00053
South Alpine Cover	18	22795	0.00079
Penninicum	22	30792	0.00071
Helveticum	28	37055	0.00076
Northern Molasse	3	15885	0.00019
Prealps	1	2018	0.00050
Aar Massif	0	527	0.00000
Gotthard Massif	0	163	0.00000

Figure 18 Rock type affected by rock avalanches in the European Alps	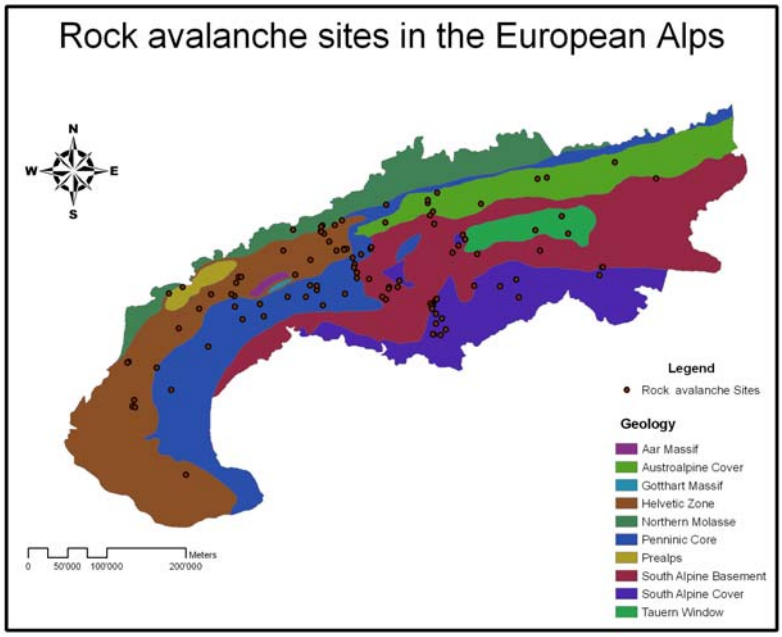
	A major dispositional factor for rock avalanches is the orientation (i.e. dipping and striking) of geologic boundaries and discontinuities, antecedent shear or fracturing conditions, or folding driven by gravitational spreading [Evans et al. 1994, Schramm et al. 1998, de Vries et al. 2001, Friedmann et al. 2003, Weidinger 2006]. This role of hillslope-scale discontinuities in compromising rock-slope stability is indicated by the fact that less fractured, but weakly cemented, rocks also gave rise to catastrophic rock avalanches. In certain cases, ore mineralisation may contribute to large-scale rock-slope instabilities [Weidinger et al. 1996, Weidinger et al. 2002].
Figure 19 View from Manang Valley, Nepal Himalaya, towards the south-dipping beds (s) on the southernmost flanks of Manang Himal (6058 m, mh)—the pre-existing structure and sliding surface (-.-.-) for the mountain collapse; md=direction of movement, ld=rockslide material of Braga (- - -), gf=glacio-fluvial gravel in the foreground; standing point: 4 km NW of Pisang, alt. 3280 m, view towards NW [Weidinger 2006].	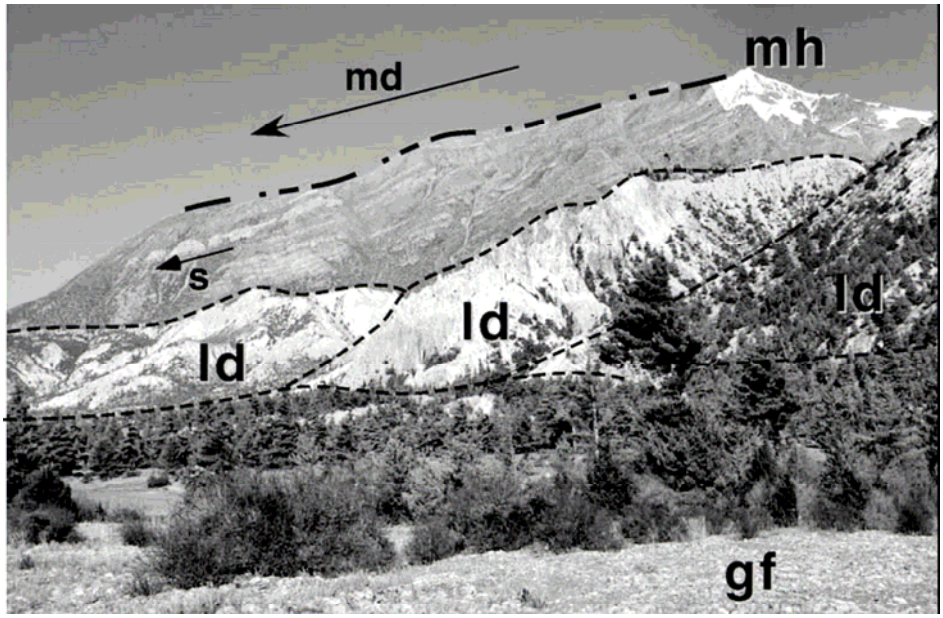
	Daylighting of failure planes in the slope faces appears to be a general prerequisite for rock avalanching, and many rock avalanches are known to have occurred on dip slopes

	in sedimentary rocks [e.g. Chigira et al. 2003]. It is notable that, where geological preconditions remain somewhat constant, reactivations in the form of successive rock avalanches at a given site may occur [e.g. Shang et al. 2003]. One of the most well known examples is that of Tsaoling, Taiwan, where four major (10^7 to 10^8 m^3) rock avalanches occurred repeatedly on sedimentary dip slopes during the 20th century [Chigira et al. 2003]. In any case, the kinematic conditions, i.e. the geometric arrangement of slope face and rock-mass discontinuities along which failure may occur, to trigger a rock avalanche need to be satisfied. It is important to realise that rock avalanches may occur as a direct consequence of a variety of rock-slope failure modes including rock fall, rock topple, or rock sliding (including wegde failures).
Rock-mass discontinuities and deterministic failure models	Many deterministic limit-equilibrium models of rock-slope stability are assuming pre-existing discontinuities, which are treated using simplified internal and external hillslope geometries, which may be adjusted for local oversteepening by either fluvial, glacial, or anthropogenic undercutting.
Figure 20 Simple mechanistic model of trapezoidal rock-block failure along well-defined discontinuities. No seismic or external forces are considered. Parameters are described in the text.	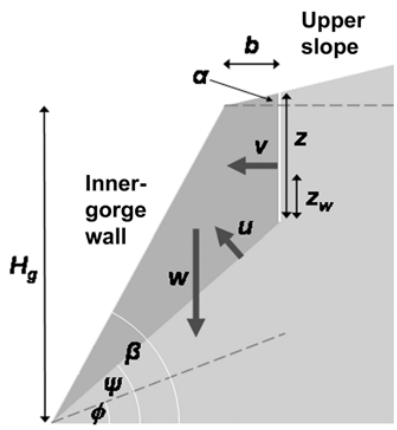
	The simplest models thus assume planar sliding of a trapezoidal block below a vertical tension crack (Fig.). The ratio of hillslope strength to effective shear stress is expressed as $$F_S = \frac{c' A_s + (w\cos\psi - u - v\sin\psi)\tan\phi}{(w\sin\psi + v\cos\psi)}, \quad (2)$$ where F_S is the Factor of Safety, c' is the cohesive strength of the failure plane, A_s is the area of the failure plane, ψ is the angle of the failure plane, w is the weight of the rock block above the failure plane, u is the uplifting water force along the failure plane, and v is the driving water force along the tension crack [e.g. Wyllie and Mah 2004]. Equation (2) can be written in dimensionless groups as

$$F_S = \frac{\frac{2c'}{\gamma_r H_g} p + \left(\frac{q}{\tan\psi} - r(p+s) \right) \tan\phi}{q + \frac{rs}{\tan\psi}}, \tag{3}$$

with

$$p = \frac{\frac{1}{\tan\beta} + x}{\cos\psi}, \tag{4}$$

$$r = \frac{\gamma_w}{\gamma_r} \frac{z_w}{z} \frac{z}{H_g}, \tag{5}$$

$$s = \frac{z_w}{z} \frac{z}{H_g} \sin\psi, \tag{6}$$

$$x = \frac{b}{H_g}, \tag{7}$$

$$y = 1 - \frac{\tan\psi}{\tan\beta}, \text{ and} \tag{8}$$

$$q = \left(\frac{y}{\tan\beta} + 2xy + x^2(\tan\alpha - \tan\psi) \right) \sin\psi, \tag{9}$$

where γ_w is the unit weight of water, z is the depth of the vertical tension crack, z_w is the depth of water in the tension crack, H_g is the height of the inner-gorge wall, b is the horizontal distance of the crack from the crest of the gorge wall, and α is the slope angle of the upper hillslope (Fig.). For cohesionless slopes ($c' = 0$), stability therefore depends only on slope geometry, but not on slope size. This makes this slope-stability model applicable to small block slides as well as large slope-clearing failures such as rock avalanches. For all other cases, one can expect F_S to decrease nonlinearly with slope height H_g, for a given slope geometry.

These simple deterministic models allow inclusion of transient loading due to cleft-water pressures along the tension crack and the potential sliding plane. Another advantage of the trapezoidal model is that it states a general form of a series of special cases for which the critical hillslope height H_c at limit equilibrium (i.e. $F_S = 1$) may be derived. For example, we find that, for shallow failures on a fully drained slope (z, $b \rightarrow 0$),

$$\lim_{z,b\to 0} H_c = \frac{2c'}{\gamma_r \sin\psi \cos\psi \left(1-\frac{\tan\psi}{\tan\beta}\right)\left(1-\frac{\tan\phi}{\tan\psi}\right)} . \quad (10)$$

This special case is equal to the expression for planar rock slides on a dip slope where $\psi < \beta$ [Selby 1992],

$$H_c = \frac{2c'\sin\beta}{\gamma_r \sin(\beta-\psi)(\sin\psi - \cos\psi \tan\phi)} . \quad (11)$$

Simplifying further for the limit case of a fully drained vertical gorge wall with daylighting potential failure planes [e.g. Cruden 1976], where $\beta = 90°$, and $\alpha = \psi$, one obtains

$$H_c = \frac{2c'}{\gamma_r \cos\psi(\sin\psi - \cos\psi \tan\phi)} \quad (12)$$

as a simple model of parallel slope retreat.

In practice, values of ψ are usually difficult to predict. However, the angle of the critical failure plane ψ_c in a dry rock slope can be approximated by computing for which value of ψ limit equilibrium is most readily reached, i.e. setting $\partial F_S/\partial\psi = 0$ in Equation (2) [*Wyllie and Mah*, 2004], thus obtaining

$$\psi_c = \frac{1}{2}(\beta + \phi) . \quad (13)$$

Substitution of Equation (13) into Equation (11) produces results very similar to those of the Culmann method (Equation 1), where values of *c'* are low.

Planar rock-slope failures described by these equations require tight geometric (also termed "kinematic") preconditions [Wyllie and Mah 2004]. These will not be met ubiquituously in nature, particularly where rock parcels detach by other mechanisms such as fall, topple, rotational sliding, or along two intersecting sliding planes. Factors of Safety for more common wedge failures are usually higher than those predicted by Equation (2) by a wedge-shape factor κ_w, assuming that ϕ and ψ are equal for both failure planes. Wyllie and Mah [2004] suggest that $1 < \kappa_w < 5$ for most cases. They argue that, for $F_{Sw} > 2$, dry cohesionless rock slopes are generally stable over a wide range of

dynamic loading conditions. Therefore, Equation (2) is a practical and conservative first-order approximation of a variety of failure scenarios. For site-specific calculations of rock-slope stability with well known rock-mass properties, more sophisticated numerical methods are commonly used [e.g. Crosta et al. 2003].

In the Norwegian fjords, Braathen et al. [2004] found that rockslide/avalanche detachment areas often formed on "moderately dipping slopes, where slope-parallel, basal sliding planes, or detachments (along foliation, exfoliation surfaces), bound unstable rocks". Foliated metamorphic and metasedimentary rocks are especially prone to develop major potential failure planes.

Figure 21 Detachment scars of the Tafjord and Loen rockslide/rock avalanches, Norway, and their relationship to foliation (exposed): (A) Langhammaren at Tafjord. The slide scar extents to ~800 m above sea level; (B) Ramnefjell at Loen. The upper part of the scarp is about 900 m above the local lake level [Hermanns et al. 2006].

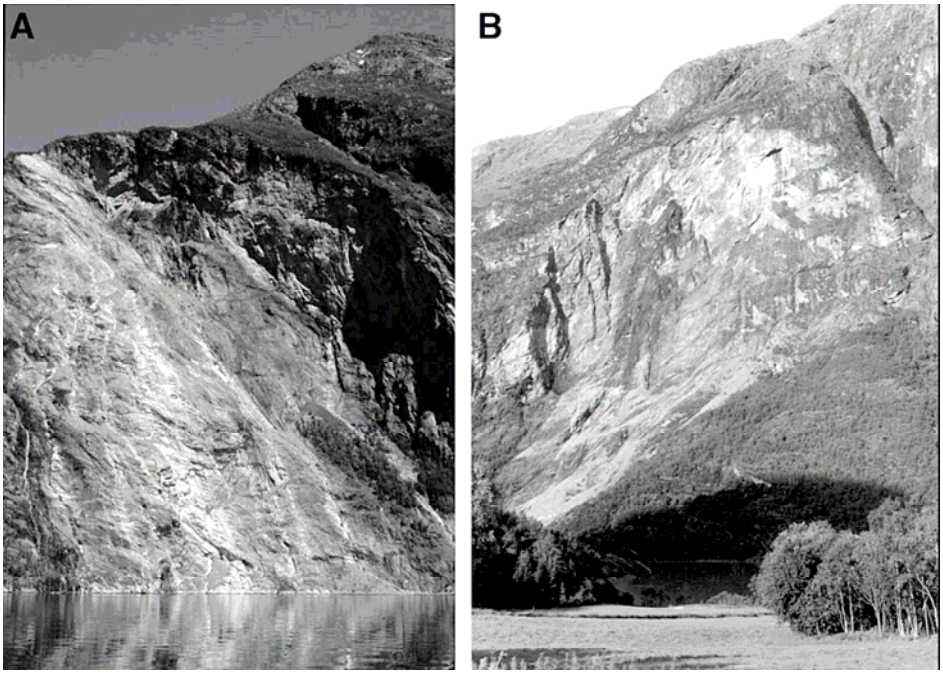

However, failure plane development along major schistosity planes (in pelitic schists, phyllites, etc.) often leads to low-velocity displacement of substantial rock masses (rock-mass creep). Despite the large amounts of rock mass involved, catastrophic long-runout rock avalanches do not develop as a necessary consequence. In other words, unstable rock slopes conditioned by dipping failures planes do not provide unequivocal conditions for rapid failure. Rock-mass creep [Chigira 1992, Chigira and Kiho 1994] creates folds, faults, and fractures, thereby contributing to reducing rock-slope stability. Using a combination of remote sensing interpretation and field work, Chigira and Kiho [1994] demonstrated that deep-seated rock-mass creep preceded at least seven large rockslide-avalanches in Japan. Although deep-seated rock-mass creep is well documented in the European Alps, very few comparable investigations there have been addressed the potential for catastrophic culmination in rock avalanching.

2.2.3 Tectonic preconditions

By tectonic preconditions we understand deformation of rocks at a scale that is larger

	than that of the individual hillslope. This in contrast to small-scale deformation that occurs in response to local shear planes, lithological discontinuities, and hillslope geometry, i.e. controls not necessarily related to the regional stress fields. However, reactivation of basement faults below volcanic edifices has recently been suggested as a cause of catastrophic flank collapse and release of large debris avalanches [Vidal and Merle 2000]. The tectonic forces working on bedrock are a major dispositional factor, as rock is weakened by faults, while ongoing fracturing also may change water infiltration and drainage. Tectonic fault-zone weakening along fault-bounded mountain ranges also seems to favour the occurrence of large rock avalanches originating from mainly cataclastic rocks and running out onto unconfined mountain forelands. Examples of large rock avalanches along thrust-bounded mountain fronts are known from the Puna Plateau in Northwestern Argentina, the northern Pamir-Tien Shan, and the Southern Alps in New Zealand [Hermanns and Strecker 1999; Strecker et al. 2003; Korup 2004]. It has been suggested that a combination of catastaclasis during fault movement, hanging-wall shattering, and hydrothermal alteration of the rock mass may contribute to reducing rock-mass strength in these settings. A recent example is the disastrous 2006 Leyte rock avalanche, which initiated along a weakened segment of the active Philippine Fault that experienced strike-slip motion of up to 25 mm/yr [Evans et al. 2007].

Figure 22 (A) Oblique aerial view (to the northwest) of Guinsaugon landslide, Leyte Island, Philippines, February 2006. (U.S. Navy photograph by M.D. Kennedy). (B) View of debris toward the source area of the rockslide-debris avalanche, March 2006 [Evans et al. 2007].	
	For example, the Goldau rock avalanche, Swiss Alps, announced itself weeks before the actual event by smaller rockfalls, cracking and building of fractures in the slope surface. These fractures increased in size until catastrophic failure took place. Notably, conspicuous weak planes, e.g. master joints, faults, bedding planes or foliation surfaces were dipping out of the slope. There exist some examples where tectonic faults are assumed to be the main dispositional factor for rock avalanches. The Haiming rock avalanche in Austria at the confluence of the Ötz and Inn rivers is such an example. Here the displaced mass is previously disaggregated and failed with a shear plane built of a fault [Abele 1974].
	2.2.4 Climatic preconditions
	Rock avalanches are documented from all major climatic zones throughout the world. It is generally accepted that climate controls rock-slope stability through effects of weathering, water infiltration, and groundwater conditions.

Long-term climatic causes: glaciation and deglaciation	One of the most immediate, if not most cited, examples of climate as a precondition of large-scale rock-slope stability is the remaining effect of Pleistocene glaciations [e.g. Smith 2001, Wilson and Smith 2006]. Glacial oversteepening of rock walls, and subsequent debuttressing during deglaciation is often invoked as an important precondition for large and catastrophic rock avalanches. Several models have been proposed that argue for an increased rock-slope failure response immediately after deglaciation. However, recent advances in geochronological methods provide increasing evidence that rock avalanches continue to occur well beyond the Last Glacial Maximum. This does not necessarily imply that glacier fluctuations are irrelevant for the occurrence of rock avalanches. The most pronounced, if not singular, cluster of large rock avalanches on Earth, both in terms of spatial density and total volume, occurs in the deeply incised valleys of the upper Indus River basin, Karakoram Himalayas, where locally hillslope height exceeds 4 km. There the Indus River cuts through the rapidly uplifting Nanga Parbat-Haramosh Massif, and local relief is as much as 7.2 km from the channel bed to the highest summit, over a distance of about 21 km. However, the highest part of the detachment zones of the rock avalanches identified to date lie below 4000 m a.s.l., and one-third are below 3500 m a.s.l. In other words, they derive from slope segments, spurs, or minor interfluves with much less than the total relief available in the region. This observation supports the notion that most of these rock-slope failures discovered to date descended into ice-free but formerly glaciated river valleys and originated on rock walls oversteepened by glaciers [e.g. Hewitt 1998, Hewitt 2001]. Moreover, Neoglacial advances may indeed by linked to some catastrophic rock avalanches [e.g. Evans and Clague 1994, Holm et al. 2004, Deline 2005], although further supporting evidence will be necessary to strengthen these causal links. For example, Holm et al. [2004] demonstrated that in southwestern British Columbia, Canada, bedrock landslide response to glacial retreat varies appreciably according to lithology and the extent of glacial scour below glacial trimlines dating to the Little Ice Age. Valleys carved in weak Quaternary volcanics show significant erosional oversteepening and contain deep-seated slope movement features, active rock fall, rock slides, and especially rock avalanches near glacial trimlines, whereas harder granitic rocks showed lesser slope-failure response. Capra [2006] noted that during the past 30,000 years major volcanic flank collapses occurred during rapid deglaciation in the wake of peak glacier stands, and argued that a combination of "glacial debuttressing, load discharge, and fluid circulation coupled with the post-glacial increase in humidity and heavy rains" may have contributed to major slope instability on volcanic flanks. Such and similar inferences about the influence of past climate change on the occurrence of rock avalanches are, however, dependent on • sufficient resolution and correlation of geochronological dating methods [e.g. Bull and Brandon 1998];

	• reliable palaeoclimatic records; • appropriate geotechnical back analyses that help discard other potential causes and triggers of rock avalanches; as well as • complete coverage of large debris avalanches. A major problem of unequivocally linking prehistoric climate change with rock-avalanche activity is that seismic ground shaking during large earthquakes must be excluded [e.g. Schuster et al. 2000]. This trigger mechanism may also trigger several coeval rock avalanches, which geochronological dating techniques may not resolve sufficiently, thus leaving the potential for misinterpretations as climate-driven slope instability. Therefore any hypothesis of climate-triggered rock avalanches must discard a palaeoseismic origin. In turn, however, any earthquake trigger also needs to be supported by such evidence as proximity to active faults, occurrence of modern analogues, limiting equilibrium back analyses and demonstrated synchroneity of failure with fault rupture [Crozier et al. 1995].
Figure 23 Graphical representation of exhaustion model of the timing of rock slope failure following deglaciation (Ballantyne 2002).	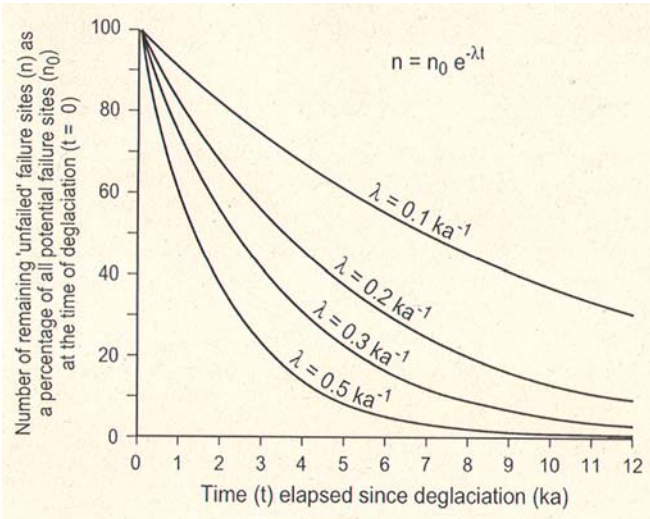
	The temporal post-glacial distribution of rock avalanche occurrence stands in contrast to recent models of total potential sites of rock slope failures after deglaciation. These models propose a high frequency and/or magnitude of rock slope failures “directly” after last deglaciation and a decline of these high frequency and/or magnitude in time, whereas the intensity of this reduction in magnitude and/or frequency may vary.

Short-term causes: climatic variability	Several authors suggested that short-term climatic variability may exert strong control on rock-slope stability. Though alpine regions experience large variabilities in rock surface temperature, the Alps are exposed to intense solar radiation and to temperatures varying from over 30°C until to -40°C. The diurnal, seasonal, and annual freeze-thaw cycles contribute to the development of near-surface fracturing, thus mainly affecting shallow rock-slope stability such as rock fall processes. Where fractures reach deeper into the rock mass, though, freeze-thaw cycles may play a more important role in affecting large-scale slope stability. This may include frost wedging effects [Braathen et al. 2004] or blocking of subsurface drainage by ice lenses, as well as increased meltwater infiltration. However, few studies have attempted to quantify such physical links.
Figure 24 Rock avalanche occurrence set into relation to glacial and climatic variability of the last 14kyr (Gruner 2006)	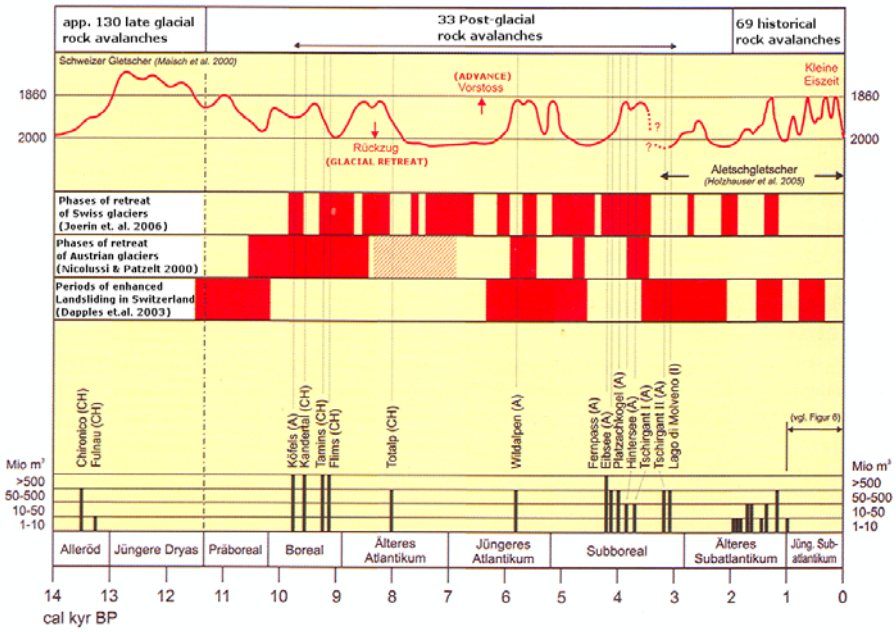
Figure 25 Rock avalanche occurrence set into relation to glacial and climatic variability of the last 1kyr (Gruner 2006)	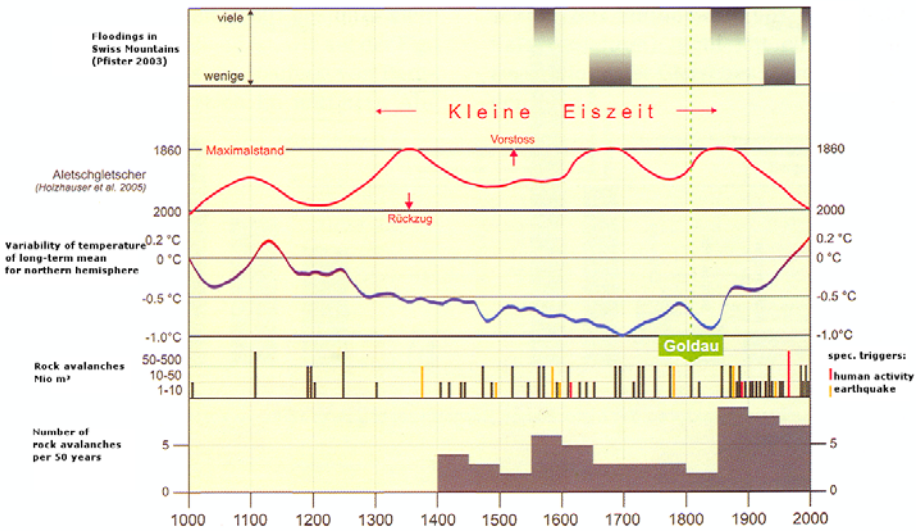

Permafrost in alpine and high-latitude regions is another thermal phenomenon that is thought to directly affect slope stability by added apparent cohesion of the rock mass [e.g. Shang et al. 2003]. Permafrost characteristics and their direct influence on rock-slope stability are notorituosly difficult to quantify, and there exists few compelling evidence that relates rock avalanching to degradation of perennial ground ice. Therefore, although physical links may seem plausible, they also remain speculative [e.g. Bottino et al. 2002], and require further proof.

The local and regional pattern, and type, of precipitation (Fig.) is another important factor of variable disposition, as it exerts a prime control on infiltration rates and cleaft-water pressures. Rainfall intensity and duration, however, vary significantly in mountainous regions, and can be very localised, i.e. affecting single catchments. However, there are few studies that have explicitly linked precipitation as a caustive factor of rock avalanches. Long-term records of precipitation are needed to better assess its role in affecting rock avalanching.

Figure 26 Distribution of rock avalanches and high precipitation areas in the European Alps (Gruner 2006)

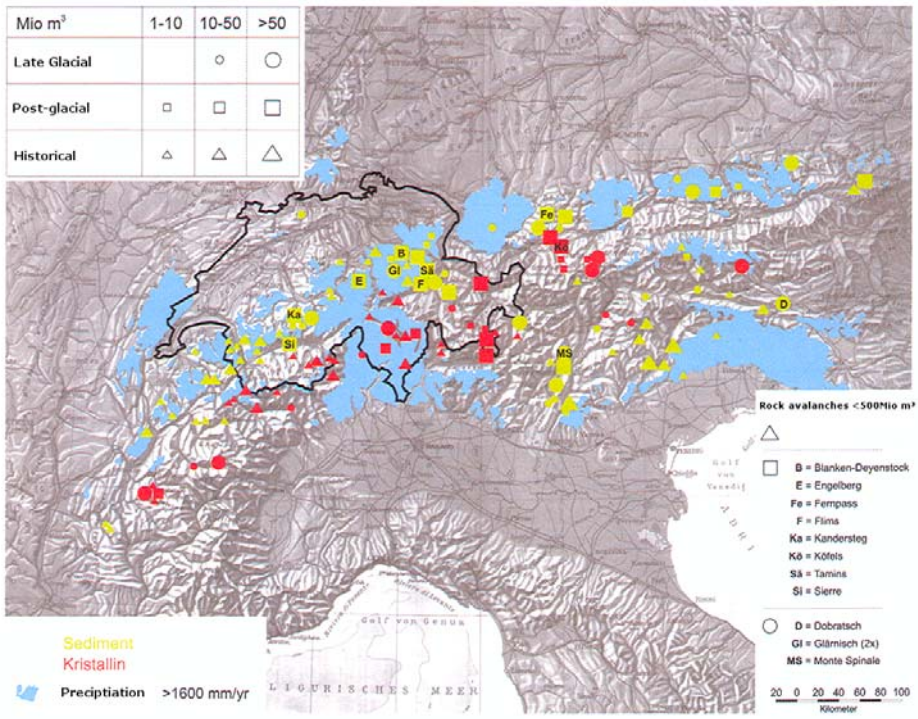

These findings underline that very little is known about the potential effects of global climate change on the occurrence of catastrophic rock avalanches.

2.2.5 Human factors

It is important to realise that in some cases human activity may also serve as a dispositional, if not triggering, factor of rock avalanches. There are two examples of rock avalanches in the European Alps that underline this instance. The Elm rock

avalanche occurred in 1881 following intensive mining of schists, so that the counter bearing was removed and the slope could move. Another case of mining-induced rock avalanching is the Piuro rock avalanche of 1618. Further and more recent examples may include the famous Frank Slide, Turtle Mountain, Canada in 1903 [Cruden and Hungr 1986], and a 70×10^6 m^3 rock avalanche in close proximity to mining wastes in the Ok Tedi River of Papua New Guinea in 1989 [Hearn 1995].

2.3 Triggering mechanisms

2.3.1 Earthquakes

Earthquakes are one of the main triggers of rock avalanches. In contrast, however, tock avalanches are generally the least numerous of the types of earthquake-triggered landslides [Keefer 1999]. A worldwide review suggests that triggering events have a magnitude of M >6 [Keefer 1984]. This generic notion is based on observations in seismically active regions such as the Himalaya-Karakorum, Alaska, Latin America, and the Southern Alps in New Zealand [Keefer 1984]. Conversely, earthquakes with M <5 will not necessarily trigger rock avalanches despite widespread triggering of disrupted soil slides, falls, slumps and block slides, as well as rock falls or rock slides [Keefer 1984]. Earthquakes magnitudes 5< M <6 may trigger rock slumps, rock-block slides, soil slides and subaqueous slides with respect to Keefer's [1984] dataset.

Such empirical approaches have limited and at best regional validity only. Jibson et al. [2006], for example, found that the M = 7.9 2002 Denali earthquake, Alaska, USA, triggered by far less landslides than one would expect from empirical observations. This earthquake also triggered several large and spatially clustered rock avalanches, which indicates the strng controls of local topographic and rock-mass effects on the occurrence of such extremely rapid mass movements. What is more, there are examples of earthquake-triggered rock avalanches that occurred during M <6, e.g. the Gros Ventre Valley rock avalanche, Wyoming, USA, in 1925. This particular rock avalanche occurred during two earthquakes, which occurred within few minutes, each of magnitude M ~3.5. The Gros Ventre Valley rock avalanche was apparently triggered by the second event, and it is possible that the rock mass had been weakened by the initial rupture and developed a potential failure plane during the first earthquake. This example demonstrates the importance of antecedent conditions in the rock mass stability, including, among others cleft-water pressures or precursory slope unloading by erosion. This highlights that a combination of causative factors eventually determines the susceptibility of a rock slope to fail catastrophically during a given earthquake magnitude.

Few studies address the less immediate post-seismic effects of rock-slope instability. The effects of earthquake activity on rock-slope stability may preserve or gradually deteriorate stability following one or several events, but little work has been carried out to establish any physical links. One example of a rock avalanche presumably triggered some time after a relatively low-magnitude earthquake is the Vorderglärnisch rock

avalanche, Swiss Alps [Eisbacher and Clague 1984]. This event occurred 1556, i.e. nine months after a $M = 4.2$ earthquake which occurred in late 1555. The link between earthquake triggers and the rock avalanche is not compelling, but no other extraordinary climatic or tectonic event occurred in between, so that the authors connected these events [Eisbacher and Clague 1984].

As a general observation, only few earthquake-triggered rock avalanches are documented in the European Alps or the Norwegian Caledonides [Abele 1974, Eisbacher and Clague 1984]; however, one has to keep in mind that trigger mechanisms of prehistoric rock avalanches are rarely documented in these mountain belts. This is partly because the palaeoseismological records for most European mountain belts are still being reconstructed. For example, since the beginning of recordings of earthquakes in Switzerland 14 earthquakes of M ≥6 and 88 earthquakes of 5< M <6 were recorded [SED database, 2006]. There are only few indications on postglacial fault ruptures in the Norwegian Caledonides [Blikra et al. 2004].

One impressive example for earthquake-triggerd rock avalanches was the earthquake of Nov. 3rd 2002 with a moment magnitude of 7.9 which triggered thousands of landslides and rock falls along the Denali fault in the Alaska Range.

Figure 27 Map showing area of Denali Fault earthquake. Area enclosed by heavy dashed line shows zone of concentrated landslides triggered by the 2002 earthquake. Earthquake subevent locations from Frankel (2004); liquefaction locations from Kayen et al. (2004).(Jibson et.al. 2006)

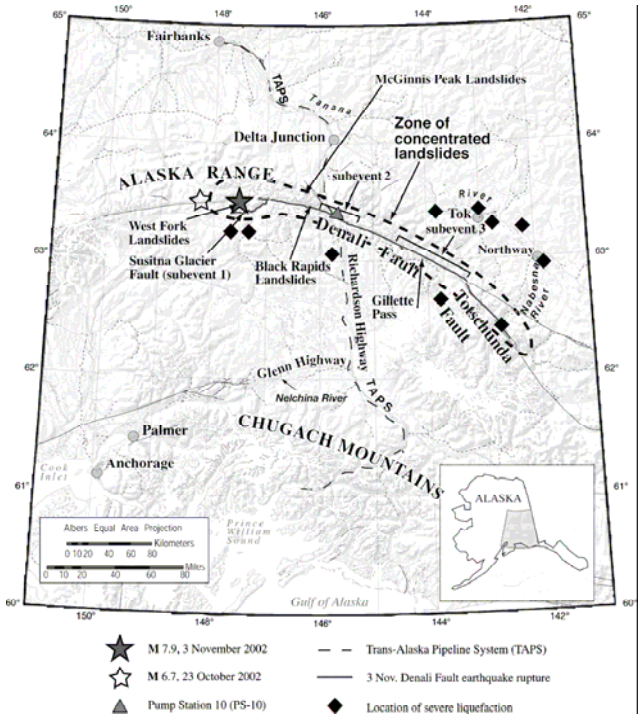

Altogether about 8-10.000 landslides were triggered by this event, but nevertheless far below the proposed number of events of about 80.000 published in Keefer (1984).

Also the majority of the landslide occurred in a narrow 30km wide and 300km long corridor along the the Denali Fault rupture zone, not as Keefer (1984) proposed in circles from the epicentre, in this case a circle with app. 200km diameter..

Under these landslide also some rock avalanches were occurring. These rock

	avalanches presented in this example were all triggered by this event. Velocities of the rock avalanches were estimated to be up to 200 km/h The geology of the Alaska Range consists mainly of schists with a generally high dip (up to 90°) and a Mainly E-W strike.
Figure 28 Map showing McGinnis Peak rock avalanches. Topographic base from USGS Mt. Hayes (C-5) quadrangle, original scale 1: 63,360, contour interval 100 ft (30 m), datum mean sea level. Strikes and dips of schistosity from Nokleberg et al. (1982), (Jibson et.al.2006).	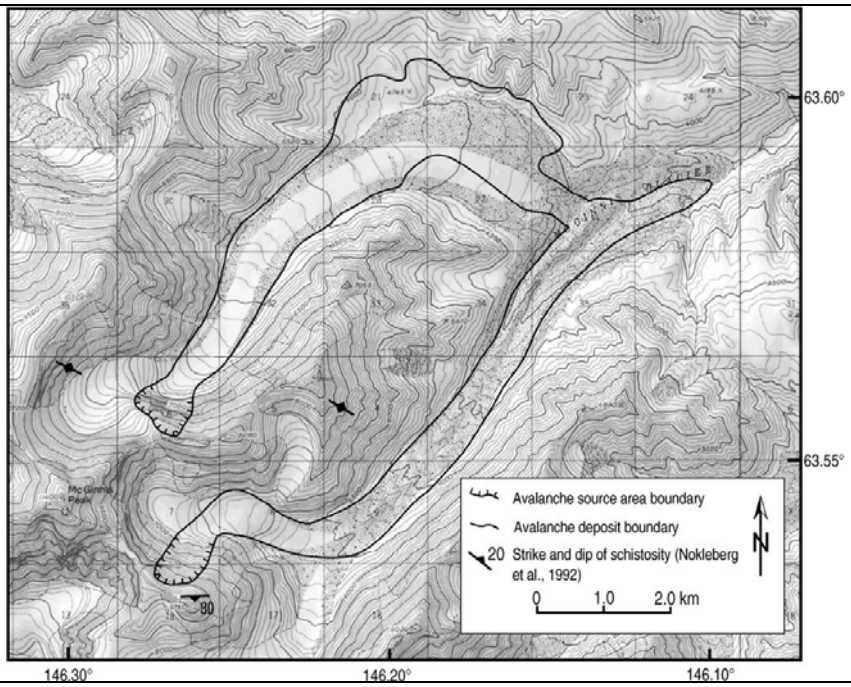
	In the Alaska Range the rock avalanches flowed onto glaciers which might have helped to reduce friction and increase the run-out length. (figures 1 and 3), on figure 2 one can see the intense fracturing of former intact rock durin the process.
Figure 29 Photograph of the rock avalanches on Black Rapids Glacier. The Glacier is about 2km wide at this location. *Note smaller Landslides on the right side of the valley. Also there are several lobes on the rock avalanche surface, indicating semi-independent movements*	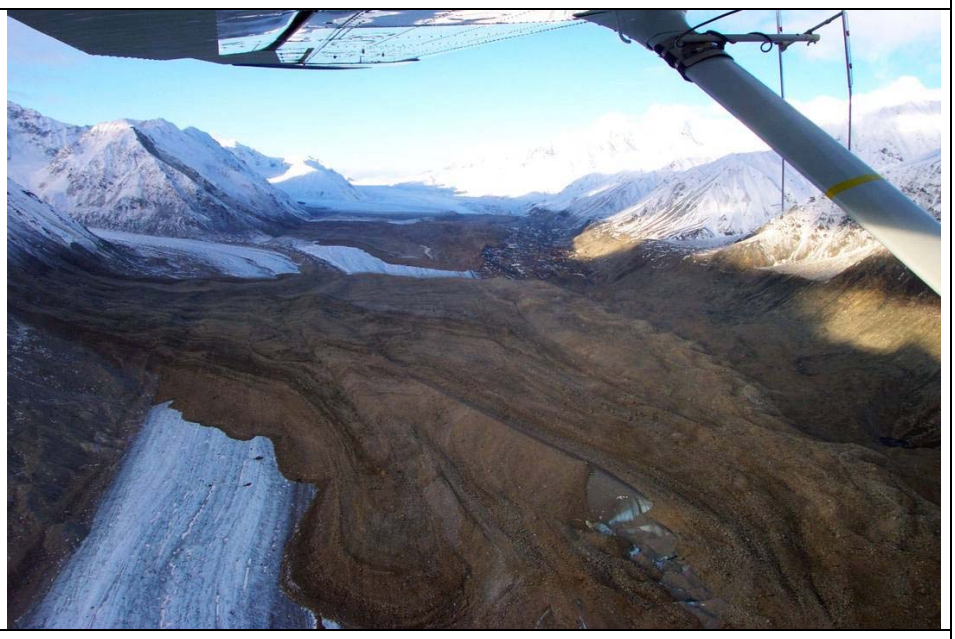
Figure 30 Map showing Black Rapids rock	

avalanches. Topographic base from USGS Mt. Hayes (B-5) quadrangle, original scale 1: 63,360, contour interval 100 ft (30 m), datum mean sea level. Strikes and dips of joints from Nokleberg et al. (1982). (from Jibson et.al. 2006)	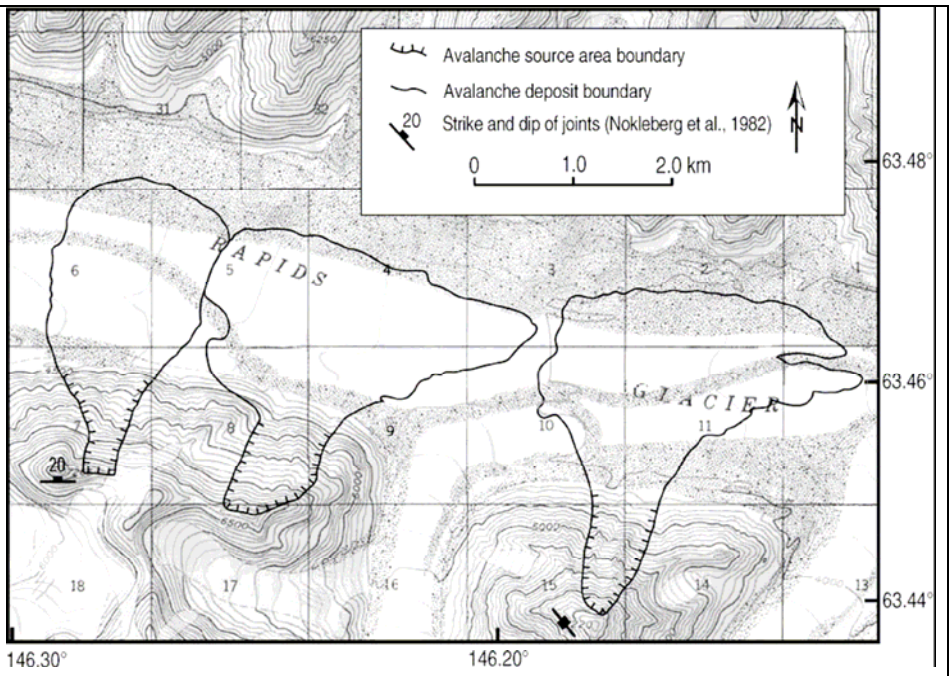

Figure 31 Black Rapids rock avalanches triggered by 2002 Denali earthquake (M = 7.9). The valley glacier is about 2-km wide here. The Denali Fault extends beneath the glacier near the mountain front. (a) Westernmost rock avalanches; note several smaller landslides extending along the ridge to the right. (b) Eastern rock avalanche; note multiple lobes of material that moved semi-independently of each other [Jibson et al. 2006].

(a)

(b)

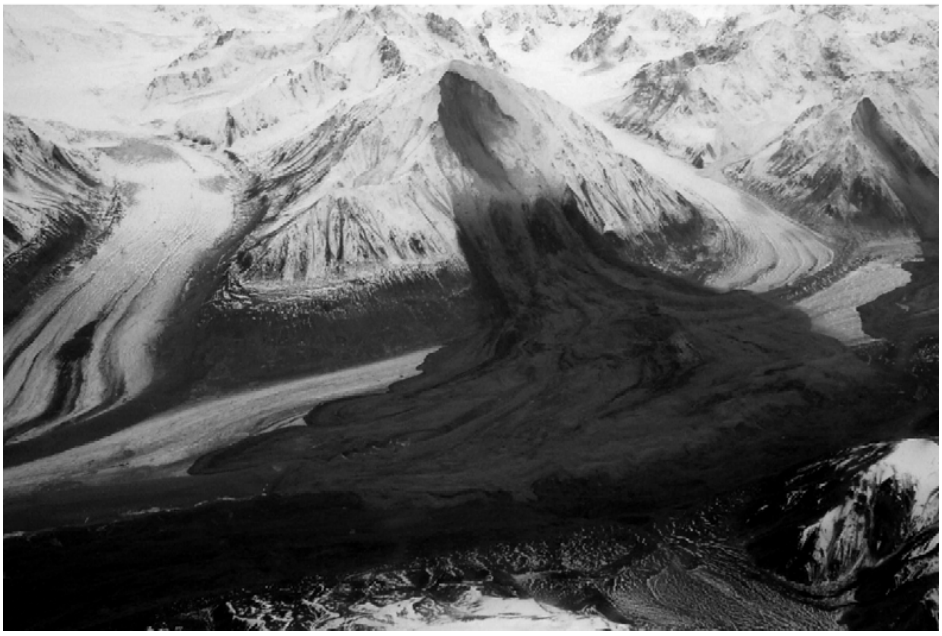

Figure 32 Triggers of rock avalanches in the European alps

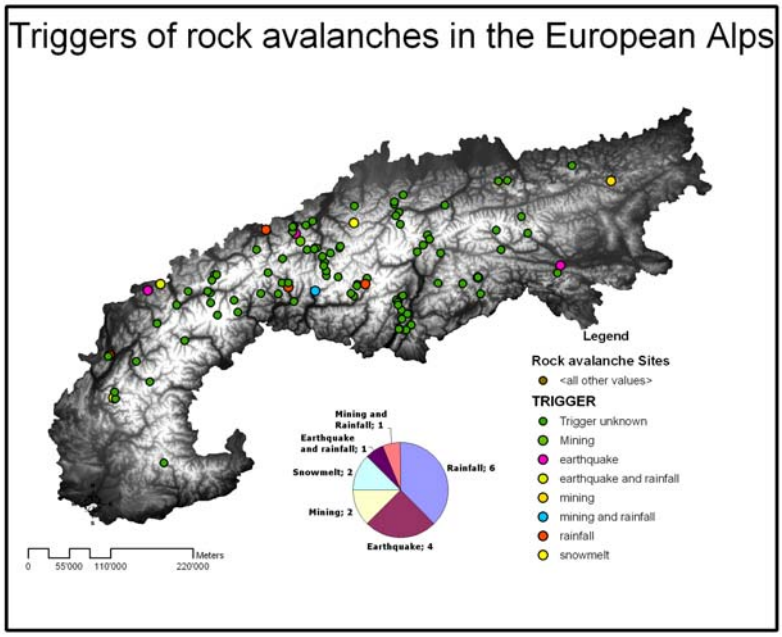

The impact of an earthquake on a specific area may vary because of different rock types and topographic conditions [Keefer 1984, Crozier 1995]. High mountain ridges are more prone to earthquakes; the seismic waves accelerate and increase their destructive power, an effect commonly subsumed under the term of topographic amplification [Crozier 1995]. Also, different rock shows different sensitivity to earthquake-induced ground acceleration and dynamic loads. Weakly cemented, weathered, sheared, intensely fractured or closely jointed rocks show the strongest sensitivity to earthquake shaking [Keefer 1984].

Table 7 Selection of earthquake-triggered rock avalanches

Location	**Earthquake magnitude**	**Volume (10^6 m^3)**	**Date**	**Reference**
Gros Ventre Valley, USA	3.5 and 3.2	38	June 23, 1925	Keefer, 1984
Vorderglärnisch, Switzerland	4.2	0.1	July 3, 1594	Eisbacher & Clague, 1984
Yvorne, Switzerland	6.4	10	March 4, 1584	Eisbacher & Clague, 1984
Dobratsch, Austria	Unknown	30	January 25, 1348	Eisbacher & Clague, 1984
Antelao, Italy	Unknown	Unknown	1348	Abele, 1974

The spatial extent of earthquake-induced effects on slope stability can affect areas of up to 10^5 km^2, and depends on the magnitude of the earthquake, once again judging from empirical observations [Keefer 1984]. This spatial extent was measured by counting and mapping the reported rock avalanches(?) and the area in which these events occurred was calculated, as well as the distance from the epicentre (***Figure 33***). The centre the affected areas of slope instability does not necessarily display the

	epicentre of the earthquake. These areas were irregular in shape and asymmetric with respect to the epicentres or fault ruptures, although the size of the affected area correlates well with earthquake magnitude [Keefer 1984]. The spatial extent of earthquake triggered rock avalanches is dependent of the geological conditions (rock type, faults, etc).
Figure 33 Relation of maximum distance between trigger and event (Keefer 1984)	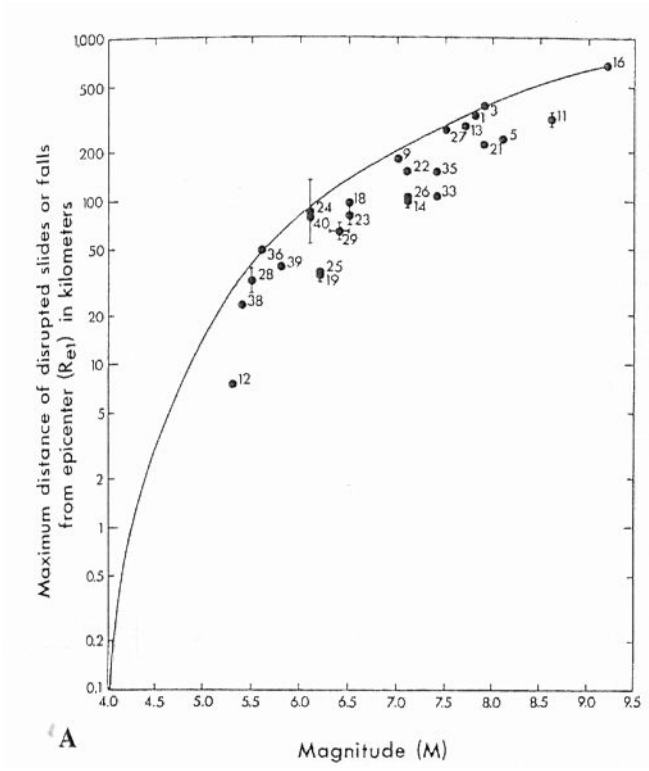
	An interesting question is whether earthquake intensity may be a useful alternative to linking rock avalanches to seismic activity instead of solely using earthquake magnitude. The Mercalli intensity scale and the Richter magnitude scale refer to observed damage and released energy, respectively. For example, the regional distribution of large landslides and landslide-dammed lakes has been used as an indicative element to spatially delimit earthquake intensity zones in mountainous terrain in New Zealand, albeit for documented historic events exclusively [Reference].
	2.3.2 Rainfall and Snowmelt
	Rainfall as a trigger of rock avalanches does generally not include short-term and high-intensity events [Crozier 1995, Crosta 2004]. More generally, rainfall-triggered rock avalanches are a consequence of prolonged periods of rain, which partly underlines the importance of antecedent groundwater conditions. For example, the 1806 Goldau rock avalanche in the Swiss Alps occurred after a longer period of intense rain. Concerning rainfall as a trigger, it is important to state that there are no established triggering thresholds of rainfall intensity or duration. The key problem of ascertaining rainfall triggers for rock avalanches is that the low number of documented cases in which the amount of fallen rain was instrumentally measured or recorded otherwise.

	Rainfall must penetrate into the system of existing fractures to trigger large-scale rock-slope failure by increased cleft-water pressures or buoyancy effects. However, much of the precipitation released during high-intensity rainstorms will be removed as superficial runoff. Such excess runoff contributes to natural drainage, and counteracts enhanced storage or pressure build-up of water in the fracture systems of potentially unstable rock masses. The duration of rainfall as a trigger for rock avalanches may exceed 24 h but this duration does not necessarily trigger rock avalanches. The 24-h duration period is commonly used for defining triggering threshold for events like debris flows or soil slides, but for deep-seated rock avalanches a 24-hour rainfall does generally not destabilize rock sufficiently [Crosta 2004].

Figure 34 Scar area (left middle) and runout area (debris moved valley up- and downwards) of the 1987 Val Pola rock avalanche, Northern Italy	
	The 1987 Val Pola rock avalanche, Italy, which reactivated an old landslide body, may serve as a rare example for rainfall-triggered rock avalanches. This slope failure was preceded by a week's enduring rainfall totalling more than 600mm, making half of the mean annual precipitation for this area [Crosta 2004]. At the same time, exceptionally high temperatures prevailed. The 0° isotherm rose up to 3500-4000 m asl. The rock avalanche itself occurred on July 28th 1987, 8 days after the intense rainfall. This time gap is typical for rainfall-triggered landslides [Crosta 2004]. ***Figure 35*** shows the temporal distribution of cumulative rainfall of three rain gauges near the rock avalanche area. There are few other documented examples, such as the Piuro rock avalanche of 1612 with heavy rain over 10 days [Eisbacher and Clague 1984].

Figure 35 Cumulative rainfall diagram of the Val Pola area June-July 1987 (Crosta 2004)

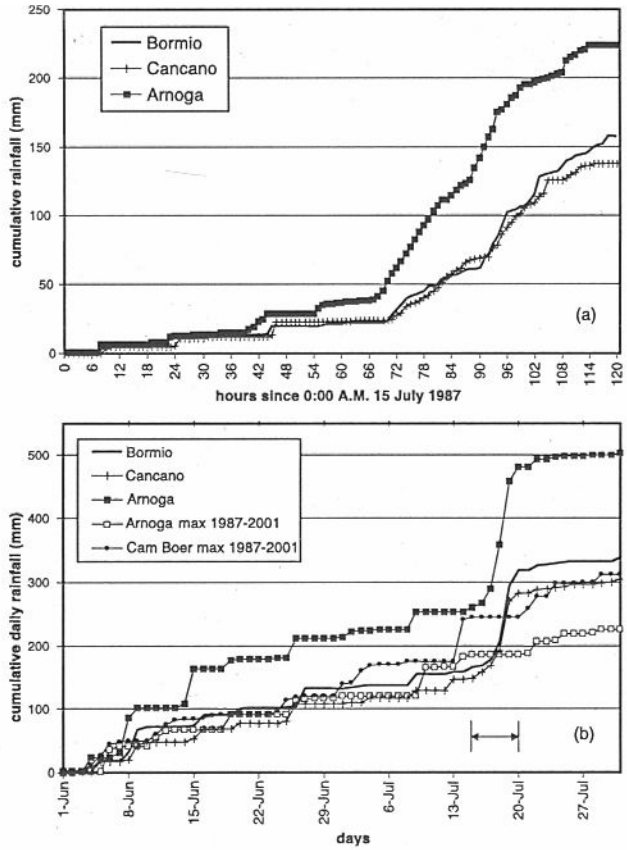

Long-term effects of rainfall infiltration into heavily fractured volcanic rocks may serve to gradually deterioriate rock-mass strength, especially in hydrothermally and clay-rich volcanic rocks. For example, the increasingly strong buildup of excess porewater pressures together with infiltration sealing and rock-mass strength decay by formation of hydrothermal smectite clays have been proposed to trigger the 1998 debris avalanche from Casita Volcano, Nicaragua [Opfergelt et al. 2006].

Few occurrences of rock avalanches may be linked to conspicuous temperature changes [e.g. Shang et al. 2003]. Once again, a combination of triggers rather than a single mechanism may be the best explanation for the triggering of rock avalanches. For example, the 2006 Southern Leyte rock avalanche/mudslide, Philippines, occurred following intense monsoonal precipitation, which amounted to more than 2000 mm in ten days. Some days after this rainfall, however, a minor earthquake (M ~2.6) occurred and eventually triggered the failure. (***Table 8***). In such cases, it remains very difficult, if not untractable, to distinguish between a seismic and a climatic trigger properly.

Table 8 Selection of rainfall-triggered rock avalanches

Location	**Intensity of rainfall**	**Volume (10^6 m^3)**	**Date**	**Reference**
Lannigou, China	600mm in 50days	450	1971	Wen et.al. 2004
Sesa, Italy (rockslide)	400mm in 15days	2	1993	Crosta 2001
Touzaigou, China	209mm in 8days	40	1997	Wen et.al. 2004
Val Pola, Italy	600mm in 7days	40	1987	Crosta 2004

Snowmelt in combination with intense rainfall has also been reported as a climatic

trigger of rock avalanches. This combination of climatic triggers has been illustrated by the 2002 Pink Mountain rock avalanche in northeastern British Columbia, Canada. Due to an exceptionally cold spring snowmelt occurred as late as June and July. Additionally five days of intensive rainfall totalled to ~150 mm cumulative rainfall (***Figure 36***). A small earthquake with a magnitude *M* ~2.9 occurred at ~ 150 km distance of Pink Mountain. Yet it was assumed that the rock avalanche was triggered by high cleft-water pressure following combined rapid snowmelt and high precipitation. There exist some other examples of snowmelt-triggered rock avalanches. Further examples of snowmelt-triggered rock avalanches are listed in ***Table 9***.

Figure 36 Diagram of rainfall-equivalent snowmelt and rainfall in comparison to long-term mean values (Gertseema et.al.2006)

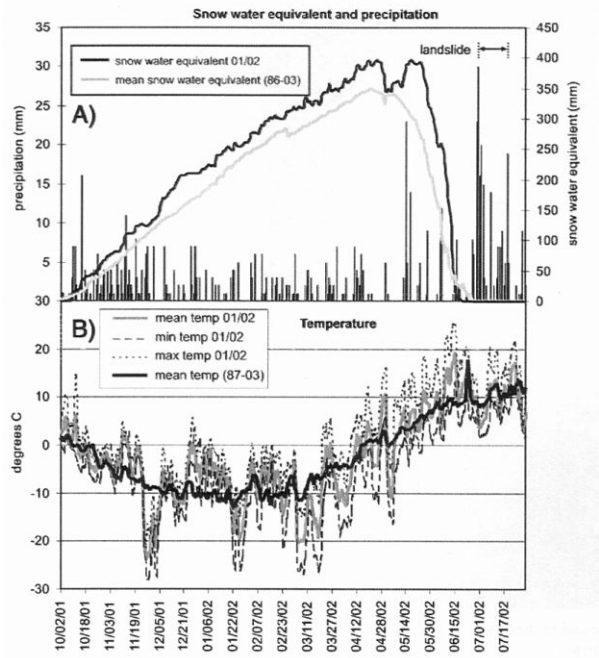

Table 9 Selection of snowmelt-triggered rock avalanches

Location	**Volume (10^6 m^3)**	**Date**	**Reference**
Blisadona, Austria	2.5	1892	Eisbacher and Clague, 1984
Lac de Vallon, France	2	1943	Eisbacher and Clague, 1984
Pink Mountain, Canada	1.04	2002	Gertseema et.al. 2006
Yigong, China	200	2000	Wen et.al. 2004

The case histories of the Val Pola, Leyte and Sesa rock avalanche show an apparent delay between the onset of the triggering rainfall event and the failure of the rock avalanche. This time lag is about 36 to 48 hours from the cessation of the triggering rainstorm. The long delay time has not been fully understood. Hydro-geological conditions determine the time it will take to increase the cleft-water pressure [Czurda and Xiang 1993].

2.3.3 Human activity

There are several documented cases, where human activities have episodically served as the main trigger of rock avalanches. The 1881 Elm rock avalanche, Switzerland, involved a volume of about 10 Mm^3. This event occurred during a wet period, but also

	the mining of schists at the toe of the affected slope is considered to be the most important trigger [Heim 1932]. Further examples of mining-induced rock avalanches have been mentioned above. Another example of a human-induced rockside/rock avalanche is the one at Vaiont, Italian Dolomites, in 1963. In this case a water supply dam was built into a valley [Hendron and Patton 1987]. The filling of the artificial reservoir with water lead to an increase in cleft-water pressure of the valley slopes, which were partly made up by fossil landslide deposits. On the southern slope of this valley an outcrop of a geologic layer discontinuity was destabilized by this increasing water pressures and failed. About 270×10^6 m^3 slid into the lake, causing a flood wave, which overtopped the dam and moved down the valley, killing more than 2000 people, while leaving the dam intact. Rock avalanches have also been triggered by explosives both advertently and inadvertently. Nuclear underground tests on Novaya Zemlaya during Soviet times triggered a large rockslide/rock avalanche, which had subsequently blocked a river. There are also several accounts of artificially triggered rock avalanches that served as artificial dams for hydropower generation and debris flow protection on the territory of the former Soviet Union (References).
	2.3.4 Rock avalanche without evident trigger
	Although the main trigger for historic and current rock avalanche events is known [Eisbacher and Clague 1984], some events occurred seemingly just "accidental", with no trigger being evident, i.e. detectable or measurable [e.g. Hancox et al. 2005]. One of the more recent events without any observed trigger is the Zymoetz rock avalanche in Canada [Boultbee et al. 2005]. A probable trigger may have been increased snowmelt and a more than usually rainfall, but there is no clear evidence for this [Boultbee et al. 2005] (***Figure 37***).

Figure 37 Climatic conditions before and during the Zymoetz rock avalanche (ZRRA) (Boultbee et.al.2005)

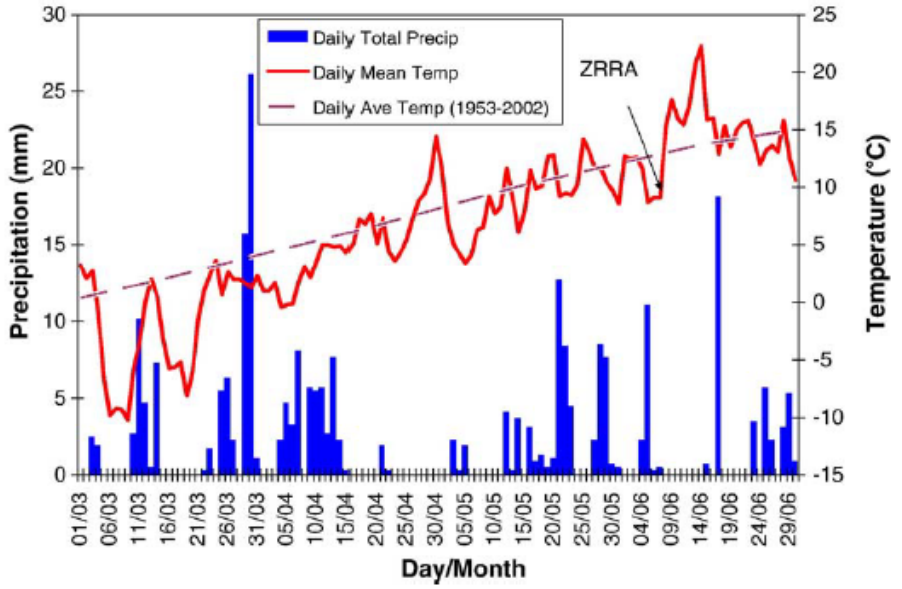

2.4 Conclusion

- Rock avalanches are an extreme end member of rock-slope failure that amy arise from a variety of failure modes (fall, topple, slide or creep). Sufficient, but not necessary, topographic conditions for the occurrence of rock avalanches include high relief and slope steepness.

- Rock avalanches occur in all rock types and climate zones. However, the local occurrence is more tightly constrained by seismotectonic history, lithology, and orientation of major discontinuities and their intersection with slope geometry. Therefore, the causes of rock avalanches are linked more closely to the long-term development of mountain belts rather than the short-term distribution of surficial sediment and soil cover.

- Earthquakes are common trigger mechanisms of rock avalanches, especially in tectonically active areas. The overall lack of documented or well-constrained trigger mechanisms for prehistoric rock avalanches makes an overall assessment of the role of earthquakes as triggers difficult.

- Rock avalanches can be triggered a few days following extended periods of excessive rainfall, which often occurs in combination with other hydrological processes, such as snowmelt. Corresponding case studies are even less documented than those for earthquakes. In several instances, a combination of different synchroneous or slightly sequenced trigger mechanisms is the most plausible explanation.

- Contrary to established critical triggering thresholds, very few quantitative values exist to better constrain, and eventually predict, the occurrence of rock avalanches as a function of terrain characteristics, earthquake magnitude, or rainstorm intensity and duration. Rock avalanches are very localised hillslope

	failures, which are notoriously difficult to predict at a regional scale. This is another characteristic that distinguishes rock avalanches from other extremely rapid mass movements such as snow abalanches or debris flows. • Human activities have occasionally triggered rock avalanches.

Chapter 3

TRIGGERING OF SNOW AVALANCHES

3.1 Introduction

Introduction

An avalanche is the rapid downhill movement of a snow mass of variable size under the force of gravity. It always corresponds to a breakdown in the equilibrium conditions governing the mechanical and structural stability of a snowpack.

The snow material and its different grains which constitute the different layers of the snowpack strongly influence the different types of avalanche according to the main physical properties of the snow. The objective of the chapter 3.2. is to describe the material and the different elements which can modify it.

Three factors, detailed chapter 3.3, can explain the avalanche, how it occurs and its size. These are the structure of the snowpack, the additional load that the snowpack can handle and the topography of the site.

Finally, avalanches and the triggering causes are described in the chapters 3.4 to 3.7.

3.2 Snow properties and crystal types

3.2.1 Snow crystal types

The snowpack is composed of layers of different snow crystal types. One of the main characteristics of the snowpack is its permanent metamorphism due to changes in environmental factors. All the snow layers have thus an own continuous evolution of

their crystal type and physical properties during all the season which deeply influences the full snowpack stability. As most of the physical parameters of the layer depends on the grain type, it is very important to define first these different types of crystals which govern the entire stability of a snowpack.

Snow crystals can thus be classified in two categories: crystals before metamorphism (generally recent snowfall) and crystals resulting from dry or wet metamorphism (metamorphism is explained in chapter 3.2.3).

3.2.2.1 Crystal before metamorphism

They are generally named precipitation particles or new snow or fresh snow. The different forms and dimensions of these crystals are very numerous. It is due to the very different meteorological conditions that can exist in the cloud where the crystal is formed. Among these meteorological parameters, temperature and humidity in the cloud are dominant to explain the crystal shape and size.

However the International Commission on Snow and Ice (ICSI) has defined mainly 8 types (***Table 10***).

Table 10 ICSI Classification for freshly fallen snow crystals

Name	symbol	Shape
Columns		Short prismatic crystal, solid or hollow
Needles		Needle-like, approx. cylindrical
Plates		Plate-like, mostly hexagonal
Stellars dendrites		Six-fold star like, planar or spatial
Irregular crystals		Cluster of very small crystals
Graupel		Heavily rimed particles
Hail		Laminar, internal structure, translucent or milky, glazed surfac
Ice pellets		Transparent, mostly small spheroids

If hail and ice pellets are rare in an alpine snowpack, graupel is sometimes present. Graupels are generally associated to convective clouds (cumulonimbus type). As long as the snow is dry, the evolution of these crystals is very slow, mainly due to the low water vapour pressure. As the presence of a thin layer of graupels in the snowpack decreases its stability (it is one possible way to generate weak layers), it is important to identify them.

	The size of the crystal is extremely variable in precipitation particles. Snowfalls are not the only way to add ice crystals to the snowpack. Condensation (solid condensation) can create a surface hoar layer in case of meteorological conditions with a high air humidity and an important difference between the air temperature and the snowpack surface temperature. As for graupels, the presence of a thin surface hoar layer in the snowpack causes instability sometimes (other source of weak layer) for a long time due to a very low evolution of these crystals in the snowpack.
	3.2.2.2 Crystal after metamorphism
	Five grain types can mainly be distinguished. The different metamorphisms of the initial fresh snow explain theses different types (Metamorphisms are explained in chapter 3.2.3). The different types are described in ***Table 11***. Usually, grains size completes the description.

Table 11 Main grain types resulting of a snow metamorphism

- partly decomposed precipitation particles (recognizable particles) : the snowfall is recent. Metamorphism has begun and affects, specially, the branches of the crystal. But it is still possible to recognize the initial crystal type during the snowfall.	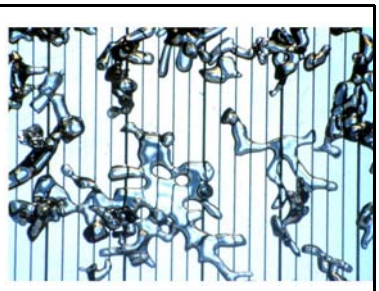
- rounded grains : the grains are well rounded. The size is generally little (between 0.2 and 0.8mm). They can be the result of the effect of the wind or of the low gradient metamorphism. The size and the shape allow a lot of bonds between the grains.	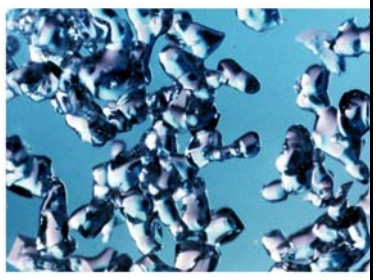
- faceted crystals : angles can be seen on the crystals. The typical form of the crystal is hexagonal. These crystals are the result of medium or large temperature gradient metamorphism. The size is generally equivalent or bigger than rounded crystals. The shape of the crystals does not allow a lot of bonds between the grains.	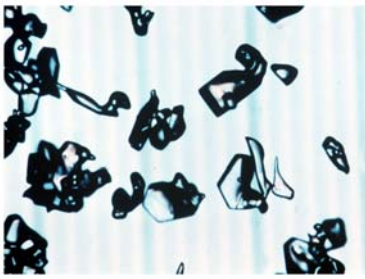
- Depth hoar : crystal has a cup shaped and is striated. The crystal size may be very high (several millimetres) . It is the result of several days with high gradient metamorphism. This metamorphism is mainly possible at the beginning of the winter when the snowpack is not thick. The number of bonds between the grains is very low.	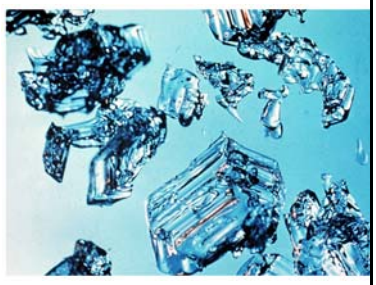
- Wet grains : these grains are the result of the wet metamorphism. Grains are rounded. The size can vary, but is usually between 0.4 and 1mm. A wet grain may be at negative temperature, which means that this grain was wetted in the past (melt-freeze cycle) and is presently frozen. Cohesion in a wet grain layer is variable. A refrozen wet grain will have an excellent cohesion. If the temperature is at 0°C, cohesion is depending on the liquid water content (section 3.2.2.1). Melt-freeze cycle of wet grains is typical during a spring day.	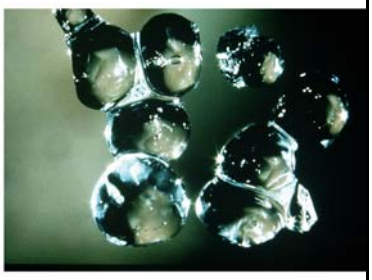
- crust : layer with high density. Crust can have different causes : melt-freeze cycle, frozen rain water, wind. A crust has a very high cohesion, but, often, cohesion is bad between the crust and the above or underneath grains.	

3.2.2 Snow physical parameters

Snow is a porous material. It consists of ice, air with water vapour and sometimes liquid water. These three water components give particular physical properties to the snow.

Liquid water content, density, temperature, grains (type and size) (explained in chapter 3.2.1) gives important information on a snow layer. Knowledge of these parameters allows us to estimate other parameters (conductivity, albedo, etc.) and helps also to determine the cohesion of the different layers, a very important parameter in the avalanche triggering.

In this chapter, these different parameters are described at the scale of the layer. We must keep in mind that this scale is not sufficient to understand all physical processes which, often, must be considered at the grain scale.

3.2.2.1 Liquid water content

Snow can be wet or dry. A snow layer will be wet if the Liquid Water Content (LWC) is not null and then snow temperature will be at 0°C. A wet snow is very different of a dry snow, mainly, metamorphism and cohesion differ.

Liquid Water Content is often represented by several expressions whether one uses volumes or masses and is expressed in % :

LWC vol = liquid water volume / snow volume (ice, liquid water and air)

LWC mas = liquid water mass / snow masse (ice, liquid water and air)

LWC por = liquid water volume / (snow volume – ice volume)

This parameter is very important to estimate the cohesion. A threshold, around 7 vol %, is often used. Under this threshold, the snow will have a good capillary cohesion, above the cohesion will rapidly decrease with the liquid water content. Above 15 vol %, the snow is said slush and is flooded with water.

Rain or snow melting brings liquid water into a snowpack. In the spring, many avalanches are due to the increasing of the LWC due to liquid precipitations.

3.2.2.2 Density

Density is also a very important parameter to characterize a snowpack. It is the rapport between the mass of a given snow volume and the corresponding snow volume. It is generally expressed in kg/m3.

Snow density is very variable, but it is generally smaller than 600 kg/m3 for non permanent snow cover (firn density being comprised between 600 and 800 kg/m3) . So, snow density is always widely lower than the ice density (917 kg/m3) due to the air

	presence. Concerning recent snowfalls, density is usually comprised between 20 and 300 kg/m^3. In fact, density after a snowfall depends mainly on 2 parameters : air temperature and wind speed. A snowfall with a cold air temperature (-15°C) and without wind will gives a very light deposited snow (20 to 50 kg/m^3). In opposite, if the air temperature is warmer and if the wind is strong, densities can reach 250 to 300 kg/m^3. Usually, density increases rapidly after the snowfall in the first day, and slowly later (settlement). Density is also an important parameter to estimate the cohesion of a layer so as other parameters, in particular conductivity. Cohesion and conductivity increase also with the density. For instance, between 200 and 300 kg/m^3, conductivity in a dry snow will be comprised between 0.1 and 0.23 Js^{-1}m^{-1}K^{-1} (multiplication the conductivity by 2).
	3.2.2.3 Main mechanical properties
	The formation of snow avalanche is determined by the mechanical properties of snow and its failure is a result of applied stresses. On a slope, a snowpack undergoes different stresses, mainly in compression and traction. Due to the cohesion between grains, a snowpack has plastic and viscous properties. These properties explain why snowcover is able to stay on a slope or initiate an avalanche. In mountain, a slope presents convexity and concavity areas. In a convexity area, the snowpack undergoes tension, in a concavity area, it will be in compression. It is important to know that snow properties are mainly efficient against compression but very less in tension (with a ratio between 10 to 20 concerning failure strengths) . So, convexity areas will be very sensitive to the avalanche danger.
	3.2.2.3.1 Cohesion
	Cohesion in snow is directly linked to the way which the snow grains are bonded. Cohesion also depends on density and grain shape. It explains why these 2 parameters are so important. Different types of cohesion are existing: - the felt-like cohesion : in the precipitation particles, it is due to the shape of the crystals. The dendrites are tangled. This cohesion is low and disappears rapidly after the snowfall. - the sintering cohesion : in the rounded grain (but general in a dry snow), the grains bond together with an ice neck at each contact point . The cohesion is very efficient, but it allows the propagation of fractures (It explains fractures observed in the slab avalanches). - capillary cohesion : in the wet snow, liquid water around crystal grains explains this

	cohesion (capillary pressure). As explains in chapter 3.2.2.1, the quality of this cohesion is depending on the liquid water content. - refrozen cohesion : initially with a wet snow, if the liquid water around the crystal freezes, we obtain a very good cohesion between the crystals.
	3.2.2.3.2 Plasticity and viscosity
	Snow is a plastic and viscous material. Plasticity is the propensity of snow to undergo permanent deformation under load; depending on the plasticity ,distortion without break will be more or less easy. Viscosity indicates the snow capacity to deform under shear stress on a slope and describes the snow internal resistance to flow. Plasticity and viscosity mainly depend on density, temperature and grain shape.
	3.2.2.3.3 Fractures and toughness (from Schweitzer et al., 2004)
	The release of a dry-snow slab avalanche involves brittle fracture in the framework of a non-linear problem. It generally happen at the interface between slab and weak layer or alternatively within the weak layer. Fracture toughness describes how well the snow material can withstand failure and is so one of the key factor to assess fracture propagation propensity and hence slope stability. Toughness is fully dependant of the materials, so of every grain types constituting the slab structure(see 3.3.1.5) , density and temperature. Current experiments (Schweizer et al. , 2004) indicate that typical values of the snow fracture toughness were 500-1000 Pa m1/2 which shows that snow is one of the most brittle material known to man and leads to estimate a critical crack size under shear failure to be about 1 m.
	3.2.2.4 Thermal properties
	Most of the thermal properties of snow (and significant to avalanche formation) are related partly or largely to snow density. These density values are also significant to the problems of evaluating and forecasting runoff from snow melt and snow surface parameters.
	3.2.2.4.1 Calorific capacity and latent heat
	Water in a snowpack may be present in the solid, liquid or gas state. Usually, the capacity of the snow is estimated to be equal to the ice capacity (2090 J/kg/K). It means that 2090 Joules are necessary to increase 1kg of snow of 1°C. In comparison, 334 000 Joules are necessary for the melting of the same quantity of snow at 0°C. Very important energy is so needed during the changes of state of the water.
	3.2.2.4.2 Conductivity
	Due to the presence of air in the snow, thermal conductivity is low. It explains the difference in the temperature that can be measured in a snowpack. For example, it is not rare to have 0°C at the bottom of the snowpack (thanks to the heat of the ground)

	and –20°C at the top. As mentioned in chapter 3.2.2.2, conductivity mainly depends on the density (in fact of the air quantity in the snow).
	3.2.2.5 Energetic budget at the surface
	A snowpack loses and receives energy mainly at its top (atmosphere - snowpack interface, ***Figure 38***). Solar radiation and long wave radiation from the atmosphere bring energy to the snowpack. However, local conditions must be considered; for example the energy received in a south slope will be very different than energy received in a north slope. Of course, date in the year and time in the day will also modify considerably these quantities. Snow reflects a large part of the solar radiation; the albedo defines this part which mainly depends on the age of the snow, on the grains shape and on the received wavelengths. A good estimation of this parameter is very important to avoid errors in the energy budget evaluation. Turbulent exchange between the top of the snowpack and the atmosphere must also be consider, even if quantities are generally less than those of radiation. Turbulent exchange increases with the wind. As snow cover approximates nearly a black body radiator, it mainly loses energy by long wave radiation. Depending on air temperature during the precipitation, rains and snowfalls bring also energy to the snowpack. Temperature (and so temperature gradient, see chapter 3.2.3) and liquid water content (wet snow avalanche) in the snowpack will be deduced from this budget. As these 2 parameters are very important to analyse the snowpack structure and stability, a correct energy budget evaluation must be performed.

Figure 38 Short wave, long wave radiation and turbulent exchange at the snow surface

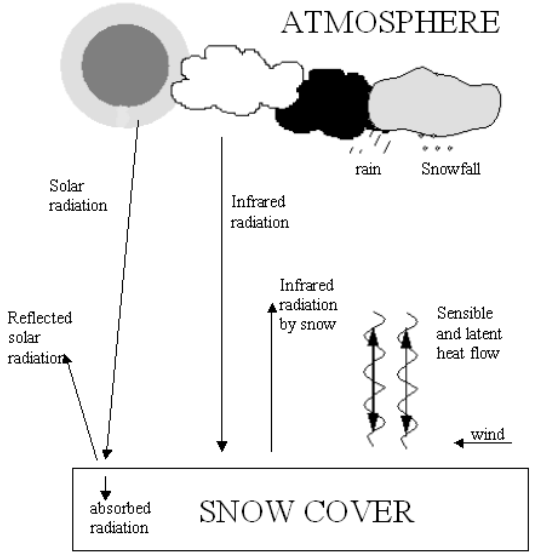

For instance, during a spring day without cloud, the impact of the energy budget on the snow cover is particularly less appreciated by skiers because of surface melting. In the night, snow loses energy by long wave radiation and a refrozen crust can appear. In morning, solar radiation becomes stronger than long wave radiation of the snow, snow begins a transformation at the surface. In afternoon, liquid water content increases. If air temperature is high, wet snow avalanches are possible.

3.2.3 Metamorphism

Once deposited, snow crystals begin to change form immediately. Stellar crystals or plates disappear and the evolution of snow is permanent inside the snowpack until the end of the season. This process has been called snow metamorphism. The term metamorphism includes changes in form due to temperature (heat flow) called thermodynamical metamorphism and overburden pressure or snowdrift called mechanical transformation. The objective of this chapter is to describe all these crystal transformations and to explain the main necessary conditions. As cohesion depends on the grain types, these transformations are important for avalanche fracture and release.

3.2.3.1 Mechanical transformation

2 causes can be distinguished :

- the wind effect during the snowfall or after a recent snowfall.

- the settlement of the snow inside the snowpack.

Wind is the cause of collision between crystals. The consequence is a transformation of the original crystal. Rapidly, fresh snow evolves to rounded grains. It generally implies an increase of cohesion and density and explains cornices and wind slab by sintering effects. This point is very important in avalanche forecast and is longer described in

chapter 3.3.1.3.

The other mechanical transformation is the settlement of the snow. A snow layer undergoes the weight of the layers above. This settlement causes an increase of the density, but also an evolution of the fresh snow towards more rounded grains.

3.2.3.2 Thermodynamical metamorphism

Thermodynamical metamorphism is a slow process compared to the mechanical transformation; usually, several days are necessary.

Metamorphisms in a wet or in a dry snow are completely different. In a dry snow, grain transformations are only due to the sublimation or solid condensation phenomenon. Vapour flow leads to modify grains shape. In a wet snow (snow temperature at 0°C), liquid water is present and vapour flow can be neglected. In this case, liquid water content is the main element in which governs the transformation.

Concerning crystal forms, results are also very different between dry or wet snow. In dry snow, evolution will be towards rounded grains, faceted grains and depth hoar. In wet snow, evolution will only be towards wet grains.

These modifications will be shortly presented in the following items and are synthesised in ***Figure 39***.

Figure 39 Scheme exhibiting the different snow metamorphisms according to the grain type

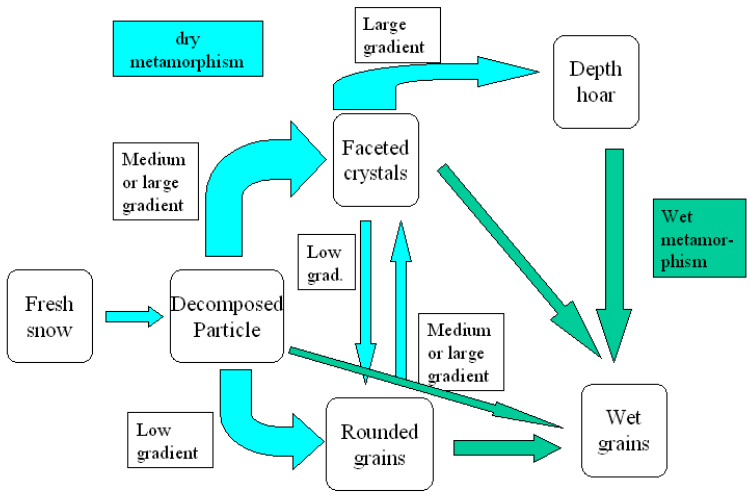

3.2.3.2.1 in dry snow

Usually, snow temperature is about 0°C at the bottom and decreases toward the snow surface (low snow conductivity explains this differences of temperature inside a snowpack). So, a temperature gradient (variation of the temperature on a vertical in the snowpack, expressed in degree Celsius by meter) with significative vertical variations is usual in a snowpack. This temperature gradient is the most important factor of the grains transformation. Since saturated warm air can content more water vapour than saturated cold air, a higher overall water vapour pressure exists in the pores of the

	snow near the warm part and the water vapour is forced to move up from the warm to the cold part. In addition, differences of saturated vapour pressure can come from the shape of the grain surface curvature and imply also water vapour transfers. In all cases, the speed of the transformation increases with temperature. Generally, in a dry snow, 2 thresholds on the gradient, 5 and 20°C/m, are defined. These 2 thresholds define 3 kinds of gradient metamorphisms : Metamorphism at low gradient : gradient is comprised between 0 and 5°C/m Metamorphism at medium gradient : gradient is comprised between 5 and 20°C/m Metamorphism at large gradient : gradient is greater than 20°C/m - low gradient In this case, all the snow crystals in the layer are nearly at the same temperature so as the air in the pores. No significant difference in water vapour pressure due to temperature gradient exists but different convex and concave parts are present on the different grains. The water vapour flows thus from the convex to the concave parts of the grain in inducing sublimation at the points of stronger curvature (convex) to the benefit of the smaller curvature points (concave) where direct condensation occurs. This metamorphism leads gradually towards rounded grains in blunting needles and sharp angles. Rounded grains have a good cohesion, so low gradient in a layer leads generally to an increase of the cohesion. Typically, fresh snow, partly decomposed precipitation particles and faceted crystals undergo this kind of metamorphism. The same phenomena also occurs when two different grains are set in close contact, generally through the wind action, in creating quickly an ice neck due to the important initial curvature between the two grains. This sintering effect is an important factor in the cornices and wind slabs formation and is at the root of many artificially triggered avalanches. Most of the accidents in backcountry-skiing are due to this kind of avalanche (see 3.3.1.3, 3.3.1.5, 3.5.2) . - medium gradient As the temperature gradient is there significant, the water vapour is forced to move up from the warm to the cold parts. The temperature gradient leads to the formation of faceted grains. Medium gradient is frequent in a snowpack. So, faceted crystals are often present and generally well seen by observers. The cohesion of theses layers is low. It is important to mention such layers inside a snowpack because it can be representative of a weak layer into a slab structure (see chapter 3.3.1.5). Faceted crystals can evolve in a dry snow. A low gradient will be efficient on these grains and will conduct to an increasing of the cohesion. On the other hand, a large

	gradient will modify crystals and a decreasing of the cohesion will be the consequence. - large gradient When the temperature gradient is large, the crystal growth rates are important depending also on the crystal pores (density). These conditions produce angular or faceted grains which can later develop steps and striations on their surfaces; the final result is a large cup crystal called depth hoar. A depth hoar layer is the "typical" model of weak layer (see chapter 3.3.1.5). Crystal size can be very large (several mm) with a very low cohesion. Moreover, depth hoars are less affected by low or medium gradient, so after their creation, they stay in the snowpack under this form. Only, a wet metamorphism will cause their disappearance. In fact, large gradients are not rare in a snowpack. Temperatures are often very different between surface and bottom, especially with dry, cold and no-cloudy meteorological conditions. So, when the snowpack is not thick (usually at the beginning of the winter), temperature gradient can be very large.
	3.2.3.2.2 in wet snow, melt metamorphism
	In this case, temperature is near 0°C, Liquid Water Content governs the metamorphism process in slightly decreasing the melting temperature according to the curvature and capillarity pressure. The liquid water appears first on the bonds between grains and surrounds the crystals with a small liquid film. In the neighbouring of concave parts, this film generally refreezes and gives back energy. This heat quantity is so available to make the smallest grains melt so as the most convex parts of the bigger grains. The small grains so disappear and the bigger ones become more rounded with homogenised sizes as presented in ***Figure 40***. Some water liquid is thus available in order to continue the process. Generally, this transformation is faster than in a dry snow (several hours or a day may be sufficient) due to the facts that liquid water is 20 times better thermal conductor than air and that no air vapour diffusion occurs. The initial crystal is not very important in a wet metamorphism, all crystals are affected and, always, wet grains are the result of this transformation. If wet grains is rapidly present, the increasing of the grain size may be longer and will mainly depend on the Liquid Water Content.

Figure 40 Rounding and size increasing mechanisms in wet snow metamorphism (from CEN/CS)

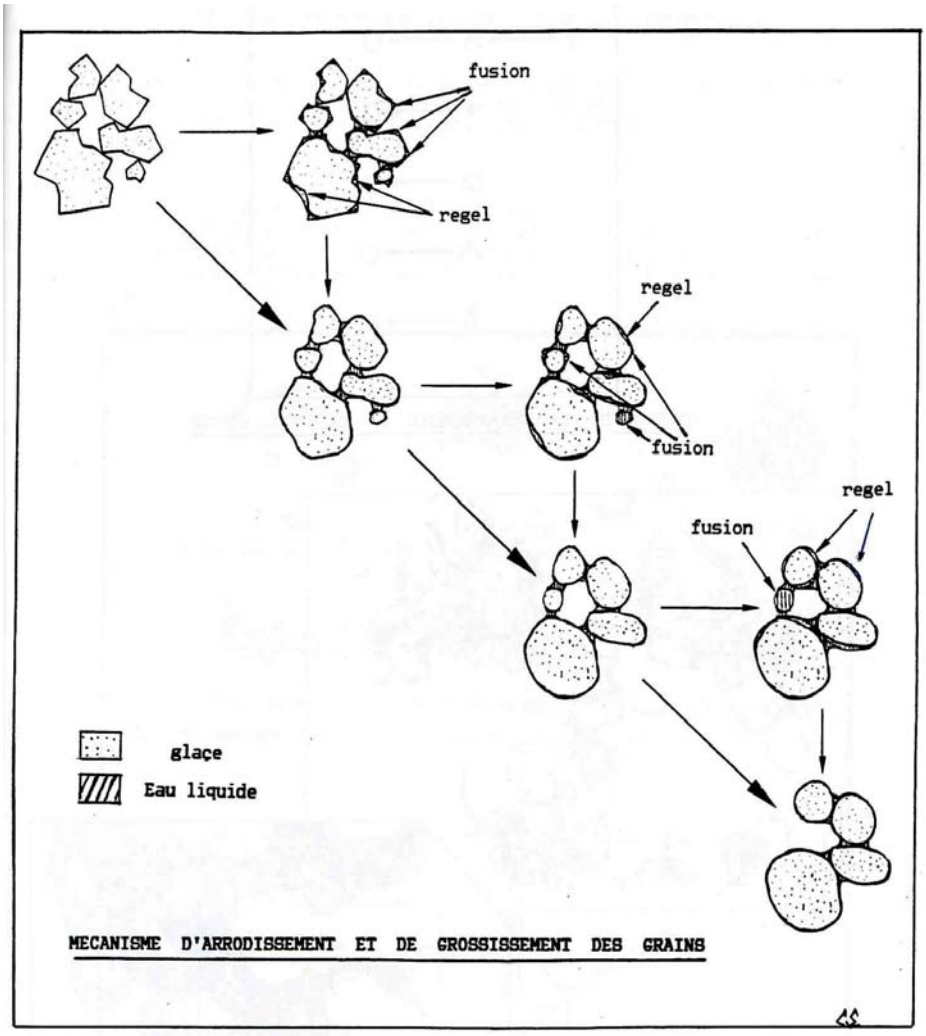

3.3 Instability factors and procedures

This chapter describes main causes that may lead to an instable snowpack. Typically, these causes are classified in 2 groups: meteorological events in a first group and the causes which are linked to the topography in a second group. The factors of the second group are invariable while the first group can vary in both time and space and may include a random component.

3.3.1 Meteorological causes

3.3.1.1 Snowfall

The number of avalanches likely to occur depends directly on the quantity of new snow or, more precisely, on two interdependent factors, the quantity and the duration of snowfalls. The shorter the duration for a given quantity of snow, the greater the number of avalanches, i.e. they will occur on more slopes with decreasing angles.

	3.3.1.2 Rain
	Rain has 2 consequences; it increases the liquid water content and the weight of the snow layers. Rain is a very effective and often spectacular cause of snowpack destabilisation. Widespread heavy rainfall on a snowpack can lead to multiple avalanches over a short period of time. The effect is all the greater when the snow receiving the rain (primarily on the surface of the snowpack, but also subsequently inside) is not yet highly stabilised (the most frequent case being of course new or recent snow).
	3.3.1.3 Wind
	Snowdrift is the main cause of slab creation (wind slab), an element of the slab structure. Wind during the snowfall or for a period of days after will produce the same effect on the snow particles. The snow crystals break up and their size is considerably reduced. The effects are variable, depending on the duration and intensity of the phenomenon. The grains quickly bond together with an ice neck at each contact point (sintering cohesion). The speed at which the ice necks form depends on the temperature, but above all on the size of the grains (inversely proportional), i.e. the smaller the grains, the faster sintering takes place. At a temperature of -10°C, an ice neck with a length equal to one tenth of the grain radius can form between two spherical grains approximately 0.1 mm in diameter in just a few seconds [Hobbs and Mason]. Consequently, small grains, resulting from the action of the wind, rapidly show good cohesion, which explains, for example, why cornices form during periods of high wind. In addition, the smaller the grains, the greater the number of contact points that form, with as a result greater cohesion and higher density. The location of slabs is therefore directly related to the effects of wind. On windward slopes, part of the snow is removed and drifts form near obstacles. On the lee side of ridge lines, cornices generally form and a bit lower, where the wind slows, the transported snow accumulates, creating wind slabs. Though, generally speaking, the slabs form on the lee slope (if the wind direction is constant), near the ridge line, this is not an absolute rule and slabs may be found far lower if obstacles on the slope block the wind and provoke further snow deposits in the sheltered zone downwind. Intimate knowledge of the terrain and careful observation of wind and snow-transport conditions help in locating high-risk sectors. Snow blowing over high ridge lines or wind during snowfall are signs that slabs are probably forming. In addition, a number of clues confirms the presence of wind slabs: • cornices on the most exposed summits (which are also helpful in determining the local prevailing wind), like ***Figure 41***; • particular snowpack surface conditions (ripples, compacted snow on windblown slopes).

Figure 41 Different topographies that can produce wind slabs

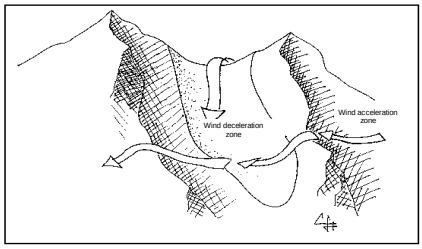

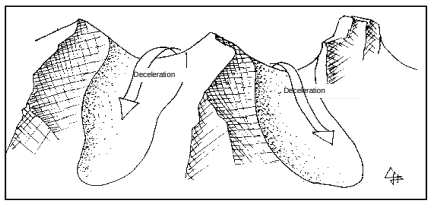

Strong winds are not required. At only 25 km/h, a slab can form in a few hours by snow grain saltation in the 20 to 30 centimetres above the surface.

Concerning the effect of wind on slab formation, studies carried out at the Col du Lac Blanc experimental site (altitude 2700 metres in the Grandes Rousses massif of the French Alps) have determined the wind speeds (measured at approximately 5 metres above ground) required to initiate transport of different types of snow (***Table 12***).

Table 12 Thresholds on the wind speed required to initiate transport

Type of snow	**Wind thresholds (m s^{-1})**
New/recent snow	4
New snow with fragmented particles (50% / 50%)	6
faceted grains	7.5
2/3 fragmented particles, 1/3 rounded grains	8
rounded grains and faceted grains (50% / 50%)	8.5
2/3 rounded grains, 1/3 fragmented particles	10
rounded grains (diameter 0.3 mm)	12
Wet grains (diameter 1.0 mm)	20

3.3.1.3 Temperature and temperature gradient

A rapid increase in the air temperature, rising above 0°C and accompanied by strong solar radiation, can result in major destabilisation of part or all of the snowpack if a significant percentage of liquid water is produced (due to melting of a varying proportion of the snow grains). The greater the quantity of liquid water, the greater the destabilisation.

Often, presence of weak layers is due to medium or large temperature gradient in the snowpack. These layers are necessary to make a slab structure (3.3.1.5 section). Such gradients are not rare in high mountains. For example, dry weather during 2 weeks can

be enough to generate depth hoar, especially in the north faces.

Cold temperatures, after a snowfall, affect the settlement of the new snow layers. So, stability of these layers will increase more slowly than with warmer temperatures.

3.3.1.5 Snowpack conditions: the slab structure

A snowpack is composed of different layers (***Figure 42***); one of the most dangerous structures is composed of a slab over a weak layer.

A snowpack with a slab structure made up of:

- One or more snow layers showing a degree of sintering cohesion that depends on the time since the snowfall occurred and the speed of the wind during the snowfall. Formation of the vast majority of these layers is due to wind. They may also be formed by metamorphic processes taking place at low temperature gradients, but this takes much longer.

- A weak underlying layer on which the above layer can collapse and slide, forming an avalanche.

Figure 42 The slab structure

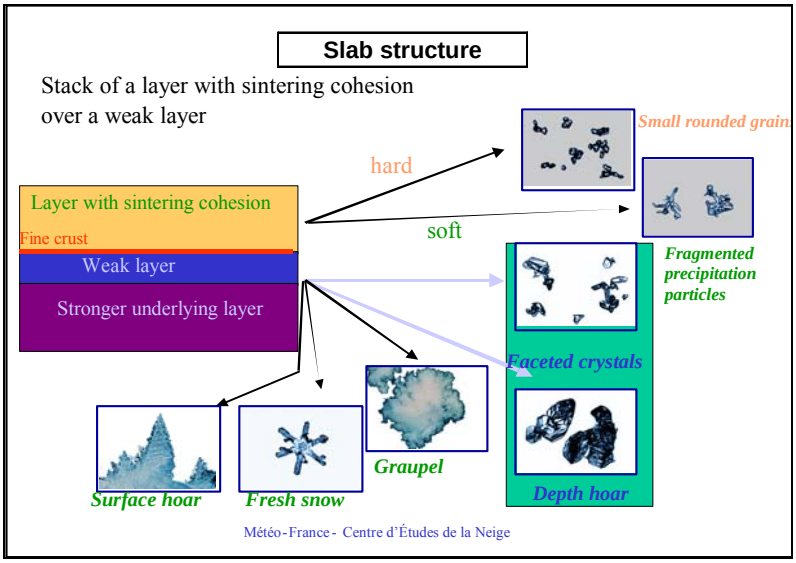

Slab formation. The upper layer, showing greater cohesion, is generally formed by the wind during or just after a snowfall. The conditions for the surface snow and wind are discussed in the 3.3.1.3 section. Cohesion is often enhanced if the temperature gradient within the snowpack is low. Wind is not always the cause of the creation of slabs, sometimes, low gradient may lead also to these formations.

Formation of weak layers. Layers are said to be weak when their intergranular cohesion is lower than that of more recent layers. Layers composed of depth hoar, faceted grains or, to a lesser degree, buried surface hoar or graupel are examples of layers with low cohesion. Weak layers may also be made up of recent snow not

	subjected to little or no wind.
	3.3.2 Environnemental causes (Terrain in the avalanche starting zone)
	Slope angle. Because gravity is the basic cause of flow, the steeper the slope, the greater the risk under otherwise equal conditions. However, on slopes steeper than 45°, the snow generally flows spontaneously during snowfall. Inversely, avalanches rarely occur on slopes with angles less than 20°. Note however that powder avalanches (with a powder cloud) can cause damage even on slopes opposite those where avalanches occur. Changes in slope are often the cause of triggering due to the increase in snowpack deformation (new distribution of stresses) due to tension. **Aspect**. Exposure to the sun is an essential factor in the modifications that take place in the snowpack. The absence of sunlight on north-facing slopes slows settlement (and consequently stabilisation) of the snowpack. Solar radiation is the driving force behind melt-freeze metamorphism in the spring on slopes facing east, south or west, depending on the time of day. Note that the amount of solar energy received at the snow surface depends on the angle and aspect of the slope with respect to the position of the sun in the sky. At mid-latitudes of the Northern Hemisphere, slopes with a southern aspect generally receive more solar radiation than an equivalent flat surface, especially in winter and early spring. **Vegetation and ground**. Forests protect against triggering in starting zones due to their capacity to "fix" the snowpack, as long as the forestation is sufficiently dense. Low-lying vegetation can increase the roughness of the ground, thereby increasing friction with the snow, but at the same time slows settlement of the snowpack, thereby reducing cohesion. Grass that is neither mown or grazed favours gliding and full-depth slab avalanches. Rough ground (presence of blocks, scree, etc.) offers better resistance (higher friction) to snowpack slip. Inversely, schist slabs or other smooth surfaces offer far less retention. **Snow surface conditions**. The roughness of the surface layer of snow can play a major role in snowpack stability following a subsequent snowfall. A surface pockmarked by rain or grooved by the wind offers a better grip for a layer of new snow than an icy or smooth surface. **Altitude**. Altitude is not a decisive direct factor because avalanches occur at all elevations. However, it does have a direct impact on snow and weather characteristics (quantity of snow, metamorphism, etc.).
	3.3.3 Instability procedures and break process
	The weight of the snow induces a gravity stress. When the snowpack is on a slope, this stress can be decomposed in a slope perpendicular component, the compressive stress (settlement), and a slope parallel component, the shear stress. In general, shear stress is related to instability and compressive stresses to stability. The shear stress increases

	with the slope. Anchors and cohesion between grains of the layer are opposite to the shear stress and are synthesised by the shear strength which allows the snowpack to stay on the slope. 2 events may suppress this balance : increasing of the stress or decreasing of the cohesion : - increasing of the stress : Usually, we distinguish rapid and gradual increasing of the stress. Consequences may be different, because, in case of gradual increasing, settlement will allow an increasing of the cohesion. A gradual increasing is usually associated to meteorological conditions : snowfall, rain, or wind (which may create local accumulation). At the opposite, a rapid and sometimes temporary increasing will be, often, associated to an exterior factor, typically, falling cornice, animal, explosive or skier. - decreasing of the cohesion : The typical case is the snow melting. It causes an increase of the liquid water content and can induce a decreasing of the cohesion. Rain for the same reasons may also affect cohesion in the snowpack. Medium or large temperature gradient also affects cohesion. However, this transformation is slow and settlement has an opposite effect and increases cohesion. So, this metamorphism is rarely a direct cause of avalanche release. Majority of deaths by avalanche is due to the presence of a human on a slope when the snowpack has a slab structure. So, it is important to explain this particular case. In this example, we consider the case of a skier (***Figure 43***).
Figure 43 Skier on a snowpack with a slab structure. In this case, the weak layer undergoes an additional stress due to the skier weight	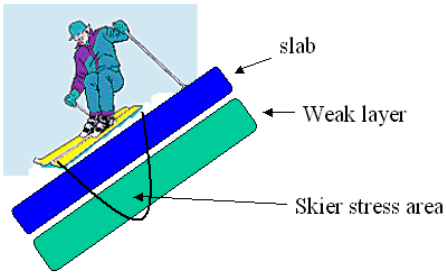
	The snowpack undergoes an additional shear stress due to the skier. The slab is able to receive this stress (sintering cohesion) and propagates it easily. In the weak layer, the cohesion (shear strength) may be too low, and, if the rate of deformation is fast enough, cracks initiate in the weak layer. Then, fracture develops that spreads upslope and across the slope. This fracture reduces the attachment of the slab and rapid tensile fracture occurs from the bottom to the top of the slab to form the crown. It is the beginning of the avalanche.

	Several parameters have thus to be taken into account to evaluate the avalanche hazard in such conditions: - parameters linked to the skier : weight of the skier, ski characteristics, movement of the skier , the skier is isolated or in a group, … - parameters linked to the snowpack : depth and shear strength of the weak layer and slab, thickness and hardness of the slab, fresh snow at the surface (skier sink in the snow), … The additional stress due to the skier decreases with the depth. Usually, when the weak layer is, at least 1 meter buried down the surface, it may be neglected.
	3.4 Avalanches description and definition
	3.4.1 Triggering classification
	Avalanche triggering may have a number of causes. If the structure of the snowpack (directly related to past and present weather conditions) is the only cause, the avalanche is said to be **spontaneous**. Otherwise, the avalanche is said to have been **released**. In this case, it results from an external factor, i.e. the additional load is not directly related to weather conditions. Without the external factor, the snowpack would not have moved and there would have been no avalanche. There are four types of avalanche triggering. • **Spontaneous avalanches**. The avalanche is due to changes in the snowpack, themselves directly related to weather and snow conditions. • **Naturally released avalanches**. The avalanche is caused by an external, non-human factor (fall of cornices, seracs, rocks, passage of animals, earthquakes, etc.). • **Accidentally released avalanches**. The avalanche is caused by an unintentional, human factor (skier, snowboarder, snowshoer, etc.). • **Artificially released avalanches**. The avalanche is caused by an intentional, human factor (artificial triggering).
	3.4.2 Avalanche classification
	Recent-snow avalanche (powder and soft slab) Slab avalanche Wet-snow avalanche **Recent-snow avalanches**

	Dry snow (T < 0°C) with low cohesion (density <= 100 kg/m3) Type of starting zone: Point or linear Powder avalanches. When spontaneous, these avalanches are triggered primarily during or just after snowfalls. Soft-slab avalanches. The dry snow has low to moderate cohesion (100 kg/m^3 < density < 200 kg/m^3). It is deposited on a weak layer. When spontaneous, these avalanches are triggered primarily during or just after snowfalls. They can also be triggered well after the snowfall by wind-transported snow deposited on the slab. These avalanches can also be released naturally, accidentally or artificially a fairly long time after snowfalls (several hours to a few days). **Slab avalanches** Dry snow (T < 0°C) Type of starting zone: Linear Cause of 80% of avalanche accidents The snow has high cohesion (density > 200 kg/m^3). It is deposited on a weak layer. When spontaneous, avalanches are triggered primarily during snowfalls on the slab. These avalanches can also be released naturally, accidentally or artificially a long time after snowfalls. **Wet-snow avalanches** Wet snow (T = 0°C) Type of starting zone: Point or linear The snow has a low to high liquid-water content (density > 200 kg/m^3) caused by solar radiation, rain or the humidity of falling snow. These avalanches are generally spontaneous and only occasionally released naturally, accidentally or artificially. This classification has been adopted by the majority of European avalanche-forecasting services. Other classification criteria encountered are the types of triggering (presented above) and often the flow dynamics (dry, dense-flow, powder).
	3.4.2 Avalanche zones and flows
	The triggering of a rapid downhill gravitational flow in the form of an avalanche

requires special conditions concerning the snow, slope and instability of the snowpack. The term "rapid" is used here to distinguish between avalanches and "gliding" snow that moves slowly on smooth ground at velocities of a few millimetres to metres per day. However avalanche velocities can vary greatly depending on the type of snow involved.

Rather than speaking of a "classification", which would appear poorly suited to a phenomenon related to modifications in the snowpack, we prefer to speak of types of avalanches and to group similar avalanches (***Table 13***). This presentation is based essentially on the snow conditions (types of crystals, density, etc.) in the starting zone and on the mechanical triggering conditions. The types of avalanches correspond basically to the various stages in the transformation of the snow deposited on the ground and depend significantly on the past and present conditions affecting the snowpack.

An avalanche takes place in three phases: starting, flow and stopping. Each phase corresponds to a zone and each zone has its own classification criteria. Among the main criteria are the type of starting zone, condition of the snow, position of the bed surface, topography, type of flow, appearance and content of the deposited snow, etc. A number of criteria must therefore be considered when classifying an avalanche.

When considering aspects related to snow and weather conditions, the starting zone must be given priority. Here lie the causes of the movement of part or all of the snowpack. The significant criteria that we will use to classify the main types of avalanches will therefore be, in addition to the type of triggering mentioned above, the **type of starting zone** and the **condition of the snow** set into motion in the zone.

Other classification criteria are possible, notably concerning the type of flow (powder or dense-flow avalanches) or the position of the bed surface (ground or a layer in the snowpack). These characteristics are used primarily in determining the consequences of an avalanche (damage) rather than the causes, i.e. in view of protecting against the phenomenon.

Starting zone. This is where movement begins, the initial phase in avalanche triggering. It is also called the accumulation zone. Its topographical characteristics, exposition to wind, the sun, etc. all contribute, in addition to the snow conditions, to the avalanche-triggering conditions. There are two types of starting zones, point or linear (***Figure 44***), that depend essentially on the degree of snow cohesion. A point start occurs with loose snow (low cohesion, dry or wet), whereas a linear fracture (***Figure 45***) is characteristic of a slab of dry snow with greater cohesion. In the latter case, a number of vertical cracks may be observed.

Figure 44 Point start	
Figure 45 Linear start	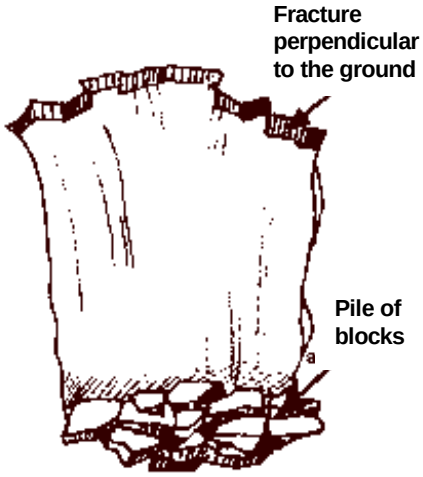
	Flow zone (Track). Generally speaking, the flow zone is directly influenced by the topography, vegetation and the snow conditions. Most often, it is a couloir, slope, etc. In certain cases, snow pick-up occurs, i.e. the avalanche gains mass during the flow phase with the addition of snow along the track. **Deposition zone** (Runout). This is where the avalanche gradually looses its energy and finally stops. The moving mass of snow is deposited in this zone, also called the sedimentation zone. The zone may be clearly or poorly defined, depending on the type of flow. In the event of a powder avalanche, for example, the zone is very large, but hard to identify.

Table 13 Avalanche morphology classification criteria (CEMAGREF/CEN)

ZONES	CRITERIA		DISTINGUISHING CHARACTERISTICS
Starting zone	**Type** of triggering		◆ **Spontaneous**. Internal causes within the snowpack (spontaneous avalanche) ◆ **Released**. External causes (released avalanche) ● Natural (non human), i.e. cornices, seracs, rocks, animals, etc. ● Human ○ Unintentional (accidental) ○ Intentional (artificial)
	Type of starting zone		◆ **Point**. Avalanche starts from a point, fanning out downhill (inverted V shape) ◆ **Linear**. Slab avalanche with a distinct fracture line at the top
	Snow **conditions**	Liquid-water content	◆ Zero. **Dry snow** ◆ Low. **Moist snow** ◆ High. **Wet snow**
		Cohesion	◆ Low. Avalanche of **powder** or **wet** snow ◆ Low to moderate. **Soft slab** ◆ High. **Hard slab**
		Type of snow	◆ **Recent** ● Not wind transported, fresh or fragmented particles ● Wind transported, fragmented particles or small rounded grains ◆ **Metamorphosed** • faceted grains / round grains
	Position of the bed surface		◆ **Within the snowpack** (surface-layer slab avalanche) ◆ **On the ground** (full-depth slab avalanche)
Flow zone (Track)	**Type** of terrain		◆ **Open slope** ◆ **Couloir** or gulley
	Dynamics (Type of flow)		◆ **With cloud** of airborne snow particles: ● at the avalanche front ● behind the front ◆ **Without cloud** (dense-flow avalanche)
	Snow pick-up		◆ **Yes** ◆ **No**
	Blocks and/or other debris		◆ **Yes** (slab chunks, ice, rocks, trees) ◆ **No**
Deposition zone (Runout)	Surface **roughness**		◆ **Smooth** (fine deposit) ◆ **Rough** (coarse deposit with blocks, lumps, etc.)
	Snow **conditions**		◆ **Wet** (wet deposit) ◆ **Dry** (dry deposit)
	Visibly **contaminated** deposit		◆ **Yes** (avalanche contaminated with soil, ◆ **No** (clean avalanche)

3.5 Triggering causes and mechanisms

3.5.1 Recent-snow avalanches

	This type of avalanche involves dry snow with a low degree of cohesion and occurs after recent heavy precipitation. However, recent-snow avalanches can also be composed of wet snow if, following snowfalls, rain makes the snowpack heavier and less stable. In the latter case, the avalanche is of the wet-snow type. The air temperature during the snowfall, wind and changing precipitation intensities significantly influence snow conditions on the ground. The starting zone is generally the point type, with the flow fanning out downhill and the volume of snow increasing with the track distance, as long as the slope and snow conditions remain favourable. The snow is generally new and/or made up of fragmented particles. The density is most often less than 100 kg/m3. In short, it is recent snow that fell with little wind. If wind and air temperature are very low, the result is a powder avalanche described below. If sintering cohesion (caused by the wind or rounding due to a low temperature gradient) has started on or near the surface of the snowpack, a linear start may occur, in which case it is a soft-slab avalanche (described below). The flow velocity depends on the slope. If the slope becomes less steep or turns upward, triggering is often limited to a sluff (small snow slide) commonly seen on the surface of the snow pack after snowfalls. If the slope is steeper and the mass of flowing snow greater, a powder avalanche may occur (see the section on powder avalanches below). The conditions of the underlying surface (snow layer or ground) also play a decisive role in the triggering of recent-snow avalanches. The type of snow on the surface of the snowpack when the snowfall occurs determines the bond with the new layer. For example, an ice crust or snow with very low cohesion, such as surface hoar, increases the risk of an avalanche. Inversely, a surface with some relief, such as small ripples or waves caused by the wind, will bond better with the new snow. Triggering is most often spontaneous and takes place during or just after heavy snowfalls. Note however that snow stabilises much more slowly on north-facing slopes than on slopes exposed to the sun. Triggering depends primarily on the weight and intensity of precipitation. The unstable accumulation of fragile snow crystals does not have the time to settle before reaching the failure point. Although fresh snow can hold on fairly steep slopes due to crystal interlocking, the balance is delicate and the slightest disturbance or increase in weight due to more falling snow can trigger an avalanche.
	3.5.1.1 Powder avalanches
	Depending on the slope, and consequently the velocity, and on the mass of available snow on the track, a powder cloud of snow and air (an aerosol) forms in front of the avalanche (***Figure 46***). The flow velocity produces turbulence that picks up the lighter snow particles and mixes them with the air. This mixture flows at high speed downhill.

	The flow velocity of the aerosol can exceed 200 km/h. This type of avalanche has a high energy level that pushes the air in front, creating an air blast. Major damage is caused more by the air blast and the velocity of flow than by the mass of the moving snow. In the absence of damage to life and property, the passage of a powder avalanche is often difficult to detect. The flow follows a straight line and damage may be caused on the opposite slope. This phenomenon is called a powder avalanche. Because powder avalanches follow major snowfalls, hikers and other mountain recreationists are rarely present. However, in some cases, these avalanches can damage homes, forests and roads, for example the avalanches that occurred in February 1999 in Montroc (France), Evolène (Switzerland) and Galtür (Austria).
Figure 46 Powder avalanche	
	3.5.1.2 Soft-lab avalanches
	The upper layer is made up of fragmented particles, often with small rounded grains, and there is low to moderate sintering cohesion (necks at contact points between grains). This layer has a density between 100 and 200 kg/m^3. It is often formed by a low to moderate wind during or just after the snowfall. This type of avalanche, made up of light, dry snow, may produce a powder cloud (***Figure 47***), because the moving slab breaks up to a large extent during the flow. In some cases the slab may be covered with new snow (no cohesion), which will increase the powder content of the flow.

Figure 47 The fracture line is clear and an aerosol (powder cloud) rapidly forms in front of the flow	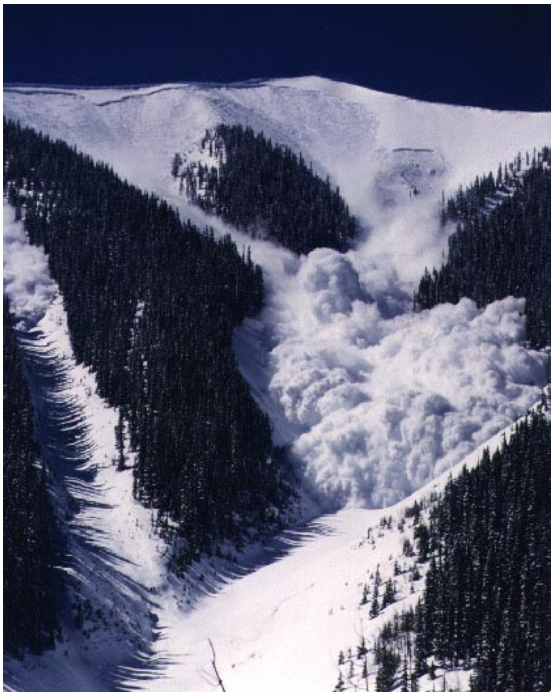
	3.5.2 Slab avalanches
	It is difficult to locate slabs, particularly if they are covered with a thin layer of new snow. It is also difficult to estimate slab instability because it depends on conditions inside the snowpack. Whether the slab is hard or soft, this type of avalanche is the most dangerous for mountain recreationists and is the cause of virtually all accidents. Once they have occurred, slab avalanches are easy to identify due to the fracture line at the top of the starting zone (***Figure 48***). The fracture may measure a few metres or several hundred metres if identical conditions prevail over an entire slope (see the photo below).
Figure 48 The fracture line spans the entire slope. Note the overhanging cornice, a sign of wind accumulation	
	Depending on the degree of cohesion and the density of the snow in the starting zone, there are two types of slab avalanches involving either soft slabs and hard slabs. The

	distinguishing features are essentially the type of movement and the type of deposit. If the layer of snow breaks up rapidly, it is a soft slab (one type of recent-snow avalanche). An avalanche made up of compact blocks of snow is the result of a hard slab. The density boundary between the two types of slab is approximately 200 kg/m3, however, the slope conditions (angle and length) are also important factors in determining the type of avalanche. Slab avalanches are triggered by a fracture in the upper part of the snowpack, made up of a cohesive layer (sintering cohesion) on top of a weak layer, caused by an additional load which locally breaks the weak layer. Triggering may be spontaneous (snowfall, rainfall, wind-transported snow) or the avalanche may be released unintentionally by one or more persons (on foot, snowboards, skis, snowshoes, etc.) or naturally by the fall of a cornice, rock, etc. The rigidity of the slab, even minor rigidity, contributes to propagating the fracture over distances that can be very long. Note that the stresses produced by skiers decrease with the thickness of the snowpack. Consequently, most unintentional triggering takes place when the slab is less than one metre thick. Another aspect is that a slab rarely has a constant thickness over the entire slope. It is often thicker in the middle than on the edges. Skiers propagate the stresses in the snow via their skis. If two or more skiers gather together, the stresses exerted by each skier may cumulate and set the slab in motion, whereas skiers maintaining a certain distance between each other could have avoided the avalanche. In-depth knowledge on the internal modifications of the snowpack as a function of the observed weather conditions is required and indeed indispensable to better gauge the risk of slab avalanches. These avalanches may occur a number of days after the formation of the slab. Stratigraphic, penetrometric and stability tests are most useful in determining the local stability of the snowpack. However, the often high degree of spatial variability of the snowpack limits the representativeness of a given observation point and complicates efforts to determine stability in the field. A slab, generally created by the wind, is made up of compact snow, i.e. a majority of rounded grains and possibly fragmented particles, with a density ranging from fairly high to high (200 to 400 kg/m^3). The avalanche is characterised by blocks of snow along the track and in the deposition zone (see ***Figure 49***). In comparison with a soft slab, note that a hard slab will better resist the passage of a skier because the stress due to the weight is more superficial and consequently the risk of reaching the underlying weak layer will be less. However if triggering does occur, the resulting fracture line is longer and the result is a larger avalanche. Note that the strength of a hard slab also depends on its thickness. The distribution of snow in slabs created by wind is highly variable and triggering often occurs in the thinnest sections, however the fracture is propagated over large distances and sets major quantities of snow in motion.

Figure 49 The fracture is linear, the snow compact (likely deposited under windy conditions) and blocks are found along the track	
	3.5.2 Wet-snow avalanches
	This type of avalanche occurs in snowpacks made up, in part or in whole, of wet grains resulting from the metamorphosis of wet snow. The risk of triggering is directly related to the presence of liquid water because the temperature of the snow is 0°C. There are two possible sources of the liquid water. The first is melting of the snowpack, generally in the spring, on slopes facing east, south or west, depending on the time of day. The second is rain which, in addition to increasing the weight and consequently the stresses in the snowpack, contributes to saturating the upper layers. Point starts are most common, but in snowpacks where certain layers still show a degree of sintering cohesion, fracture lines may occur. The wetting of the layers is not always uniform and high sintering cohesion may persist locally. The slopes most exposed to the sun (depending on the season) will be the first to trigger. Avalanches may occur on slopes only slightly steeper than 25°. These avalanches often take place on known tracks, well identified because they depend mainly on topography. They can cause significant erosion. However, entire slopes may be affected by this type of avalanche and grassy areas in particular are ideal triggering zones. The frequency of avalanches means vegetation does not have time to grow in the track and results in bedrock being exposed. The pressure exerted by the avalanche on obstacles in the track represents several dozen tons per square metre. That explains why trees and rocks are picked up and transported. This type of avalanche transports vast quantities of snow, often with other debris, to the valley bottom. The deposition zone comprises rough blocks with high densities (up to 500 or 600 kg/m^3), piled up in a runout cone that can be many metres deep. In such a case, the pile

of snow may remain in the valley late in the season, even after the surrounding vegetation has long turned green.

Wet-snow avalanches are triggered by an increase in the liquid-water content (LWC). Snow layers subjected for the first time to a high LWC rapidly lose cohesion. The water tends to filter through the snowpack and accumulates in certain layers. If it meets an impermeable layer (melt-freeze crusts or ground) or a less permeable layer, the liquid water accumulates, its runoff serving as a lubricant, and the layer may constitute a bed surface for an avalanche.

In addition to the decrease in friction between certain layers, there is also a decrease in strength due to the considerable loss of cohesion. The layers of snow that were initially dry, with low cohesion (faceted grains, depth hoar, new snow, fragmented particles, graupel) are the layers primarily affected by the destabilisation.

Even though wet-snow avalanches can occur throughout the winter season (during warm periods with heavy rainfall), they generally take place in the spring when solar radiation is stronger and longer, and the snow albedo lower, particularly during the afternoon when the energy absorbed by the snowpack is at a maximum. That being said, if certain weather conditions prevent refreezing during the night, triggering may occur at any time. The aspect of the slope also plays an important role. Depending on the time of day and the season, slopes facing east (in the morning, particularly in the spring), south and west (until the end of the afternoon on hot days) are particularly dangerous.

Monitoring of snowpack LWC at different altitudes and on slopes with different aspects is useful to assess the risk of triggering for this type of avalanche.

Rain falling on recent snow is a major cause of wet-snow avalanches that can occur in large numbers under such conditions (as in February 1980 and December 1990 and 1991 in the Alps). Wet-snow avalanches can also occur in the middle of winter for the same reasons (additional load, melt-freeze metamorphism, a reduction in the stability of the snowpack, etc.).

3.6 Main triggering thresholds

The triggering thresholds for spontaneous avalanches involved the following meteorological parameters:

the quantity of new snow over a limited time period (a few hours to a few days), and the accompanying wind conditions, that cause recent-snow avalanches,

the quantity of rain falling on the snowpack and/or significant and rapid temperature rises, that cause wet-snow avalanches.

The quantity of new snow is the parameter that most frequently causes major, spontaneous avalanches. Examples are Val d'Isère (France) in February 1970, Montroc

	(Chamonix-France) in February 1999 or Galtür (Austria), also in February 1999. Heavy rainfalls have a frequency of occurrence that depends on the location in question. For example, they are frequent in the Pyrenees and in the western half of the French Alps, but less frequent in the north-eastern part of the Alps. Concerning temperature rises without precipitation, though they often cause avalanche activity (occasionally sustained) on sunny days in spring, they rarely produce major, spontaneous avalanches (one exception, however, was at the end of March 1996 on the French side of the eastern Pyrenees).
	3.6.1 Recent-snow avalanches
	Quantity and duration of snowfalls are the 2 mains parameters to consider. But it is also necessary to take into account the presence of any snow having fallen more or less recently and that may have retained the characteristics of "recent snow", due essentially to cold temperatures and the lack of exposure to the sun (typical conditions during the main winter months). Note that variations in intensity frequently occur during a single snowfall. This phenomenon tends to increase the instability of the layer of new snow. The wind is also a factor in that it creates large drifts and cornices that further contribute to instability. However, at the same time, it tends to localise the most unstable zones of the snowpack. Concerning the size of avalanches, this depends on a number of criteria. The first is the total thickness of new snow plus recent snow, which can be referred to as the quantity of available snow for an avalanche. There are other important parameters. Some concern snowpack conditions, e.g. the existence of a certain thickness of snow likely to be picked up by an avalanche along the track, thus increasing its volume, or the presence of a sufficiently thick snowpack at intermediate and lower altitudes on which the avalanche can slide more easily to reach low altitudes where human residences and infrastructure are located. Others are topographical, of which the most important are the angle and length of the slope on which the avalanche flows, as well as the roughness of the slope (e.g. presence of numerous trees or large rocks).
	3.6.1.1 Quantity of new snow
	Practically speaking, it is possible to define depth thresholds corresponding to different levels of avalanche activity. The thresholds are in fact ranges due to the influence of the many factors mentioned above. - 30 to 60 cm: avalanches only on steep slopes and usual locations - 60 to 90 cm: avalanches on moderate slopes (between 30° and 40°) and large avalanches cutting transportation routes - ≥ 90 cm: widespread danger, very large avalanches endangering residences and

	transportation routes The latter threshold, which corresponds to an exceptionally high level of spontaneous avalanche activity, can be broken down as a function of the intensity. in 24 hours: 60 to 80 cm in 48 hours: 70 to 90 cm in 3 days: 90 to110 cm in 4 days: 100 to 140 cm in 5 days: 130 to 160 cm in 6 days: 140 to 180 cm in 7 days: 150 to 200 cm
	3.6.2 Slab avalanches
	Strictly speaking, triggering thresholds do not exist for slab avalanches. Wind (past and present) is an important factor to monitor. It can give information on the possible presence and localisation of slab. It is difficult to indicate weakness thresholds for the weak layers that cause tripping of slab avalanches. That being said, observations indicate that for angular snow grains, if the density decreases or the diameter increases, cohesion drops.
	3.6.3 Wet-snow avalanches
	The water-retention threshold of a snow layer depends on the type of snow and its density. It is approximately 10% in weight (10% in LWC weight for snow with a density of approximately 250 kg/m^3 and 7% for snow with a density of 500 kg/m^3). Penetration of the liquid water into the inner layers of the snowpack is often highly variable and follows specific routes (percolation paths). If the water meets an impermeable or less permeable surface in the lower layers of the snowpack, the snow collects the water, which may lead to destabilisation of the snowpack and an avalanche.
	3.6.3.1 Rain
	The quantities are not as clearly defined as those for new snow. It is, however, possible to indicate a minimum quantity required for major destabilisation of at least a part of the snowpack (the upper layer(s)) and a maximum quantity above which any further rain produces no effect. Roughly speaking, the minimum quantity is approximately 10 mm over 24 hours for major destabilisation of the upper layers where the snowpack is made up of recent snow (low density) and not very thick. The maximum quantity is between 30 and 70

	mm over 24 hours for destabilisation of a significant part or of the entire snowpack, depending primarily on the total thickness of the snowpack and its average density (or the water equivalent of all the snow layers).
	3.6.3.2 Significant and rapid temperature rises
	Again, it is not possible to set precise thresholds because the effect of a significant and rapid temperature rise depends on the snow and meteorological conditions, i.e. the condition of the snow affected by the warming and, more generally speaking, the weakness of the layers, which itself depends on other meteorological factors such as the wind and the amount of solar radiation. Note that the consequences of temperature rises on the snowpack differ depending on the duration. For example, following a rise of several degrees over a few hours, the upper layers of the snowpack are destabilised and may trigger a surface-layer slab avalanche, generally with a limited volume. For a more significant increase over a number of days, a much thicker layer of the snowpack is likely to participate in an avalanche or even the entire snowpack, with as a result a full-depth slab avalanche with a large volume.
	3.7 Typical meteorological situations causing major spontaneaous avalanches
	Though the situations would be expected at first glance to be very different for the various mountain regions considered in Europe, they in fact differ only in details and it is possible to determine typical situations. That is because all the mountains covered by the study have the same type of climate, i.e. the ocean climate of temperate zones. The differences between regions are due simply to regional variations in the standard climate (standard ocean, cold ocean, ocean with more or less continental trends, Mediterranean, etc.), to which the local influence of the relief must be added. Heavy snowfalls and rainy warm spells, the cause of major, spontaneous avalanches, occur during highly active weather disturbances that generally move from west to east. There are, however, two main types of weather situations that produce serious, spontaneous avalanches due to the high level of precipitation: - passage of a highly active disturbance, generally from west to east, where the direction can in fact be any westerly direction between north to south, - passage of the northern part of an active disturbance, during which the winds blow in the opposite direction, i.e. in any easterly direction from north to south. This type of situation featuring an easterly return is often given a special name locally, for example, the "Lombarde" in the French Alps along the Italian border. This is the case when the centre of the depression causing the disturbance is located in low latitudes, not far from the mountain region in question.

	In both cases, the exact wind direction (or high-altitude flow) that causes the heaviest precipitation over a mountain region depends on the latter's geographic location with respect to the entire mountain range and the orientation of the major neighbouring valleys. Once again, in each case, the quantity of new snow brought in by the disturbance depends on the intensity of the precipitation and the time during which the disturbance affects the given mountain region. Consequently, a relatively moderate disturbance that holds over a region for a number of days may cause a level of avalanche activity comparable to that of a highly active disturbance that rapidly moves on. Extreme avalanche situations result when a disturbance is highly active and stagnates or moves very slowly, e.g. the very active easterly return that hit the eastern Queyras mountains in France for six days in January 1978. Below are listed typical meteorological conditions that create exceptional avalanche conditions for mountain regions in certain countries, together with dates of examples that have occurred.
	3.7.1 French Alps
	• Northern Alps - Highly active disturbances from the west to north-north-west. Examples are February 1970 in Val d'Isère, end of January/beginning of February 1978 in the Savoie, Haute-Savoie and Isère departments, January 1981 in the Savoie and Isère departments, February 1984 in the Savoie and Isère departments and February 1999 in Chamonix-Montroc (Haute-Savoie). • Southern Alps - Highly active disturbances from the south to west. Examples are February 1984 in the Thabor region (west wind), January 1996 Haut-Var/Haut-Verdon region (Estenc - south-west wind) and beginning of March 2001 in the Mount Pelvoux region (Le Monêtier - west-south-west wind). - Highly active easterly returns of very large disturbances running from west to east, with an isolated depression in the Mediterranean near the Gulf of Genoa (the concerned zone is a narrow band just a few dozen kilometres wide running along the French-Italian border and extending from the Mercantour to the Haute-Tarentaise region). Examples are mid-January 1978 in the eastern part of the Thabor region (Montgenèvre) and in the Queyras (Ristolas) and end of January 1986 in the eastern part of the Queyras (Abriès).

	3.7.2 Corsica
	Disturbances from virtually any direction, but mainly from the west to south-west and, for the Renoso region, from the east to north-east (eastern return), where the heaviest snowfalls most often occur in the beginning of February. Examples are February 1927 (strong east wind), February 1934 (violent east wind) and February 1969 (very strong west wind).
	3.7.3 French Pyrenees
	• Western and Central Pyrenees - Highly active disturbances from the west to north. Examples are January 1972 in La Pierre-St-Martin (Pyrénées-Atlantiques department), end of December 1993 (strong north-west wind) and end of January 2003 (strong, very cold north wind) in La Mongie (Haute-Bigorre region). • Eastern Pyrenees - Highly active disturbances from the west to north. Examples are January-March 1935 in the Capcir-Puymorens region (north, followed by north-west winds), January 1972 in Serra Dal (Capcir-Puymorens region, eastern return followed by disturbances from the north-west) and mid-February 1978 in the Capcir-Puymorens region (west to north-west wind, followed by an eastern return). - Highly active Mediterranean depressions centred near the Balearic Islands. Examples are December 1971 in the Canigou region (three-day eastern return, three weeks after a five-day eastern return), end of January 1986 in the Capcir-Puymorens and Cerdagne-Canigou regions (two-day eastern return).
	3.7.4 Spanish Pyrenees
	Western and Central Pyrenees Disturbances with south winds. Disturbances with north-west winds (particularly in the western section of the Pyrenees). Cold advection of oceanic polar air. Val d'Aran

	Disturbances from the north and north-west. Eastern Pyrenees Disturbances from the west and north-west. Mediterranean depressions centred near the Balearic Islands.
	3.7.5 Italy (provided by AINEVA)
	Regione Valle d'Aosta: The NW area is affected by north-westerly flows; the SE area is affected by southerly flows; the central area is drier than the previous ones. The border area of our Region are the most affected by avalanche events. Regione Piemonte: Usually cyclonic condition which carries southern current upon western Alpine range; in the north-western boundary zone of the Alpine range of Piemonte considerable avalanche hazards may occur with north-western current stream too. Regione Lombardia: Northern streams: cold winter powder avalanches. Wet southern streams: wet spring canalised avalanches. Provincia Autonoma Trento: Main causes of avalanches in the Tridentine Alp and Pre-Apls are due to snowfall (abundant with stream from E and SE, modest or weak with stream from W, modest with stream from N in the northern Dolomiti), widespread presence of windy snow deposits, spring heating. Provincia Autonoma Bolzano: With streams from N and W the weather in the northern regions will grow stormy, while in the southern ones it will usually be good due to foehn;. With streams from S the southern regions will be interested by heavy precipitations while the northern ones, except for a central strip, will be interested by weak precipitations. Streams from E are not frequent and give cold weather with weak precipitations. Precipitations and prevalent winds upon various regions with snowpack state and the other parameters draw up the complex avalanche chart. Regione Veneto: Main causes of avalanches in the of the Veneto region Dolomiti and Pre-Alps are due

	to snowfall (abundant with stream from E and SE, moderate or weak with stream from W, moderate with stream from N in the northern Dolomiti), widespread presence of windy snow deposits after intense winds from N, NW and W. Regione Friuli Venezia Giulia: Usually cyclonic condition which carries southern current upon eastern Alpine arc; strong wind from NE.

Annex 1: Questionnaire (sent to various European avalanche hazard forecasting organisations)

irasmos

Survey concerning avalanche causes and forecasting

I) Avalanches causes (D1.1)

1. What is your classification of snow avalanches?

2. For you, what are the main physical causes (mechanical, snow pack state, weather…) of avalanche triggering? (list in decreasing order)?

3. What are the triggering thresholds related to snow and weather parameters that you use in operational forecasting of avalanche hazard?

4. What environmental factors do you take into account regarding the avalanche hazard and related flows? (topography, slope angle and aspect, vegetation, soil, snow state in avalanche paths and at different elevations …)

5. What are the relations between the different climate types of your country and snow avalanches situations? (perhaps with details for different regions)

6. What is the frequency (or return period) of situations characterised by a very high avalanche activity (level 4 and level 5 in the European Danger Scale)?

7. What kind of catalogue and corresponding databases of past avalanche situations are available in your service?

II) Avalanche forecasting and modelling (D1.3)

1. What is the size of the area (km^2) covered by your forecast?

2. How many times a week do you issue a forecast?

3. How long is your forecast valid for?

4. How high (%) do you estimate the hit rate (percentage of correct forecasts) of your forecast? Do you carry out some kind of verification?

5. Which datasets and observations (snow, avalanche, weather) are available to you for avalanche hazard assessment?

   5.1. human observation (number of stations, parameters)

   5.2. automatic measurements (number of stations / parameters / time frequency {periodic? after events? other?})

6. What tools or methods do you use to collect and process these data?

7. Which methods do you use for avalanche forecasting? (deterministic / statistical / expert …; human/ automatic …… spatial and temporal scale)

8. Do you forecast triggering probabilities? (spatial and temporal scales?)

9. Do you predict or estimate avalanche characteristics in your forecasts? (flow/ speed/ pressure/ extension/ density/ snow taken up along the path ….) and, if yes, by what methods?

Questionnaire results
"Survey concerning avalanche causes and forecasting"
WP1 D1.1

Service de prévision avalanche →	**SM Catalogne Spain**	**Val d'Aran (Catalogne) Spain**	**LWZ Austria**	**SLF Swizerland**	**CMT (INM) Spain**	**CEN France**	**ZAMG Autria**
1 Classification	Powder, fresh wet, hard slab, soft slab, ground avalanche, melt snow	Idem SMC	Classification based on the hazard scale (1-5)	Triggering type: spontaneous, skier, artificially (explosives) Process type:. (dry, wet snow, powder) Consequence type: non damage, with)	New snow and soft slab, hard slab, wet snow	Recent snow and soft slab, hard slab, wet snow.	Wet, dry, ground surface, size
2 Physical causes	Snow pack state (weak layer, hard layer, interfaces, mechanical (rutshblock, shovel tests) weather (new snow, snowdrift, radiative periods, rain, air temp. and humidity, …)	Idem SMC	Mechanical snowpack conditions; additional stress (people and/or naturally factors)	Mechanical, snowpack state and weather without priority because of heavily interlinked. Mechanical is of high priority because high frequency of skier triggered avalanches Weather is probably the bottleneck in avalanche forecast, since precipitation is difficult to predict with reasonable spatial and temporal certainty	Recent snow: weather, mechanical, snowpack state Hard slab: mechanical, snowpack state, weather, topo. Wet snow: snowpack state, weather, slope aspect	Weather factors: heavy snowfalls, temp. rise, sun radiation. Snow and weather: Snow mobility, Cohesion of snow layers, freezing crust, snow in gullies Topography: Accumulation zones, slope shape, soil roughness	Snow pack state, mechanical, weather
3 Triggering thresholds	New snow: 30cm/24h et 60/72h wind >30km/h	Idem SMC	Spontaneous, high and low level – based on the hazard scale (1-5)	No precisely snow and weather threshold for fixing the danger level. European avalanche danger scale apply	Slope > 25° (angle increasing), weak layers, tempe equal to 0°, precipitation intensity, wind speed >4 m/s,	See text	No thresholds but probabilities of triggering

4 Environmental factors	Vegetation, aspect (wind, sun) Altitude, slope angle,…	Idem SMC	Snow state and snow conditions; topography and shape aspect; slope angle	Topography (e.g. near to or far from crest in case of wind transport) Local forecast: slope angle and aspect.	Topography, roughness, snowpack state, weather situation.	Slope angle and aspect, slope shape, accumulation zone or not, vegetation and soil type, presence of ridge	All of them
5 Relation with climate types	See text	See text	See text	See text	See text	See text	See text
6 Frequency of high avalanche activity (levels 4 and 5)	4: 5.1% 5: 0.4%	4: 10days/year 5: 2 years	4: 5-7 days/year 5: nothing since season 98-99	5: 3 periods since 1999	4 et 5: around 7%	**Risque 5**: Savoie: 4,5% Isère & Htes-Alpes: 3 % Alpes de Hte-Provence & Maritimes: 1,5% Corse: 0 % Pyrénées Atlantiques & Htes-Pyrénées: 1% Pyrénées Orientales: 1,5% Hte-Garonne & Ariège: 0,1% **Risque 4**: Haute-Savoie, Isère & Hautes-Alpes: 18 % Savoie & Alpes de Hte-Provence: 14% Alpes Maritimes: 7% Corse: 2,5 % Pyrénées Atlantiques:11% Hautes-Pyrénées: 12% Hte-Garonne & Ariège:10 % Pyrénées Orientales:8 %	4: 10 days/year 5: not every winter
7 Data base	before 03-04 GIS past avalanche database	NIVOLOG + SIG + Images	Notations about weather and snow since 1952-1953	Detailed data base of damage avalanches Detailed recording of avalanches in region of Davos	NIVOMET	BDNIV: snow and weather observations, avalanche report and risks	Avalanche activity

Survey concerning avalanche causes and forecasting
(provided by AINEVA).
Indagine riguardante le cause e la previsione delle valanghe

I) Avalanches causes (D1.1)	**Regione Valle d'Aosta**	**Regione Piemonte**	**Regione Lombardia**	**Provincia Auonoma Trento**	**Provincia Autonoma Bolzano**	**Regione Veneto**	**Regione Friuli Venezia Giulia**
1. What is your classification of snow avalanches ?	The classification of snow avalanches we use is the one proposed by ICSI (UNESCO, 1981). Other references to the avalanche frequency and size are expressed according to the indications given in the last European Avalanche Warning Services meeting (Davos, 2005).	According to what defined in the report by the international group of the avalanche warning services.		The WMO classification according to the AINEVA standard	In size: sluff, small, mean, big; snow kind: wet or dry; trigger cause: spontaneous or caused.	The WMO classification according to the AINEVA standard	According to what defined in the report by the international group of the avalanche warning services.
2. For you, what are the main physical causes (mechanical, snowpack state, weather….) of avalanche triggering? (list in decreasing order) ?	The main physical causes of avalanche triggering are: a) intense snowfall accompanied by wind b) snowpack structure c) human accidental triggering	Snowpack structure Meteorological conditions Mechanical factors Terrain Slope aspect	Snowpack, meteorological ,mechanical conditions.	It depends on the meteorological trend of the current winter season. a)Avalanches during or after snowfalls. b)Spring avalanches or due to temperature rise. c)Avalanches after windy days. d)Ski-triggered avalanches.	Natural or accidental overload, temperature.	It depends on the meteorological trend of the current winter season. a)Avalanches during or after snowfalls. b)Spring avalanches or due to temperature rise. c)Avalanches after windy days. d)Ski-triggered avalanches.	Snowpack structure Meteorological conditions Mechanical factors Terrain Slope aspect
3. What are the triggering thresholds related to snow and weather parameters that you use in operational forecasting of avalanche hazard ?	We don't use any thresholds in our forecasting.	We don't use any predefined thresholds in our forecasting., but we use an approach based on the experience of the forecaster.		We don't use any thresholds in our forecasting. It's more a joint analysis of weather and snow factors.	We don't use any thresholds in our forecasting, as avalanche activity and avalanche hazard greatly depend on snowpack state, which is not standardizable.	We don't use any thresholds in our forecasting. It's more a joint analysis of weather and snow factors.	Until 30 cm of forecasted new snow, the avalanche level remain 2, it becomes 3 if the forecasted new snow is 30-60 cm and 4 or 5 with more than 60 cm.

4. What environmental factors do you you take into account regarding the avalanche hazard and related flows ? (topography, slope angle, shape aspect, vegetation, soil, snow state into paths and at different elevations …)	We usually define to macro-scale the avalanche hazard level on 3 sectors. We detail the further information to local scale related to: slope angle shape aspect vegetation	Slope angle, vegetation, soil, slope aspect, snow distribution and snowpack characteristics at different altitudes.	Slope angle, snow properties, slope aspect.	Environmental factors: a)snowpack structure b)elevation c)terrain morphology (soil surface, forest cover, channels, concave terrain etc.) d)slope angle e)slope aspect	general topographic parameters; snowpack state; snow height; snow limit on he ground altitude) and ts seasonal characteristics; vegetation and ground oughness.	Environmental factors: a)snowpack structure b)elevation c)forest cover d)slope angle e)slope aspect	Snow distributions, snow properties, wind, slope angle, vegetation, slope aspect, soil.
5.What are the relations between the different climate types of your country and snow avalanches situations? (maybe detailed by region)	See text	See text	See text.	See text	See text	See text	See text.
6.What is the frequency (or return period) of situations characterized by a very high avalanche activity (level 4 and level 5 in the European Danger Scale)?	The frequency of situations with a very high avalanche activity (level 4 and/or level) is on average at least once per year.	Risp.: Return period of about 5-10 years.	8-10 years	ut 2-5 days with level 4. Since 1994 no day with level 5.	From 1 or more n a year in some sites, to return period of 5 or more year.	ut 2-5 days with level 4. Since 1994 no day with level 5.	1 or 2 days per year with level 4. Return time of 5-10 years for level 5
7. What kind of catalogue and corresponding databases of past avalanche situation are available in your service?	We have a regional database composed by avalanche digital maps and paper identity cards of each avalanche where single event is reported.	Seasonal reports since 1983. Avalanche historical and topographical database since 1845 for the Provincia of Cuneo and Torino		Avalanche digitalized and georeferenced cartography with a related database. All the data are available on internet.	t is available a elation into the annual pubblication meteorological and avalnche state)	Only avalanche cartography on paper.	CLPV of all the Region with about 4500 avalanche sites and avalanche database with about 22.000 registered avalanche events. The data are available in digitalized form.

	References
Chapter 1	
Triggering of debris flow	Ardizzone F., Cardinali M., Carrara A., Guzzetti F. & Reichenbach P. - Uncertainty and errors in landslide mapping and landslide hazard assessment. Natural Hazards and Earth System Sciences, Vol. 2:1-2, 3-14., 2002 Armanini A., Gregoretti C., "Triggering of debris-flow by overland flow: A comparison between theoretical and experimental results". Rotterdam:Balkema, p. 117-126., Atti del convegno: "Debris-Flow Hazard Mitigation: Mechanics, prediction and assessment", Taipei, 16-18 Aug. 2000 Ashida, Takahashi, Mizuyama, Study on bed load equations for mountain streams, Japan Society of Erosion Control Engineering, Vol.30 No.4, Ser. No.107, April 1978 Ashida, Takahashi, Mizuyama, Study on the initiation of motion of sand mixtures in a steep slope channel, Japan Society of Erosion Control Engineering, Vol.29 No.4, Ser. No.103, March 1977 Baum, R.L., Savage, W.Z., and Godt, J. W., 2002, TRIGRS - A Fortran program for transient rainfall infiltration and grid-based regional slope-stability analysis: U.S. Geological Survey Open File Report 02-0424. Bardou, E., and Delaloye, R. 2004: Effects of ground freezing and snow avalanche deposits on debris flows in alpine environments, Natural Hazards and Earth System Sciences, 4, 519-530, 2004 Bardou, E., Niggli, M., and Musy, A. 2003: The role of snow in the generation of debris flow in small watersheds of the European Alps, Geophysical Research Abstracts, 5, 05672, 2003 Bertoldi G., and Rigon R. , Flood Peaks: a GIS based model for the estimation of the maximum flood peaks. User Manual, Dipartimento di Ingegneria Civile ed Ambientale/CUDAM, 2003 Bertoldi G., and Rigon R., . GEOTOP 0.75: A Hydrological Balance Model; Technical Description and Users Guide . Dipartimento Ingegneria Civile ed Ambientale/ CUDAM, 2001-2003 Beven K.J e M. Kirkby M.J, A physically based variable contributing area model of basin hydrology, Hyrological Science Bulletin, 24(1), 43-69, 1979 Beven K.J e M.J. Kirkby (ed), Channel Network hydrology, Wiley, 1993 Beven K.J., Rainfall-runoff Modelling, Wiley, New York, 2000 Beven, K J and Kirkby, M J. 1979 A physically based variable contributing area model of basin hydrology Hydrol. Sci. Bull., 24(1),43-69. Bishop D.M., Stevens M.E. 1964: Landslides on logged areas, southeast Alaska, Res. Rep. NOR-1, 18 p., For. Serv., U.S. Dep. Of Agric., Juneau, AK Bovis M.J., Jones P. 1992: Holocene history of earthflow mass movements in south-central British Columbia: the influence of hydroclimatic changes, Can. J. Earth Sci., 29, 1746-1754 Brardinoni F., Hassan M.A. 2006: Glacial erosion, evolution of river long profiles, and the organization of process domains in mountain drainage basins of coastal British Columbia, J. of Geophysical Research, 111 Buchanan P., Savigny K.W. 1990: factors controlling debris avalanches initiation, Can. Geotech. J., 27, 659-675 Campbell R.H., 1974 : Debris flows originating from soil slips during rainstorms in Southern California. Q. J. Engng. Geol., vol. 7, 339-349. Campbell, C. S. (1990) Rapid granular flows. Annu. Rev. Fluid Mech. 22, 57-92. Campbell, R.H.. Soil slips, debris flows, and rainstorms in the Santa Monica Mountains and vicinity, southern California. Professional Paper 851. Menlo Park, CA: U.S. Geological Survey; 51 p. , 1975 Cannon, S. H. Regional rainfall-threshold conditions for abundant debris-flow activity, in Ellen, S. D., and Wieczorek, G. F., eds., Landslides, floods, and marine effects of the storm of January 3-5, 1982, in the San Francisco Bay region, California: U. S. Geological Survey Professional Paper no. 1434 , 35-42. 1988 Cannon, S.H.; Ellen, S.. Rainfall conditions for abundant debris avalanches: San Francisco Bay Region, California. California Geology, December, 1985: 267-272, 1985 Carey S.K., Woo M.K. 2000: The role fo soil pipes as slope runoff mechanism, subarctic Yukon, Canada, J. Hydrol., 233, 206-222 Carrara A., Agnesi V., Macaluso T., Monteleone S., Pipitone G., Reali C., Sorriso-Valvo M., Modelli matematici per la valutazione della pericolosità connessa con i fenomeni di instabilita' dei versanti. Geologia Applicata e Idrogeologia, 10(2) I, 63-91, 1985. Carrara A., Cardinali M., Detti R., Guzzetti F., Pasqui V., Reichenbach P., GIS techniques and statistical models in evaluating landslide hazard. Earth Surface Processes and Landforms, 16, 427-445, 1991. Carrara A., Cardinali M., Guzzetti F., Reichenbach P., GIS Techniques in Mapping Landslide Hazard. In: Geographical Information Systems in Assessing Natural Hazards, A. Carrara and F. Guzzetti (eds.), Kluwer Academic Publishers, Netherlands, 135-175, 1995. Carrara A., Landslide hazard mapping: aims and methods. Association Francaise de Géographie Physique. Colloque de CAEN, 141-151, 1984.3 Chen 1997: Debris flow hazard mitigation: Mechanics, Prediction and Assessment, San Francisco, American Society of civil engineers Chen H. 2006: Controlling factors of hazardous debris flow in Taiwan, Quaternary Int., 147, 3-15 Chung CH. F. Fabbri A. G., & Van Western C.J.,. Multivariate regressionanalysis for landslidehazard zonation. In: Geographical information System in Assessing Natural Hazards Carrara A., Guzzetti F. (eds), Kluwer Pub., Dordrecht, The Netherlands, 107-142,1995. Chleborad A.F. 1997: Temperature, Snowmelt and the Onset of Spring Season Landslide in the central Rocky mountains (USGS Open-file Report 97-27, 35 pp.), US Geological Survey, Reston VA

Chleborad A.F. 1998: Use of Aier Temperature Data to Anticipate the Onset of Snowmelt-season Landslide (USGS Open-file Report 97-27, 35 pp.), US Geological Survey, Reston VA
Costa J.E., Williams G.D. 1984 Debris Flows Dynamics (USGS Water Resources Division, Open-file Report 84/606, Video). US Geological Survey, Reston, VA
Crosta G. Rainfall thresholds applied to soil slips in Alpine and pre-Alpine areas In: Proceedings 1st International Symposium on protection and development of the environment in mountain areas, Ponte di Legno, 20–24 June, Montana- Graf Galeati, pp 141–153., 1994
Dave Savage, 2205: National Operational Hydrologic Remote Sensing Center, National Weather Service,NOAA,Minneapolis,Minnesota http://www.nohrsc.nws.gov/technology/pdf/Snow_Induced_Debris_Flows_1.pdf
D'Odorico, P., S. Fagherazzi and R. Rigon, Landslides and rainstorm hydrology, submitted to Journal of Geophysical Research –ES, 2003
Dietrich, W .E., Reiss, R., Hsu, M., and Montgomery, D. R., 1995, A process-based model for colluvial soil depth and shallow landsliding using digital elevation data, Hydrological Processes, Vol. 9, 383-400.
Dietrich, W. E., C. J. Wilson, D. R. Montgomery, and J. McKean, 1993, Analysis of erosion thresholds, channel networks and landscape morphology using a digital terrain model, J. Geology, Vol. 101, No.2, p.161-180.
Dietrich, W. E., C. J. Wilson, D.R. Montgomery, J. McKean, and R. Bauer, 1992, Erosion thresholds and land surface morphology, Geology, v. 20, p. 675-679.
Dietrich, W.E. and Sitar, N., 1997 : Geoscience and geotechnical engineering aspects of debris-flow hazard assessment. Proc. of the 1st Intern.Conf. : Debris-flow Hazard Mitigation, S.Francisco.
D'Odorico, P., S. Fagherazzi and R. Rigon, Frane superficiali e idrologia dei versanti: un possibile metodo di indagine, XXVIII Convegno di Idraulica e Costruzioni Idrauliche. (vol. V, pp. 177-184), 2002
Duzgoren-Aydin N.S., Aydin A., Malpas J. 2002: Dostribution of clay minerals along a wheathered pyroclastic profile, Homg Kong, Catena, 50, 117-40
Ekanayake J.C., Philipps C.J. 2002: Slope stability thresholds for vegetated hillslopes: a composite model, Can. Geotech. J., 39, 849-862
Endo T., Tsuruta T. 1969: The3 effect of the tree's roots on the shear strength of soil, Annual Report, 1968, pp. 167-182, Hokkaido Branch, For. Exp. Stn., Sapporo, Japan
Evans S.G., Clauge J.J. (1994): Recent climatic change and catastrophic geomorphic processes in mountain environments. Geomorphology, 10, 107-128
Fernandes N.F., Netto A.L.C., Lacerda W.A. 1994: subsurface hydrology of layered clluvium mantles in unchannelled valleys-south eastern Brazil, Earth Surf. Process. Landforms, 19,609-626
Fleming R.W., Ellen S.D., Algus M.A. 1989 Trasformation of dilative and contractive landslide devris into debris floes: an example from Marin County, California, Engineering Geology, 27, 201-223
Fujiwara K. 1970: A study on the landslides by aerial photographs, Res. Bull. Exp. Forest Hokkaido Univ., 27(2), 297-345
Genevois R., Tecca P.R., Analisi probabilistica della stabilità dei versanti: applicazione per la realizzazione di una carta della pericolosità nella media valle del Fiume Tammaro (BN). Atti Convegno Le Scienze della Terra nella Pianificazione Territoriale, Chieti, Mem. Soc. Geol. It., 37(1), 150-170, 1987.
Gray D.H., Megahan W.F, 1981: Forest vegetation removal and slope stability in the Idaho Batholit, Res. Pap. INT-271, 23 p, For Serv US Dep of Agric, Ogden Utah
Greenway D.R. 1987: Vegetation and slope stability, in slope Stability, Geotechnical Engineering and Geomorphology, edited by M.G. Anderson and K.S. Richards, pp. 187-230, John Wiley & Sons, Chichester, UK
Guthrie R.H. 2002: The effects of logging on frequency and distribution of landslide in three watersheds on Vancouver Island, British Columbia, Geomorphology,43(3/4),273-292
Guzzetti F., Cardinali M., Reichenbach P., The AVI Project: A Bibliographical and Archive Inventory of Landslides and Floods in Italy. Environmental Management, 184, 623-633, 1994.
Hewitt K. 1998: Catastrophic landslides and their effects on the Upper Indus stream, Karakoram Himalaya, northern Pakistan, Geomorphology, 26(1-3), 47-80
Horton R.E. 1938: Phenomena of the contact zone between the ground surface and a layer of melting snow. Association Internationale D'Hydrologie Scientifique, Paris, 244, 545-561
http://www.nohrsc.nws.gov/technology/pdf/snow_induced_debris_flows_1.pdf
Haeberli, W., Kaab, A., Muhll, D., and Teysseire, P. 2001: Prevention of outburst floods from periglacial lakes at Grubengletscher, Valais, Swiss Alps, Journal of Glaciology, 47, 111- 122, 2001
Huggel, C., Kaab, A., Haeberli, W., and Krummenacher, B.: Regional-scale GIS-models for assessment of hazards from glacier lake outbursts: evaluation and application in the Swiss Alps, Natural Hazards and Earth System Sciences, 3, 647-662, 2003
Hungr O., Evans S.G., Bovis M.M., Hutchinson J.N. 2001: A review of the classification of landslides of the flow type (vol 7, pg 225,2001), Environmental and Engineering Geoscience 7:21-38
Hutchinson J., Bhandari R. 1971: Undrained loading, a fundamental mechanism of mudflows and orther mass movements, Geotechnique, 21(4), 353-358
Imaizumi F., Sidle R.C. 2005: relationship between sediment supply and transport processes in miyagawa Dam catchment, Ann. Disaster Prevention Res. Inst., Kioto univ. 48C, 209-217
Iverson R.M., 1992 : Sensitivity of stability analyses to groundwater data. Landslides, Proc. 6th Int.Symp. on Landslides : 451-457.
Iverson R.M., Reid M.E, LaHusen R., 1997 : Debris-flow mobilization from landslides. Annual Rev. of Earth and Planetary Sciences, 25, 85-138.
Iverson, R. M., 2000, Landslide triggering by rain infiltration: Water Resources Research, v. 36, n. 7, p. 1897-1910.
Jones J.A.A. 1997: global hydrology: process, resources and environmental management, 399 p. Longman, Essex, UK
Lancaster S.T., Hayes S., Grant G.E. 2003: Effects of wood on debris flow runout in a small mountain watersheds, Water Reour. Res., 39(6), 1168

Lu, N., and Lycos, W, J., 2004 Unsaturated Soil Mechanics. John Wiley and Sons.
Lu, N., and Lycos, W, J., 2006 Suction Stress Characteristic Curve for Unsaturated Soil, Journal of Geotechnical and Environmental Engineering, February 2006, in press.
Mathewson C.C., Keaton J.R., Santi P.M. 1990: Role of bedrock ground water in the initiation of debris flows and sustained post-storm stream discharge. Bulletin of Association of Engeneering Geologist, 27(1), 73-78
Montgomery D.R. and Dietrich W.E., Torres R., Anderson S.P. and Heffner J.T1997: Hydrological response of a steep, unchannel valley to natural and applied rainfall, water Resour. Res. 33, 91-109
Moore P.L., Iverson N.R. 2002: Slow episodic dhear for granular materials regulated by dilatant stregthening, Geology, 30(9), 843-846
Pack, R. T., D. G. Tarboton and C. N. Goodwin, (1998), "The SINMAP Approach to Terrain Stability Mapping," Paper Submitted to 8th Congress of the International Association of Engineering Geology, Vancouver, British Columbia, Canada 21-25 September 1998
Palacios D., Garcia R., Rubio V., Vigil R. 2003: Debris flows in a weatered granitic massif: Sierra de Gredos, Spain, Catena, 51, 115-140
Paert M.R.., Zhang D.D. 2005: Landslide and sediment delivery to a drainage system: some observations from Hong Kong, J. Asian Earth Sci., 25(5), 821-836
Philipps C.J., Watson A.J . 1994: structural tree root research in new zeland: a review, Landcare Res Sci zSeries No 7,71 p. Lincoln, New Zeland
Rickenmann, D. and Zimmerman, M 1993.: The 1987 debris flows in Switzerland: documentation and analysis, Geomorphology, 8, 175-189
Rickenmann D., Chen C-I. 2003: Debris-flow hazards mitigation: mechanics, prediction, and assessment, Third International Conference. Davos, Switzerland, Millpress, Rotterdam, Netherland:1335
Rigon R., G. Bertoldi e T. m. Over, GEOTOP: un modello del ciclo idrologico . XXVIII convegno di idraulica e Costruzioni idrauliche, Potenza. (pp. 303-312).
Rigon, R., Bertoldi, G., and Over, T. M., 2006 a: Geotop: A distributed Hydrological Model with Coupled Water and Energy Budgets. Journal of Hydrometeorology, 7 (3), 371-388.
Sassa K. 1985: The geothechnical classification of landslides, Proc. 4th Int Conf and Field Workshop on Landslides, pp. 31-45
Sassa K. 1985: the mechanism of debris flow. Proceedings of XI international conference of soil mechanics and foundatuion engeneering, San Francisco p. 1173-1176 A.A. Balkema, Rotterdam, Netherlands
Savage, W. Z., Godt, J. W., and Baum, R. L., 2004, Modeling time-dependent areal slope stability, in Lacerda, W. A., Ehrlich, M., Fontoura, S. A. B., and Sayao, A. S. F., eds., Landslides: London, Taylor and Francis Group, p. 23-36.
Sidle R.C. 1984: shallow groundwater fluctuations in unstable hillslopes of coastal alaska, Z. fur gletscherkunde und Glazialgeol., 20, 79-95
Sidle R.C. 1984: relative importance of factors influencing landsliding in coastal alaska, Proc. 21st Ann. Eng. Geol. And Soils Eng. Symp., pp. 311-325, Univ. of Idaho, Moscow.
Sidle R.C., Pearce A.J., O'loughlin C.L.1985: hillslope stability and land use, Water resources monograph, vol. 11, Am. Geophys. Union, Wsahington, DC 140 p
Sidle R.C. 1992: A theoretical model of the effects of timber harvesting on slope stability, Water Resour. Es., 28(7), 1897-1910
Sidle R.C., Chigira M. 2004: Landslides and debris flows strike Kyushu, Japan, Eos. Trans. AGU, 85(15), 145-151
Sidle R.C., Noguchi S., Tsuboyama Y., Laursen K. 2001: a conceptual model of preferential flow system in forested hillslopes: evidence of self organization, Hydrol. Processes, 15(10), 1675-1692
Sidle R.C., Tsuoyama Y., Noighuchi S., Hosoda I., Fuijeda M., Shimizu T. 2000: Stream-flow generation in steep headwaters: a linked hydrogeomorphyc paradigm, Hydrol. Process, 14, 369-385
Sidle R.C., Hirotaka O. 2006 Landslide Processes,Prediction and land use, AGU
Stiny J. 1910: Die Muren, Innsbruck
Swanson F.J., Dyrness C.T. 1975: Impacts of clearcutting and road construction on soil erosionby landslides in the western Cascade Range,Oregon, Geology, 3(7), 393-396
R.Rigon, A. Cozzini, S. Pisoni, G. Bertoldi, A. Armanini, A new simple method for the determination of the triggering of debris flows, Proceeding f the tenth Interpraevent Conference, Riva del Garda, 2004
Tabata S., Ichinose E. 1973: Study on the primary factors of the mudflow disasters in Owase area. Shin-sabo [journal of the erosion control engineering society, Japan], 86, 20-24
Tharmit (1999): "Torrent Hazard Control in the European Alps: Practical tolls and methodologies for hazard assessment and risk mitigation". EVG1-CT-1999-00012 http://www.geol.unipd.it/convegni/EUtharmit.htm.
Terzaghi, K., 1943, Theoretical Soil Mechanics, John Wiley and Sons Inc., new York.
Todini, E. (1996), The ARNO rainfall-runoff model, Journ. of Hydrol., 175, 339-382
Torrance J.K. 1999: Physical, chemical and minieralogic influences on the reology of remoulded low-activity sensitive marine clay, Appl. Clay Science, 14, 199-223
Tsuboyama Y., Sidle R.C., Nogochi S., Murakami S., Shimizu T. 2000: a zero-order basin its contribution to catchement hydrology and internal hydrological processes, Hydrol. Processes, 14, 387-401
Varnes D.J. 1984. Landslide hazard zonation : a review of principles and practice. IAEG Publication. Paris, Unesco.
Villemeur A. 1988. Sûreté de fonctionnement des systmes industriels. Fiabilité. Facteurs humains. Informatisation. Collection de la Direction des Etudes et Recherches d'Electricité de France. Eyrolles.
Wang F.W., Sassa K., Wang G. 2002: Mechanism of long-runout landslide triggered by the August 1998 heavy rainfall in Fukushima Prefecture, Japan, Eng. Geol., 63, 169-185
Wang G., Sassa K., Fukuoka H. 2003: Downslope volume enlargement of a debris slide-debris flow in the 1999 Hiroshima, Japan, Rainstorm, Eng. Geol,, 69, 309-330
Wieczorek G.F. and Sarmiento J., 1988 : Rainfall, piezometric levels and debris flows near La Honda, California, in storms between 1975 and 1983 in Landslides, floods and marine effects of the storm of

	January 3-5, 1982, in the San Francisco Bay Region, California, US Geol. Survey Prof. Paper 1434. Wieczorek, G.F., 1984. Preparing a Detailed Landslide Inventory Map for Hazard Evaluation and Reduction. Bulletin, Association of Engineering Geologists, 21(3): 337-342. Wieczorek, G.F.; Sarmiento, J1983:. Significance of storm intensity-duration for triggering of debris flows near La Honda, California. Geological Society of America Abstracts with Programs 15(5): 289. Weczorek G.F., Naeser N.D. 2000: Proceedings of the second International Conference on debris-flow hazard mitigation, 16-18 August 2000 Debris-flow hazards mitigation: mechanics, Prediction and assessment. Taipei, Taiwan, Balkema:608 Weczorek G.F., Coe J.A., and Godt J.W. 2003: Debris-flow hazard assessment using remote sensing rainfall. In: D. Rickenmann and C-L. Chen (eds), Debris-flow Hazrd Mitigation: Mechanics, Prediction and Assessment: Proceeding of the 3rd International Conference, Davos, Switzerland, September 10-12 (pp. 1257-1268), Millpress, Rotterdam Willis, C.J. e McCrink, T.P., 2002. Comparing landslide inventories: the map depends on the method. Environ. Eng. Geosc. VIII (4), 279-293. Wright, R.H., R.H. Campbell, and T.H. Nilsen, 1974. Preparation and use of isopleth maps of landslide deposits. Geology, 2: 483-485. Wu T.H., McKinnel W.P., Swantson D.N. 1979: Strength of tree roots and landslide on Prince of Wales Island, Alaska, Can. Geotech. J., 16, 19-33 Yatsu E. 1966: Rock Control in Geomorphology, Sozosha, Tokio, 133 p. Ying W. & Bifan Z., 1992 : Conversion mechanism of gravelly soil to viscous debris flow. Proc. Symp. on Erosion, Debris flows and Environment in Mount. Regions, Chendu '92, IAHS Publ. n. 209, 315-323. Zhao, R. J., Zhuang Y. R., Liu X.R. and zhang Q.S. (1980), The Xinanjiiang model, in Hydrol' Forecasting IAHS Publications No. 129, Wallingfort, UK, 351-356. Zhu, J.H. and Anderson, S.A., 1998 : Determination of shear strength of Hawaiian residual soil subjected to rainfall-induced landslides. Geotechnique, 48, 1 :73-82.
Triggering of debris flow - additional	Agresti, Alan : Categorical Data Analysis. John Wiley and Sons, 734 pp. 2002. Amadesi E., Vianello G., Bonfatti G., Pignone R., Preti D., Guida alla realizzazione di una carta della stabilità dei versanti. Regione Emilia Romagna. MB T6. Ed.Pitagora., Bologna, 72 p., 1977. Amadesi E., Vianello G., Nuova guida alla realizzazione di una carta della stabilità dei versanti. Mem.Soc.Geol.It., 19, 53-60, 1978. Amanti M., Carrara A., Castaldo G., Colosimo P., Gisotti G., Govi M., Marchionna G., Nardi R., Panizza M., Pecci M., Vianello G., Linee guida per la realizzazione di una cartografia della pericolosità geologica connessa ai fenomeni di instabilità dei versanti alla scala 1:50.000. Presidenza del Consiglio dei Ministri. Servizio Geologico. Progetto CARG ,53p., 1992. Antoine P., Pachoud A. 1976. Enseignements tirés de deux essais de cartographie systématique de glissements de terrain. Bulletin de liaison des laboratoires des Ponts et Chaussées, Numéro spécial 2, vol. 1, pp. 31-39. Armanini A., L. Fraccarollo, L. Guarino, R. Martino & Y. Bin 2000 Experimental analysis of the general features of uniform debris flow over a loose bed. Second Int. Conference on Debris-Flow, Hazards Mitigation: Mechanics, Prediction, and Assessment, August 16-18 2000, Taipei, 327-334. Autori Vari, Partnership for reducing landslide risk, National Research Council, (books.nap.edu/catalog/10946.html) ,2003 Bonnet-Staub I., 1998 : Mécanismes d'initiation des laves torrentielles dans les Alpes françaises - Contribution à la maîtrise du risque, 230 p. et Annexes 133 p. Thse de l'Ecole des Mines de Paris. Bosi C, Considerazioni e proposte metodologiche sulla elaborazione di carte della stabilità. Geol. Appl. & Idrogeol., 13, 245-281, 1978. Brabb E.E., Innovative approaches to landslides hazard mapping. Proc. IV Int. Symp. on Landslides, Toronto, 1, 307-324, 1984. Bulletin International Association of Engineering Geology, 16: 69-72. Caine, N., 1980 : Rainfall intensity-duration control of shallow landslides and debris flows, Geograf. Ann., 62A, pp.23-27. Caine, N.: The rainfall intensity-duration control of shallow landslides and debris flows. Geografiska Annaler, 62A: 23-27, 1980 Cancelli A, Nova R. Landslides in soil debris cover triggered by rainstorms in Valtellina (central Alps, Italy) In: Sassa K (ed) Proceedings of 4th International Conference on Landslides, Tokyo, The Japanese Landslide Soc, Tokyo,pp 267–272, 1985 Canuti P., Casagli N., Considerazioni sulla valutazione del rischio di frana. Estratto da " Fenomeni Franosi e Centri Abitati". Atti del Convegno di Bologna del 27 Maggio 1994. Capart, H., Fraccarollo, L., Guarino, L., Armanini, A. and Zech, Y. 2000 Granular velocities, concentrations, and temperatures for loose bed debris flows in steady uniform conditions. Second Int. Conference on Debris-Flow, Hazards Mitigation: Mechanics, Prediction, and Assessment, August 16-18 2000, Taipei, 361-368. Carrara A., Multivariate Methods for landslide hazard evaluation. Mathematical Geol., 15(3), 403-426, 1983. Castro, G., 1975 : Liquefaction and cyclic mobility of saturated sands. Journal of Geotechnical Engineering, 101 : 551-569. Ceriani M, Lauzi S, Padovan N. Rainfalls and landslides in the Alpine area of Lombardia region, central Alps Italy. In: Aulitzky A (ed) Proc. of Interpraevent 1992, Bern, Switzerland, Österr. Wasserwirtsch., Klagenfurt, 2 :9–20., 1992 CNR-GNDCI – Linea 2 "Previsione e Prevenzione di Eventi Franosi a Grande Rischio". Pubblicazione n° 846, 57p., 1996. CNR-GNDCI, MAPPAVI: Censimento delle aree italiane storicamente colpite da frane e da inondazioni. Vers.1.2. CNR-GNDCI, Roma, 1998. Cojean R and Genevois R, 1999 : Debris flow triggering, 38p., in Debris Flow Risk, Final scientific report, volume 1. EC Research Programme, contract ENV4-CT96-0253. Cojean R. and Staub I., 1998 : Mécanismes d'initiation des laves torrentielles dans les Alpes françaises. 8e

Congrs de l'AIGI, Vancouver, 21-25 septembre 1998, vol. 3, pp 2075-2082.
Comité Français de Géologie de l'Ingénieur 2000. Caractérisation et cartographie de l'aléa dû aux mouvements de terrain. Paris, publication LCPC, Collection Environnement.
Corniello A., De Riso R. & Lucini P. - La franosita' potenziale del bacino del F. Tammaro (Campania). Mem. e Note Ist. Geol. Appl., XV, 1-39, Napoli, 1980
Crozier, M.J. & Preston, N.J. 1999. Modelling changes in terrain resistance as a component of landform evolution in unstable hill country. In: Hergarten, S. & Neugebauer, H.J. (eds.), Process Modelling and Landform Evolution, Lecture Notes in Earth Sciences 78, Springer, Berlin. 267-284.
Cunge J., (1969), On the subject of a flooding routing method (Muskingum method), Jour. Of Hydrul. Res., 7: 205-230
Dearman W. R., Fookes P. G. 1974. Engineering geological mapping for civil engineering practice in the United Kingdom. Quaterly Journal of Engineering Geology, vol. 7, pp. 223-256.
Doodge J.C.I., 1959, A general theory of the unit hydrograph, Jornal of Geophys. Res., 64, 241-256
Fleming R.W., Ellen S.D., Algus M.A., 1989 : Transformation of dilative and contractive landslide debris into debris flows - an example from Marine County, California. Engng. Geol., vol. 27, 201-233.
Franchini M., Wendling M. J., Obled C., Todini E.,Phisical interpretation and sensitivity analysis of the Topmodel, Journal of Hydrology, 1996, vol. 175, p. 293-338
Gostelow, T.P., 1991 : Rainfall and landslides, CEC Report EUR 12918 EN, Prevention and control of landslides and other mass movements, pp.139-161, Brussels.
Govi M., Sorzana P.F., Landslide susceptibility as a function of critical rainfall amount in Piedmont basins (NW Italia). Studia Geomorphologica Carpatho-Balcanica, 14, 43-61, 1980.
Govi, M., Mortara, G. and Sorzana, P.F. 1985 : Eventi idrologici e frane, Geologia Applicata e Idrogeologia, Vol.XX, Parte II, pp.359-375, Bari.
Hirano, M., Prediction of Debris Flow for warning and evacuation, in "Recent Developments on Debris Flow, Lectures Notes in Earth Sciences, vol 64, 7-26, Armanini A. e M. Michiue (ed), 1997
Hunt, M.L., R. Zenit, C.S. Campbell & C.E. Brennen 2002 Revisiting the 1954 suspension experiments of R. A. Bagnold. Journal of Fluid Mechanics 452, 1-24.
International Association of Engineering Geology 1976. Engineering geological maps. A guide to their preparation. Paris, Unesco
Jenkins, J.T. & D.M. Hanes 1998. Collisional sheet-flow of sediment driven by a turbulent fluid. J. Fluid Mech. 370, 29-52.
Johnson A.M., Rahn. P.H., 1970 : Mobilization of debris flows. Zeit. fur Geomorph. Suppl. Band 9, 168-186.
Johnson, A.M. and Rodine, J.R., 1984 : Debris flows in Slope Instability, Bruns-den, D. and Prior, D.B. Ed., pp.257-361, John Wiley & Sons.
Keefer, D. K., Wilson, R. C., Mark, R. K., Brabb, E. E., Brown, W. M., Ellen, S. D., Harp, E. L., Wieczorek, G. F., Alger, C. S., and Zatkin, R. S. Realtime landslide warning during heavy rainfall: Science, v 238, p. 921-925. 1987
L. Fraccarollo, H. Capart, Riemann wave description of erosional dam-break flows, Journal of Fluid Mechanics, Volume 461. June 2002. pp183-228
Larcher, M. & B. Spinewine 2002 Laboratory Report: Analysis of uniform liquid-granular flows utilizing three-dimensional Voronoï imaging methods. Università degli Studi di Trento - Université Catholique de Louvain.
Laugier P. and Cojean R., 2001 : Analyse de scénarios d'événements « laves torrentielles » dans le bassin versant de l'Arbonne (Bourg-Saint-Maurice, Savoie, France). Revue Française de Géotechnique, N° 95/96, 2me et 3me trimestre 2002, pp231-240.
Laugier P., 2002 : Contribution à l'analyse des risques naturels en montagne par l'étude géologique et géotechnique de scénarios de mouvements de versants et laves torrentielles. Application à la région de Bourg-Saint-Maurice (Savoie, France). Thse de doctorat en Géologie de l'Ingénieur, Ecole des Mines de Paris, 333p et Annexes.
Lee H.J., Ellen S.D., Kayen R.E., 1988 : Predicting transformation of shallow landslides into high-speed debris flows. Proc. of the 5th Int. Symp. on Landslides, Luglio '88.
Leroi E. 1996. Landslide hazard. Risk maps at different scales : objectives, tools and developments. Comptes rendus du VIIme Symposium international sur les glissements de terrain. Trondheim. Vol.1, pp. 35-51.
McHarg I. L. 1969. Design with Nature. New York, NHP.
Montgomery, D. R. and W. E. Dietrich, 1994, A physically-based model for topographic control on shallow landsliding, Water Resources Research, vol.30, no.4, p.1153-1171..
Montgomery, D.R, K. M. Schmidt, W. E. Dietrich, H. M. Greenberg, 2000, Forest clearing and regional landsliding in the Pacific Northwest, Geology v. 28, p. 311-314.
Mougin, P., 1914 : Les torrents de la Savoie, 1251 p., Grenoble.
Phillips, R., R. Armstrong & R. Brown 1992 A constitutive equation for concentrated suspensions that accounts for shear-induced particle migration. Physic of Fluids A 4(1), 30-40.
Preston, N.J. 1999. Event induced changes in landsurface condition. Implications for subsequent slope stability. Zeitschrift für Geomorphologie Supplementband 115. 157-173.
Sanejouand R. 1972. La cartographie géotechnique en France. Paris, Ministre de l'Equipement et du Logement (DAFU), ARMINES, LCPC.
Sassa K., 1984 : The mechanism to initiate debris flows as undrained shear of loose sediments. Int. Symp. Interpraevent '84, Villach, 73-87.
Schmidt, K. M, J. J. Roering, J. D. Stock, W. E. Dietrich, D. R. Montgomery and T. Schaub, 2001, Root cohesion variability and shallow landslide susceptibility in the Oregon Coast Range, Canadian Geotechnical Journal.
Seed, H.B. and Lee, K.L., 1966 : Liquefaction of saturated sands during cycling loading, Journal of Soil Mechanics and Foundation Division, ASCE, Vol.92, SM6.
Sorgi-de Gennaro C. 1999. Contribution à l'étude des facteurs climatiques, géologiques et géotechniques contrôlant la génération de laves torrentielles. Application au secteur de Saint-Martin-de-la-Porte (Savoie, France). Thse de doctorat (Géologie de l'ingénieur) de l'Ecole des Mines de Paris.

	Spiker, E.C., and P.L. Gori, 2000. National Landslide Hazards Mitigation Strategy—A Framework for Loss Reduction, U.S. Geological Survey Open-File Report 00-450, 49 pp. Stevenson, P.C., 1977. An Empirical Method for the Evaluation of Relative Landslide Risk. Stiny J., 1910 : Debris flow - Die Muren - Versuch einer Monographie mit besonderer Verücksichtigung der Verhältnisse in den Tiroler Alpen - Innsbruck - English translation by Matthias Jacob & Nigel Skermer, 106 p. Takahashi, T., Nakagawa, H. & Satofuka, Y. 2000 Newtonian fluid model for viscous debris-flow. Proceedings of 2nd international conference "Debris flow hazards mitigation: Mechanics, Prediction and Assessment".
Example: Triggering conditions of debris flows associated to complex earthflows	Ancey, C., 2002. Debris flows and related phenomena. In: Balmforth, N., Provenzalle, A. (Eds.), Geomorphological Fluid Mechanics, Lecture Notes in Physics, vol. 582. Springer-Verlag, Berlin, pp. 528– 547. Antoine, P., Giraud, A., Meunier, M., Van Asch, Th.W.J., 1995. Geological and geotechnical properties of the "Terres Noires" in the southeastern France: weathering, erosion, solid transport and instability. Engineering Geology 40, 223– 234. Coussot, P., Ancey, C., 1999. Rhéophysique des pâtes et des suspensions. EDP Sciences, Paris. 266 pp. Crosta, G.B., 2001. Failure and flow development of a complex slide: the 1993 Sesa landslide. Engineering Geology 59, 173– 199. Geo-Slope, 2000. SEEP/W/SLOPE/W. User Manual. Geo-Slope International, Calgary. 875 pp. Henry, J.-B., Malet, J.-P., Maquaire, O., Grussenmeyer, P., 2002. The use of small format and low-altitude aerial photos for the realization of high-resolution DEMs in mountainous areas. Application to the Super-Sauze earthflow (Alpes-de-Haute- Provence, France). Earth Surface Processes and Landforms 27, 1339–1350. Hungr, O., 1995. A model for the runout analysis of rapid flow slides, debris flows and avalanches. Canadian Geotechnical Journal 32, 610– 623. Hungr, O., Morgan, G.C., Kellerhals, R., 1984. Quantitative analysis of debris torrent hazards for the design of remedial measures. Canadian Geotechnical Journal 21, 663–677. Hungr, O., Evans, S.G., Bovis, M.J., Hutchinson, J.N., 2001. A review of the classification of landslides of the flow type. Environmental and Engineering Geoscience 7, 221– 238. Hutchinson, J.N., 1988. Morphological and geotechnical parameters of landslides in relation to geology and hydrogeology. In: Bonnard, C. (Ed.), Landslides, Proceedings of the 5th International Symposium on Landslides, Lausanne. Balkema, Rotterdam, pp. 3 –35. Iverson, R.M., 1997. The physics of debris flow. Reviews of Geophysics 35, 245–296. Iverson, R.M., Reid, M.E., LaHusen, R.G., 1997. Debris flow mobilization from landslides. Annual Reviews: Earth and Planetary Sciences 25, 85– 138. Johnson, A.M., Rodine, J.R., 1984. Debris flow. In: Brunsden, D., Prior, D.B. (Eds.), Slope Instability. Wiley, Chichester, pp. 257– 362. Laigle, D., Coussot, P., 1997. Numerical modelling of debris flows. Journal of Hydraulic Engineering 123, 617–623. Laigle, D., Hector, A.-F., Hqbl, J., Rickenmann, D., 2003. Comparison of numerical simulation of muddy debris flow spreading to records of real events. In: Rickenmann, D., Chen, C.-L. (Eds.), Proceedings of the 3rd International Conference on Debris flow Hazard Mitigation: Mechanics, Prediction and Assessment, Davos. Millpress, Rotterdam, pp. 635–646. Lambe, T.W., Whitman, R.V., 1979. Soil Mechanics. Wiley, New York. 553 p. LeMignon, G., Cojean, R., 2002. Rôle de l'eau dans la mobilisation de glissement-coulées (Barcelonnette, France). In: Rybar, J., Stemberk, J., Wagner, P. (Eds.), Landslides, Proceedings of the 1st European Conference on Landslides, Prague. Swets and Zeitlinger Publishers, Lisse, pp. 239–244. Malet, J.-P., Maquaire, O., Calais, E., 2002. The use of global positioning system for the continuous monitoring of landslides. Application to the Super-Sauze earthflow (Alpes-de-Haute- Provence, France). Geomorphology 43, 33– 54. Malet, J.-P., 2003. Les glissements de type écoulement dans les marnes noires des Alpes du Sud. Morphologie, fonctionnement et modélisation hydro-mécanique. Doctoral thesis in Earth Science, Louis Pasteur University, Strasbourg, 394 pp. Malet, J.-P., Remaître, A., Maquaire, O., Ancey, C., Locat, J., 2003. Flow susceptibility of heterogeneous marly formations. Implications for torrent hazard control in the Barcelonnette basin (Alpes-de-Haute-Provence, France). In: Rickenmann, D., Chen, C.-L. (Eds.), Proceedings of the Third International Conference on Debris flow Hazard Mitigation: Mechanics, Prediction and Assessment, Davos, Switzerland. Millpress, Rotterdam, pp. 351– 362. Malet, J.P., Maquaire, O., Locat, J., Remaître, A., 2004. Assessing debris flow hazards associated with slow-moving landslides: methodology and numerical analyses. Landslides 1, 83–90. Maquaire, O., Malet, J.-P., Remaître, A., Locat, J., Klotz, S., Guillon, J., 2003. Instability conditions of marly hillslopes, towards landsliding or gullying? The case of the Barcelonnette basin, south east France. Engineering Geology 70, 109– 130. Picarelli, L., 2001. Transition from slide to earthflow and the reverse. In: Sassa, K. (Ed.), Transition from Slide to Flow. Mechanisms and Remedial Measures, Proceedings of the Conference, Trabzon, pp. 21–54. Pierson, T., Costa, J.E., 1987. A rheologic classification of subaerial sediment-water flows. In: Costa, J.E., Wieczorek, G.F. (Eds.), Debris flows/Avalanches: Process, Recognition and Mitigation, Geological Society of American Review of Engineering Geology, vol. 7, pp. 1 –12. Richards, A.L., 1931. Capillary conductivity of liquid through porous media. Physics 1, 316– 333. Vaunat, J., Leroueil, S., 2002. Analysis of post-failure slope movements within the framework of hazard and risk analysis. Natural Hazards 26, 83–109.
Channel type initiation (entrainment of bed	Armanini, A., Gregoretti, C. (2005), Incipient sediment motion at high slopes in uniform flow condition, Water Resour. Res., 41, W12431, doi:10.1029/2005WR004001. Berti, M. and A. Simoni (2005). Experimental evidences and numerical modelling of debris flow initiated by

material)	channel runoff. Landslides 2(3): 171-182. Hungr, O., McDougall, S., Bovis, M. (2005): Entrainment of Material by Debris Flows. In Jakob, M. and Hungr, O. (Eds.), Debris-Flow Hazards and Related Phenomena, pp. 135-158. Chichester: Praxis-Springer. Papa, M., Egashira, S., Itoh, T. (2004): Critical conditions of bed sediment entrainment due to debris flow. Natural Hazards and Earth System Sciences 4: 469 – 474. Rickenmann, D., Zimmermann, M. (1993): The 1987 debris flows in Switzerland: documentation and analysis. Geomorphology, 8(2-3): 175-189.
Example: The debris flow event of August 22, 2005 in the Armancette torrent	Bardou E. (2002) Méthodologie de diagnostic des laves torrentielles sur un bassin versant alpin..PhD thesis EPFL, no 2479 (2002), Faculté de l'environnement naturel, architectural et construit ENAC, Section de génie civil. Hungr O., Morgan G.C. and Kellerhals R. (1984) Quantitative analysis of debris torrent hazards for design of remedial measures. Canadian Geotechnical Journal, 21: 663-667.
Catchment specific investigations on sediment availability	Veyrat-Charvillon S., Elaboration d'une méthode de prédiction du volume maximal d'une lave torrentielle (PREVENT), PhD Thesis of Clermont-Ferrand University, 2005 (in french). Veyrat-Charvillon S. & Memier M., Stereophotogrammetry of archive data topographic approaches to debris-flow torrent measurements: calculation of channel-sediment states and a partial sediment budget for Manival torrent (Isère, France), Earth Surf. Process. Landforms 31, 201-219, 2006.
Chapter 2	
Rock avalanches	Abele, G., 1974. Bergstürze in den Alpen. Wissenschaftliche Alpenvereinshefte, Heft 25, 230p. Augustinus, P. C., 1995. Glacial valley cross-profile development: The influence of in situ rock stress and rock mass strength, with examples from the Southern Alps, New Zealand. Geomorphology 14, 87-97. Ballantyne, C.K., 2004: Paraglacial Geomorphology. Quaternary Science Reviews 21: 1935-2017 Ballantyne, C.K. and Stone, J.O., 2004. The Beinn Alligin rock avalanche, NW Scotland: cosmogenic Be-10 dating, interpretation and significance. Holocene, 14(3): 448-453. Beget, J.E. and Kienle, J., 1992. Cyclic Formation of Debris Avalanches at Mount St Augustine Volcano. Nature, 356(6371): 701-704. Bjerrum, L., Jørstad, F., 1968. Stability of rock slopes in Norway. Norwegian Geotechnical Institute Publications 79, 1-11. Blikra, L. H., Longva, O., Braathen, A., Anda, E., Dehls, J. F. and Stalsberg, K. Rock slope failures in Norwegian fjord areas: Examples, spatial distribution and temporal pattern. In: Massive rock slope failure NATO science series, edited by S. G. Evans, G. Scarascia Mugnozza, A. Strom and R. L. Hermanns, Kluwer Academic Publishers, Dordrecht. Bottino, G., Chiarle, M., Joly, A. and Mortara, G., 2002. Modelling rock avalanches and their relation to permafrost degradation in glacial environments. Permafrost and Periglacial Processes, 13(4): 283-288. Boultbee, N., D. Stead, et al., 2005. The Zymoetz River rock avalanche, June 2002, British Columbia, Canada. Engineering Geology. Braathen, A., Blikra, L.H., Berg, S.S. and Karlsen, F., 2004. Rock-slope failures in Norway; type, geometry, deformation mechanisms and stability. Norwegian Journal of Geology, 84(1): 67-88. Bull, W.B. and Brandon, M.T., 1998. Lichen dating of earthquake-generated regional rockfall events, Southern Alps, New Zealand. Geological Society of America Bulletin, 110(1): 60-84. Capra, L., 2006. Abrupt climatic changes as triggering mechanisms of massive volcanic collapses. Journal of Volcanology and Geothermal Research, 155(3-4): 329-333. Capra, L., Macias, J.L., Scott, K.M., Abrams, M. and Garduno-Monroy, V.H., 2002. Debris avalanches and debris flows transformed from collapses in the Trans-Mexican Volcanic Belt, Mexico - behavior, and implications for hazard assessment. Journal of Volcanology and Geothermal Research, 113(1-2): 81-110. Carrasco-Nunez, G. et al., 2006. Multiple edifice-collapse events in the Eastern Mexican Volcanic Belt: The role of sloping substrate and implications for hazard assessment. Journal of Volcanology and Geothermal Research, 158(1-2): 151-176. Crosta, G.B., 2001. Failure and flow development of a complex slide: the 1993 Sesa landslide. Engineering Geology 59(1-2): 173-199. Crosta, G.B., Imposimato, S., Roddeman, D.G., 2003. Numerical modelling of large landslides stability and runout. Natural Hazards and Earth System Sciences 3, 523-538. Crozier, M.J., Deimel, M.S., Simon, J.S., 1995. Investigation of earthquake triggering for deep-seated landslides, Taranaki, New Zealand. Quaternary International 25, 65-73. Chigira, M., 1992. Long-Term Gravitational Deformation of Rocks by Mass Rock Creep. Engineering Geology 32(3): 157-184. Chigira, M. and K. Kiho, 1994. Deep-Seated Rockslide-Avalanches Preceded by Mass Rock Creep of Sedimentary Rocks in the Akaishi Mountains, Central Japan. Engineering Geology 38(3-4): 221-230. Chigira, M., Wang, W.N., Furuya, T. and Kamai, T., 2003. Geological causes and geomorphological precursors of the Tsaoling landslide triggered by the 1999 Chi-Chi earthquake, Taiwan. Engineering Geology, 68(3-4): 259-273. Crosta, G. B., H. Chen, et al., 2004. Replay of the 1987 Val Pola Landslide, Italian Alps. Geomorphology 60(1-2): 127-146. Crozier, M. J., M. S. Deimel, et al., 1995. Investigation of Earthquake Triggering for Deep-Seated Landslides, Taranaki, New-Zealand. Quaternary International 25: 65-73. Cruden, D.M., 1976. Major rockslides in the Rockies, Canadian Geotechnical Journal, 13, 8-20. Cruden, D.M. and Hungr, O., 1986. The Debris of the Frank Slide and Theories of Rockslide Avalanche Mobility. Canadian Journal of Earth Sciences, 23(3): 425-432. Czurda, K. and Xiang, W., 1993. Der Einfluss der Kationenbelegung auf das Kriechverhalten von Tonen am Beispiel einer ostalpinen Großhangbewegung. Nationale Tagung für Ingenieurgeologie, p. 33-42 Davies, T.R., McSaveney, M.J. and Beetham, R.D., 2006. Rapid block glides: slide-surface fragmentation in

New Zealand's Waikaremoana landslide. Quarterly Journal of Engineering Geology and Hydrogeology, 39: 115-129.
Deline, P., 2005. Change in surface debris cover on Mont Blanc massif glaciers after the 'Little Ice Age' termination. Holocene, 15(2): 302-309.
Eisbacher, G.H., J.J. Clague, 1984. Destructive Mass Movements in High Mountains: Hazard and Management. Geological Survey of Canada Paper 84-16, 230p.
Evans, S.G., Clague, J.J., 1994. Recent climatic change and catastrophic geomorphic processes in mountain environments. Geomorphology 10, 107-128.
Evans, S.G., Guthrie, R.H., Roberts, N.J. and Bishop, N.F., 2007. The disastrous 17 February 2006 rockslide-debris avalanche on Leyte Island, Philippines: a catastrophic landslide in tropical mountain terrain. Natural Hazards and Earth System Sciences, 7(1): 89-101.
Evans, S.G., Hungr, O. and Clague, J.J., 2001. Dynamics of the 1984 rock avalanche and associated distal debris flow on Mount Cayley, British Columbia, Canada; implications for landslide hazard assessment on dissected volcanoes. Engineering Geology, 61(1): 29-51.
Evans, S.G., Hungr, O. and Enegren, E.G., 1994. The Avalanche Lake Rock Avalanche, Mackenzie Mountains, Northwest-Territories, Canada - Description, Dating, and Dynamics. Canadian Geotechnical Journal, 31(5): 749-768.
Friedmann, S.J., Kwon, G. and Losert, W., 2003. Granular memory and its effect on the triggering and distribution of rock avalanche events. Journal of Geophysical Research-Solid Earth, 108(B8).
Friele, P.A. and Clague, J.J., 2004. Large Holocene landslides from Pylon Peak, southwestern British Columbia. Canadian Journal of Earth Sciences, 41(2): 165-182.
Geertsema, M.,O. Hungr, J.W.Schwab, S.G. Evans, 2005. A large rockslide-debris avalanche in cohesive soil at Pink Mountain, northeastern British Columbia, Canada. Engineering Geology, in press
Gruner, U. , 2006. Bergstürze und Klima in den Alpen – gibt es Zusammenhänge?. Bulletin angewandter Geologie 11(2): 25-34
Hancox, G.T., McSaveney, M.J., Manville, V.R. and Davies, T.R., 2005. The October 1999 Mt Adams rock avalanche and subsequent landslide dam-break flood and effects in Poerua River, Westland, New Zealand. New Zealand Journal of Geology and Geophysics, 48(4): 683-705.
Hearn, G.J., 1995. Engineering Geomorphological Mapping and Opencast Mining in Unstable Mountains - a Case-Study. Transactions of the Institution of Mining and Metallurgy Section a-Mining Industry, 104: A1-A18.
Hendron, J., A. J. and F. D. Patton, 1987. The Vaiont slide – A geotechnical analysis based on new geologic observations of the failure surface. Engineering Geology 24(1-4): 475-491.
Hermanns, R.L. and Strecker, M.R., 1999. Structural and lithological controls on large Quaternary rock avalanches (sturzstroms) in arid northwestern Argentina. Geological Society of America Bulletin, 111(6): 934-948.
Hermanns, R.L. et al., 2006. Examples of multiple rock-slope collapses from Kofels (Otz valley, Austria) and westem Norway. Engineering Geology, 83(1-3): 94-108.
Hewitt, K., 1998. Catastrophic landslides and their effects on the upper Indus streams, Karakoram Himalaya, northern Pakistan. Geomorphology 26, 47-80.
Hewitt, K., 2001. Catastrophic rockslides and the geomorphology of the Hunza and Gilgit river valleys, Karakoram Himalaya. Erdkunde 55, 72-93.
Holm, K., Bovis, M., Jakob, M., 2004. The landslide response of alpine basins to post-Little Ice Age glacial thinning and retreat in southwestern British Columbia. Geomorphology 57, 201-216.
Hsü, K.J., 1975. Catastrophic debris streams (sturzstroms) generated by rock falls. Geological Society of America Bulletin 86, 129-140.
Hungr, D. and Evans, S.G., 2004. Entrainment of debris in rock avalanches: An analysis of a long run-out mechanism. Geological Society of America Bulletin, 116(9-10): 1240-1252.
Jarman, D., 2002. Rock slope failure and landscape evolution in the Caledonian Mountains, as exemplified in the Abisko area, northern Sweden. Geografiska Annaler Series A-Physical Geography, 84A(3-4): 213-224.
Jibson, R.W., Harp, E.L., Schulz, W. and Keefer, D.K., 2006. Large rock avalanches triggered by the M 7.9 Denali Fault, Alaska, earthquake of 3 November 2002. Engineering Geology, 83(1-3): 144-160.
Keefer, D.K., 1984. Landslides Caused by Earthquakes. Geological Society of America Bulletin 95(4): 406-421.
Keefer, D.K., 1999. Earthquake-induced landslides and their effects on alluvial fans. Journal of Sedimentary Research 69, 84-104.
Korup, O., 2004. Geomorphic implications of fault zone weakening: slope stability along the Alpine Fault, South Westland to Fiordland. New Zealand Journal of Geology and Geophysics 47, 257-267.
Korup, 2006. Effects of large deep-seated landslides on hillslope morphology, western Southern Alps, New Zealand, Journal of Geophysical Research-Earth Surface 111 (2006) F01018, doi:10.1029/2004JF000242.
Korup, O., Clague, J.J., Hermanns, R.L., Hewitt, K., Strom, A.L., Weidinger, J.T., in press. Giant landslide, topography, and erosion. Earth and Planetary Science Letters.
Opfergelt, S., Delmelle, P., Boivin, P. and Delvaux, B., 2006. The 1998 debris avalanche at Casita volcano, Nicaragua: Investigation of the role of hydrothermal smectite in promoting slope instability. Geophysical Research Letters, 33(15).
Pierson, T.C. and Janda, R.J., 1994. Volcanic Mixed Avalanches - a Distinct Eruption-Triggered Mass-Flow Process at Snow-Clad Volcanos. Geological Society of America Bulletin, 106(10): 1351-1358.
Ponomareva, V.V., Melekestsev, I.V. and Dirksen, O.V., 2006. Sector collapses and large landslides on late Pleistocene-Holocene volcanoes in Kamchatka, Russia. Journal of Volcanology and Geothermal Research, 158(1-2): 117-138.
Reid, M.E., Sisson, T.W. and Brien, D.L., 2001. Volcano collapse promoted by hydrothermal alteration and edifice shape, Mount Rainier, Washington. Geology, 29(9): 779-782.
Schmidt, K.M., and D.R. Montgomery, 1995. Limits to relief, Science, 270, 617-620.

Schneider, JL, Pollet, N, Chapron, E, et al., 2004. Signature of Rhine Valley sturzstrom dam failures in Holocene sediments of Lake Constance, Germany. Sedimentary Geology 169 (1-2): 75-91.
Schramm, J.M., Weidinger, J.T., and Ibetsberger, H.J., 1998. Petrologic and structural control on geomorphology of prehistoric Tsergo Ri slope failure, Langtang Himal, Nepal. Geomorphology 26, 107-121.
Schuster, R.L., Logan, R.L. and Pringle, P.T., 1992. Prehistoric Rock Avalanches in the Olympic Mountains, Washington. Science, 258(5088): 1620-1621.
Seijmonsbergen, A.C., Woning, M.P., Verhoef, P.N.W. and de Graaff, L.W., 2005. The failure mechanism of a late glacial sturzstrom in the subalpine Molasse (Leckner valley, Vorarlberg, Austria). Geomorphology, 66(1-4): 277-286.
Selby, M.J. (1992), Hillslope materials and processes, Second edition, 451p., Oxford University Press, Oxford.
Shang, Y., Yang, Z., Li, L., Liu, D., Liao, Q., and Wang, Y., 2003. A super-large landslide in Tibet in 2000: background, occurrence, disaster, and origin: Geomorphology 54, 225-243.
Smith, L.N., 2001. Columbia Mountain landslide: late-glacial emplacement and indications of future failure, Northwestern Montana, USA. Geomorphology, 41(4): 309-322.
Stoopes, G.R. and Sheridan, M.F., 1992. Giant Debris Avalanches from the Colima Volcanic Complex, Mexico - Implications for Long-Runout Landslides (>100 km) and Hazard Assessment. Geology, 20(4): 299-302.
Strecker, M.R., Hilley, G.E., Arrowsmith, J.R. and Coutand, I., 2003. Differential structural and geomorphic mountain-front evolution in an active continental collision zone: The northwest Pamir, southern Kyrgyzstan. Geological Society of America Bulletin, 115(2): 166-181.
Strom, A.L. and Korup, O., 2006. Extremely large rockslides and rock avalanches in the Tien Shan Mountains, Kyrgyzstan. Landslides, 3(2): 125-136.
Ui, T., Takarada, S., Yoshimoto, M., 2000. Debris avalanche. In: Encyclopedia of Volcanoes. Academic Press, 617-626.
Vallance, J.W. and Scott, K.M., 1997. The Osceola Mudflow from Mount Rainier: Sedimentology and hazard implications of a huge clay-rich debris flow. Geological Society of America Bulletin, 109(2): 143-163.
Varnes, D. J., 1978. Slope Movement. Types and Processes. R. L. Schuster and R. J. Krizek(eds): Landslides: Analysis and control. Washington, DC, Transportation Research Board, National Academy Press. Special Report 176: 11-33.
Vidal, N. and Merle, O., 2000. Reactivation of basement faults beneath volcanoes: a new model of flank collapse. Journal of Volcanology and Geothermal Research, 99(1-4): 9-26.
de Vries, B.V., Self, S., Francis, P.W. and Keszthelyi, L., 2001. A gravitational spreading origin for the Socompa debris avalanche. Journal of Volcanology and Geothermal Research, 105(3): 225-247.
Wadge, G., Francis, P.W. and Ramirez, C.F., 1995. The Socompa Collapse and Avalanche Event. Journal of Volcanology and Geothermal Research, 66(1-4): 309-336.
Watters, R.J., Zimbelman, D.R., Bowman, S.D. and Crowley, J.K., 2000. Rock mass strength assessment and significance to edifice stability, Mount Rainier and Mount Hood, Cascade Range volcanoes. Pure and Applied Geophysics, 157(6-8): 957-976.
Weidinger, J.T., 2006. Predesign, failure and displacement mechanisms of large rockslides in the Annapurna Himalayas, Nepal. Engineering Geology 83, 201-216.
Weidinger, J.T., Schramm, J.M., and Nuschej, F., 2002. Ore mineralization causing slope failure in a high-altitude mountain crest—on the collapse of an 8000 m peak in Nepal: Journal of Asian Earth Sciences 21, 295-306.
Weidinger, J.T., Schramm, J.M., and Surenian, R., 1996, On preparatory causal factors, initiating the prehistoric Tsergo Ri landslide (Langthang Himal, Nepal): Tectonophysics 260, 95–107.
Wilson, P. and Smith, A., 2006. Geomorphological characteristics and significance of Late Quaternary paraglacial rock-slope failures on Skiddaw Group terrain, Lake District, northwest England. Geografiska Annaler Series A-Physical Geography, 88A(3): 237-252.
Wyllie, D.C., and C.W. Mah, 2004. Rock slope engineering, Civil and mining 4th edition, 431 p., Spon Press, London and New York.

Chapter 3

Guide Neige et Avalanches, coordinated by Christophe Ancey, Edisud, 1998.
La neige, ses métamorphoses, les avalanches, Laurent Rey, Anena, 1986.
The Avalanche Handbook, David McClung and Peter Schaerer, The Mountaineers, 1993.
Février 1999 dans les Alpes du nord, J. Villecrose, C. Coléou and G. Giraud, Note de Centre (Météo-France CNRM-CEN), 1999.
Notices des C.L.P.A. des massifs des Alpes, de la Corse et des Pyrénées, C.E.MA.G.R.E.F. de Grenoble-St-Martin-d'Hères, 2006.
Estimation de l'épaisseur moyenne de déclenchement pour le calcul des avalanches denses, Burkard A. and Salm B., Rapport interne n° 668, I.F.E.N.A. in Davos, February 1992.
Schweizer J., Michot G., Kirchner H.O.K., 2004. On the fracture toughness of snow. Annals of Glaciology, 38, 2004, pp 1-8.

Data bases

www.avalanches.org (SLF)
www.avalanches.fr (CEMAGREF)
BDNIV (Météo-France – CEN)
NIVOLOG (Météorisk)
NVOMET